A Szilikátipari Tudományos Egyesület lapja

építőanyag

Journal of Silicate Based and Composite Materials

A TARTALOMBÓL:

2019/2

European Materials Research Society

E-MRS now has more than 4,000 members from industry, government, academia and research laboratories, who meet regularly to debate recent technological developments of functional materials. The E-MRS differs from many single-discipline professional societies by encouraging scientists, engineers and research managers to exchange information on an interdisciplinary platform, and by recognizing professional and technical excellence by promoting awards for achievement from student to senior scientist level. As an adhering body of the International Union of Materials Research Societies (IUMRS), the E-MRS enjoys and benefits from very close relationships with other Materials Research organizations elsewhere in Europe and around the world.

23 RUE DU LOESS, BP 20 - 67037
STRASBOURG CEDEX 02, FRANCE
EMRS@EUROPEAN-MRS.COM
WWW.EUROPEAN-MRS.COM

építőanyag
Journal of Silicate Based and Composite Materials
2019/2

TARTALOM

CONTENT

A finomkerámia-, üveg-, cement-, mész-, beton-, tégla- és cserép-, kő- és kavics-, tűzállóanyag-, szigetelőanyag-iparágak szakmai lapja
Scientific journal of ceramics, glass, cement, concrete, clay products, stone and gravel, insulating and fireproof materials and composites

A folyóiratot referálja · The journal is referred by:
Cambridge Scientific Abstracts
ProQuest

A folyóiratban lektorált cikkek jelennek meg.
All published papers are peer-reviewed.
Kiadó · Publisher: Szilikátipari Tudományos Egyesület (SZTE)
Elnök · President: ASZTALOS István
1034 Budapest, Bécsi út 122–124.
Tel.: +36-1/201-9360 ▪ E-mail: epitoanyag@szte.org.hu
Tördelő szerkesztő · Layout editor: NÉMETH Hajnalka

Címlapfotó · Cover photo: GYURKÓ Zoltán

WWW.EPITOANYAG.ORG.HU
EN.EPITOANYAG.ORG.HU

Online ISSN: 2064-4477
Print ISSN: 0013-970x
INDEX: 2 52 50 ▪ 71 (2019) 33–72

Vol. 71, No. 2

Performance of dolomitic cementitious mortars as a repairing material for normal concrete in Egypt

M. E. EL-FAKHARANY ▪ Housing and Building National Research Center, Egypt
M. EZZAT ▪ Housing and Building National Research Center, Egypt
A. GAD ▪ Geology Department, Faculty of Science, Ain-Shams University, Egypt
N. G. ABDEL GHAFOUR ▪ Housing and Building National Research Center, Egypt
A. R. BAGHDADY ▪ Geology Department, Faculty of Science, Ain-Shams University, Egypt

Érkezett: 2019. 02. 12. ▪ Received: 12. 02. 2019. ▪ https://doi.org/10.14382/epitoanyag-jsbcm.2019.7

Abstract

The use of dolomitic aggregate in preparation of cementitious repairing mortar really depends on their mineralogical composition and physico-mechanical properties. The physico-mechanical properties and chemistry of the selected local dolomitic aggregates were evaluated and compared with those of natural siliceous sand minerals. The studied dolomitic aggregates have a convenient chemical composition to be used as a concrete aggregate. Whereas they show relative variations in their physico-mechanical properties especially the grain size distribution, which will of course reflect the characteristics of the repairing mortar mix.

The compatibility of some cementitious repair mortars characteristics casted by dolomitic aggregates was assessed. Showed that dolomitic aggregate possess a clear effect on the properties of cementitious mortar rather than the natural siliceous sand. Also, using of this type of aggregates improves the compatibility with most commonly concrete used in Egypt by justification of the cementitious mortar mix with the suitable admixture. Assisted that most of the studied mixes show good compatibility with the casted concrete depending of appropriate composition.

Keywords: Cementitious repairing mortar; Aggregate; Physico-mechanical properties; Dimensional stability; Drying shrinkage; Compressive strength; Bond strength.
Kulcsszavak: Cementbázisú javítóhabarcs,; Adalékanyag; Fiziko-mechanikai tulajdonságok; Méretstabilitás; Száradási zsugorodás; Nyomószilárdság; Kapcsolati szilárdság.

Maged Ezzat EL-FAKHARANY
Assistant researcher in Raw Building Materials Technology and Processing Research Institute, Housing and Building National Research Center (HBNRC), XRD laboratory member since 2010, and working on Ph.D in Geology.

Mohamed Ezzat TAHA
Researcher in Raw Building Materials Technology and Processing Research Institute, Housing and Building National Research Center (HBNRC), XRD and Petrography labs member.

Ahmed GAD
Lecturer of Geology at the faculty of Science, Ain-Shams University

Nasser Gamal Abdel GHAFOUR
Professor of Geology of Raw Building Materials, Housing and Building National Research Center (HBNRC)

Ashraf Rushdi BAGHDADY
Professor of Geology at faculty of Science, Ain Shams University

1. Introduction

Continuous rapid urbanization in Egypt was followed by the appearance of concrete deteriorating problems. Repairs would be successful in the long-term if original caused damages are avoided by applying appropriate repairing materials to resist the future deterioration, [1]. Having good experience of repairing process with higher initial quality of the used repairing material, results in postponement of repair and, in the end, a reduction of the costs for maintenance and repeat the repair. One of the most challenging and interesting tasks in the field of concrete repairing is to choose and evaluate local repairing materials used. Without knowledge about building materials used it would not be possible to build safe, efficient and long-lasting buildings. The performance of a repaired concrete structure, and thus its service life, depends mainly on the quality of the repairing material composite [2]. Today cementitious materials especially of Portland cement represent the majority of our binding materials. Cementitious materials are defined as compounds that are mixed easily and react with water results in hydration products of calcium silicates (C-S-H), which bind the constituents together. These hydrated phases contribute to cement matrices densification and thus, to improve the mechanical properties and durability [3]. Cementitious repairing mortars mixed with local dolomitic aggregate can offer a number of advantages such as availability, cheapness, easy production with large volume and its compatibility with the older local common concrete. Repairing materials only with cementitious binders can provide acceptable protection to existing concrete structures, [4]. Addition of different percentages of mineral admixtures may also enhance the performance of a cementitious repairing mortar thus improve the compatibility with concrete substrate.

Good bond between the repair and the existing concrete substrate is a primary requirement for a successful repair [5]. This generally requires that the repairing material have high strength, be well bonded and compatible with the substrate. The final requirement is the repairing material should have properties that enable it to be dimensionally stable relative to the substrate [6-8]. This frequently requires that the repair materials have a low drying shrinkage and that these materials have a coefficient of thermal expansion that is similar to the substrate. Cementitious materials are locally available and it can mix with any natural aggregate and additives. The selection of a suitable additive to make a successful cementitious repair mortar depends mostly on using a suitable elected aggregate. In this case the set properties are strongly influenced by the cementitious composites especially the characteristics of aggregate used as discussed by [9].

Fig. 1 Satellite image shows the locations of quarrying and samples, Ataqa area, Suez City, Egypt
1. ábra A kőfejtés és mintavétel helyei műholdképen, Ataqa terület, Szuez, Egyiptom

Oxide content (wt,%)	OPC	EPP	CS
SiO_2	20.61	74.69	50.6
Al_2O_3	4.72	9.91	25
Fe_2O_3	3.31	0.59	9.7
CaO	62.65	2.19	4
MgO	2.12	0.01	2.5
SO_3	2.8	0.04	0.009
Loss of Ignition (LOI)	3.11	1.48	1.05
Na_2O	0.39	5.65	1.98
K_2O	0.23	4.66	2.9
TiO_2		0.14	1
P_2O_5		0.03	0.001
Total	99.94	99.39	98.74
Ins.Res	2.71		
Na_2OEq	0.24		
C_3A	5.98		
C_3S	51		
C_2S	22.05		

Table 1 Chemical composition of the used OPC, EPP and CS admixtures
1. táblázat Az alkalmazott OPC, EPP és CS adalékok kémiai összetétele

2. Materials and methods

2.1 Raw materials used

Aggregate representative samples were collected from different quarries stockpiles at Ataqa area- Egypt and coded Dol.1, Dol.2 and Dol.3, (*Fig.1*). More than 150kg for each aggregate type was collected to measure its performance in mortar mixes for repairing concrete. Three aggregate samples were elected and coded. A natural sand sample is collected from Jabal El Sheeb quarry, 6th October City, Egypt.

The type of cement used was the Egyptian Ordinary Portland Cement (OPC-CEMI with Rank 42.5) produced by Tourah Cement Company. Its chemical analysis was performed and found to agree with the standard specifications, (*Table.1*). The mineral admixtures used were expanded perlite powder (EPP) made in Egypt by the Egyptian Company for Expanded Perlite (E.C.P.V.), Batch year 2016 and an import coal slag (CS) with cement replacement percentages (5, 10, and 15%).

2.2. Aggregate evaluation

There is recommendation to add high quality aggregate to repairing mortars according to [6].The chemical and mineralogical investigation of carbonate aggregates were done using Axios (PW4400) WD-XRF Sequential Spectrometer (Panalytical, Netherland) and X-ray diffractometer, (model X'Pert Pro, Phillips MPD – Manufactured by PANalytical B.V Co., Netherlands - ISO 9001/14001 KEMA - 0.75160) provided with (Cu) anode at 40 kv&30 mA with a scanning speed of 2° / minute. The elected aggregates will be used in a repair mortar mix should have a physical and mechanical characteristics meet the ASTM C33 specification [10].

Mortar Mix	Mix proportions (kg/m³)					
	Cement	Aggregate		Water	SP	Additive
M.Dol.1	571	1630		224	4.6	
M.Dol.2	571	1630		224	4.6	
M.Dol.3	571	1630		224	4.6	
M.Sand	568	1622		223	4.5	
		(Dol.1)	(Dol.2)			EPP CS
M.Dol.C(MD.C)	571	981	644	224	4.6	
M.D.C. 5%EPP	542	981	644	224	4.6	28.6
M.D.C.10%EPP	514	981	644	224	4.6	57.1
M.D.C.15%EPP	485	981	644	224	4.6	85.6
M.D.C.5%CS	542	981	644	224	4.6	28.6
M.D.C.10%CS	514	981	644	224	4.6	57.1
M.D.C.15%CS	485	981	644	224	4.6	85.6

Table 2 Mix proportion of the studied cementitious mortars (kg/m³)
2. táblázat A vizsgálat cementbázisú habarcsok keverési összetétele (kg/m³)

2.3. Mortars properties tests

The mixed repairing mortar was defined as all concrete constituents with a smaller aggregate particle size pass 9.5mm sieve, i.e., aggregate <9.5mm, cement, water and super plasticizer (SP), (*Table2*). For concrete substrate the proportion by mass 1:1.9:3.6 (cement: sand: carbonate aggregate) trail mix was used with W/ C ratio = 0.5, to gain normal concrete with strength reaches approximately 41 MPa. For the substrate and repairing mortars compressive strength test on 3 cubic concrete samples for each mix were performed at ages of 1, 3, 7, 28 and 90 days. In each case, this test was carried out on specimens following the procedure described by Egyptian Code for the design of concrete structures [11]. Mortar cubes water absorption was performed according to the test

procedure ASTM C642 [12]. The procedure for determining the coefficient of thermal expansion of repair mortars is used where mortar prisms are exposed to temperatures ranging from 5 to 60 °C [13]. The drying shrinkage test was carried out according to ASTM C157/C157M [14], also slant shear test according to ASTM C882 [15].

3. Results and discussion

3.1. Aggregates

3.1.1. Chemical and mineralogical composition

Chemistry of carbonate aggregate samples shows that CaO is the highest recorded oxide followed by MgO (*Table.3*). On the other hand, the sand aggregates show high content of SiO_2. These facts are related to the mineralogical composition of the studied aggregates. The carbonate aggregates are mainly composed of dolomite and calcite; meanwhile the sand aggregates are dominated by quartz (*Fig.2*). The carbonate aggregates can be classified according to their MgO % into dolomite (Dol.1&Dol.2) and calcitic dolomite (Dol.3), [16]. Dol.3 sample show relatively higher contents of SiO_2, Al_2O_3, Fe_2O_3 and loss in ignition than those of other carbonate aggregates, that may be related to the presence of impurities. All samples show low Na_2O and K_2O contents however the sand recorded relatively higher alkali contents than carbonate aggregates. SO_3% is relatively higher in carbonate aggregates than those of sand, however this percentage still in acceptable limit (0.02-0.12%). On the other hand, carbonate aggregates especially Dol.3 sample have unacceptable chloride limit according to the Egyptian specification [11].

Oxide content (wt,%)	Dol.1	Dol.2	Dol.3	Sand
SiO_2	1.09	0.48	1.32	97.16
CaO	35.6	38.42	33.7	1.54
MgO	19.3	20.61	18.7	0.11
Al_2O_3	0.23	0.12	0.55	0.05
TiO_2	0.07	0.07	0.06	
Fe_2O_3	0.19	0.17	0.21	0.05
Na_2O	0.11	0.04	0.13	0.19
K_2O	0.04	0,02	0.06	0.11
P_2O_5	0.11	0.05	0.05	
SO_3	0.1	0.12	0.02	0.01
Loss of Ignition (LOI)	42.9	39.7	45.2	0.39
Total	99.74	99.78	100	99.97
Chloride ion(Cl)	0.06	0.09	0.1	0.09

Table 3 Chemical composition of the studied aggregates
3. táblázat A vizsgált adalékanyagok kémiai összetétele

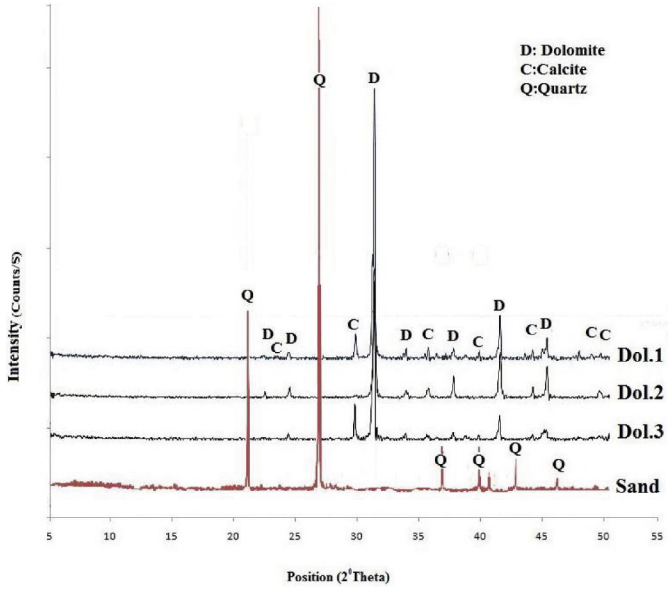

Fig. 2. XRD patterns of the different studied aggregates
2. ábra A vizsgált adalékanyagok XRD elemzése

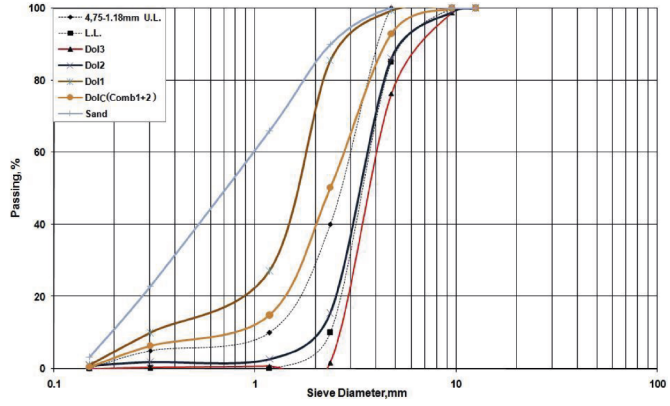

Fig. 3. Grain size distribution curve of the studied aggregates
3. ábra A vizsgált adalékanyagok szemmegoszlás görbéje

3.1.2 Physico-mechanical properties

3.1.2.1 Grading

Using of well and densely graded aggregates is highly recommended for repairing mortar, to reduce the required cement paste and minimize the risk of debonding, via shrinkage reduction [17]. Also, the grading affects the workability and finishing quality of mortar and concrete [18]. The studied dolomitic aggregates show variations in grain size distribution (*Fig.3*). The grading curves are lined near the zone of size number (9) limit according to ASTM D448 [19]. Dolomitic aggregates are falling within the coarse sand size especially sample Dol.1 when compared with the natural sand aggregate. Sample Dol.3 exceeds the upper limits of the size number (9) which disagrees with the concept of repair [20], while Dol.1 sample deviates toward the sand fractions and pass its lower limit. Void contents increase with decreasing in aggregate size to about (40%-50%) for fine aggregates [21]. This may lead to higher amount of cement paste and more shrinkage. Dol.2 sample have a good grading distribution curve and in the case of combined sample (Dol.C), the distribution curve is slightly

shifted to sand size. This combination may be helpful to use wide size range and mostly of smaller sizes as possible. Satoh et al., [22] stated that the suitable sizes of aggregates should line with treated roughness of the substrate surface for best repairing. Such these dolomitic aggregates grading could positively affect the aggregate interlock and may lead to good bonding.

3.1.2.2 Bulk density

The bulk density of the studied dolomitic aggregate samples ranges from 1.30 to 1.36 g/cm^3 with an average value of 1.32 g/cm^3. While natural sand sample shows the highest recorded bulk density value (1.47 g/cm^3) and considered the densest aggregate (*Fig. 4*). That can be attributed to the smallest sand fractions which help in fissuring and decrease voids space. Recorded bulk density values are considered reasonable to good mortar with normal weight which requires less cement. It should be known that, normal aggregate weight will have good workability and has been considered resistant to length change due to drying [23]. Variation of bulk densities values for dolomitic aggregates compared with sand aggregate may relate to their angularity and abundance of coarser size fractions. It is well known that, angularity shape of aggregate is a very important factor that causes changes in the relative density values as indicated by [24, 25]. Low bulk density values can increase voids contents between aggregate particles [21], leading to higher cement paste and so higher shrinkage. So, samples with normal weight should be used and total volume of voids can be reduced by using a combination of aggregate sizes.

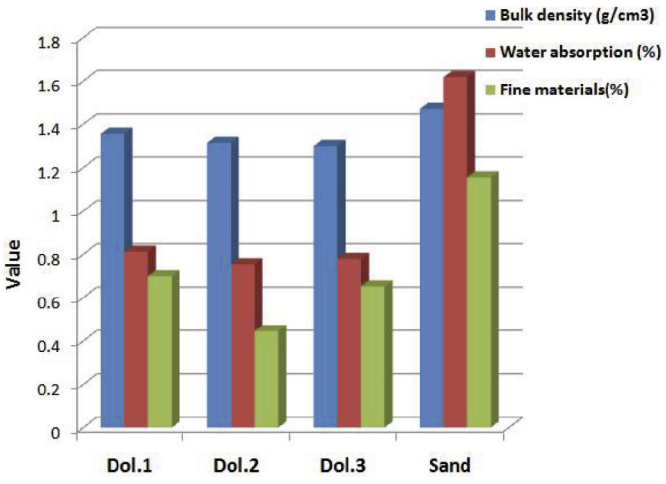

Fig. 4. Correlation between bulk density, water absorption and fine materials values of the studied aggregates
4. ábra A vizsgálat adalékanyagok halmazsűrűsége, vízfelvétele és finomrész aránya

3.1.2.3 Fine materials and water absorption

The percentages of fine materials (*Fig.4*) revealed that all studied aggregate samples don't exceed the value of 1%, except sand sample. These values agree with the ASTM C142 limits [26], that give chance to use such aggregates for a repairing mortar. There is a direct relation between the water absorption and presence of fine materials. All recorded values lie within the standard limits [27, 28]. Dolomitic aggregates seem to be relatively lower in water absorption than sand. Their values are relatively close to combined substrate aggregates values, which may enhance the compatibility. In addition to presence of fines the high water absorption may related to the iron oxide as deleterious substances which may contribute to more shrinkage. The Drying shrinkage test in BS 812 -120 [29] is limited to aggregate with water absorption less than 3.5%. Length change seems to be caused by change in surface energy of most aggregate due to absorption [23]. Generally, it shouldn't use aggregate with high water absorption which will not be more safely in repairing of concrete. Since the mechanical adherence with high water absorption may be prevented from occurring as discussed by [30].

3.2 Mortar

3.2.1Physico-mechanical properties

Suitable repair mortar mix allows cementitious repair materials to easily penetrate and hydrate into substrate cavities. The slump values of fresh mortar mixes with dolomitic aggregates ranges between 4.9 and 6.8 cm. While mortar made with natural sand show moderate value equal 5.6 cm. Therefore, all studied mixes are considered of medium workability. ACI 224.1R [31] recommended using of the lowest possible slump to reduce shrinkage and avoid occurrence of cracks, so a combination of dolomitic samples is more acceptable to use.

Dry density of studied mortar cubes already matches with bulk density of aggregates and compatible with substrate (*Fig. 5*). Dolomitic mortars show similarity in dry density which range from 2.39 to 2.41 g/cm^3. Mortar with natural sand show the dense value (2.42 g/cm^3), that related to the good packing shown by sand particles. The main causes of little difference in weight between mortars may relate to grading, shape and composition of aggregate, [21]. Spherical particles like natural sand lead to good backing and so better workability, [32]. The crushed dolomitic aggregates that yield grains with angular corners cannot be workable enough like sand [18]. They still have slightly compatible nature with the substrate density. But when additives applied, EPP mortar cubes showed decrease in dry density with increasing cement replacement unlike CS mortars. That simply relate to the relatively high specific gravity of such additive. Therefore high dosages affect on mass unit compatibility with the normal concrete substrate.

Good adherence of mortar is recommended by using amix with lower water absorption than the substrate [30]. It can be observed that water absorption of all studied mixes is lower than substrate value (*Fig. 5*). Mortar made with dolomitic aggregates shows approximately similar values with an average equal 0.9%. While the comparable sandy mortar shows the highest water absorption value (1.5%) among all studied mixes. This may be due to the higher percent of fine materials in that aggregate which influence the concrete absorption, [33]. To some extent, there is relation between the densities of the studied mortars and their water absorption values. It can be noticed that water absorption of mortars mixed with EPP increase with decreasing density and increasing cement replacement. This fact may be related to water uptake due to the high surface area gained by these additives. EPP could be

used in small quantities as a cement replacement due to its high water absorption capacity [34]. However, in case of CS there is a slight decrease with increase dosages and density that means CS did not have the ability to excess water uptake. This reflects that aggregate type and mortar composition may influence water absorption of the produced repairing mortars.

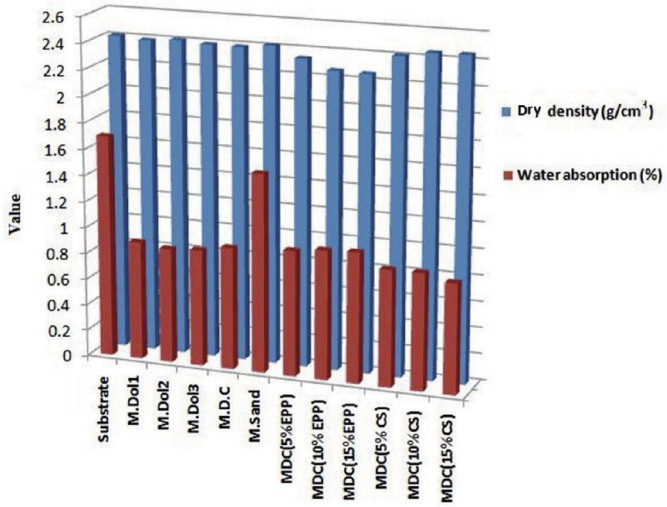

Fig. 5. Correlation between the values of dry density and water absorption of the studied cube mixes
5. ábra A kocka minták sűrűsége és vízfelvétele közötti korreláció

3.2.2 Dimensional stability

3.2.2.1 Length change (Dry shrinkage)

Cementitious mortar mix with an excess of binder may lead to high shrinkage and mortar cracking. Therefore, excessive shrinkage of a cementitious repair mortar can be a main cause of the repair failure. There is a suggestion to use very low shrinkage cementitious mortars for concrete repair by [35]. All studied mortar mixes show drying shrinkage ranging from 0.0053% to 0.01% after 28days (*Fig.6*), (*Table 4*); therefore, they are considered very low shrinkage according to [36]. Also they should be desirable since the point of view is "shrinkage of a cementitious mortar should be less than that of concrete" as mentioned by [7]. Dolomitic mortars showed relatively lower shrinkage values range between 0.0053 and 0.0086% after 28 days, and 0.0072 and 0.0092% after 2 months. While the comparable natural sandy mortar showed the highest shrinkage value (0.01%) after 28days between the studied samples, then its value seems to be constant for 2 months. However, it is considered acceptable since the repair mortar to concrete substrate relation is (R<C).

The relatively high shrinkage of natural sand mortar relate to its relatively high absorption and more fines in that aggregate. Grassl et al., [37] reported that the concretes shrinkage depends primarily on the used aggregate properties. However, some mineral admixtures are capable to reduce shrinkage as documented by [38]. Mortars with EPP and CS after 28days show drying shrinkage increasing reached to 0.0065 and 0.0072%, respectively with the replacement level 15%, although they are still compatible with the substrate.

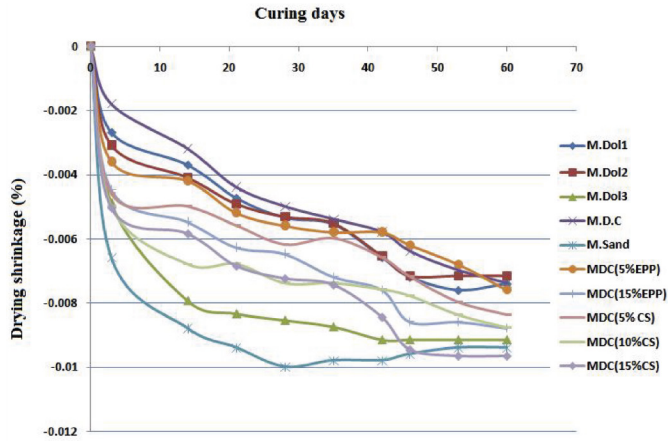

Fig. 6. The change of drying shrinkage between the studied mortar mixes.
6. ábra A száradási zsugorodás változása időben az egyes habarcskeverékek esetében

Mortar Sample	Shrinkage, 28days (%)	Shrinkage Relation	Thermal Expansion	Thermal Relation
M.Dol.1	0.0054	Classified as Very low - R<C (where the substrate shrinkage equals = 0.01444%)	4.87E-06	R<C (where thermal expansion coefficient equals = 6.77162E-06)
M.Dol.2	0.0053		5.18E-06	
M.Dol .3	0.0086		5.44E-06	
M.Sand	0.01		6.56E-06	
M.D.C	0.0054		5.44E-06	
M.D.C. 5%EPP	0.0056		5.32E-06	
M.D.C.10%EPP	0.0063		5.28E-06	
M.D.C.15%EPP	0.0065		5.18E-06	
M.D.C.5%CS	0.0062		4.85E-06	
M.D.C.10%CS	0.0074		6.48E-06	
M.D.C.15%CS	0.0072		6.76E-06	

Table 4 Shrinkage, thermal expansion coefficients values of the studied mixes and their relations with the substrate
4. táblázat A vizsgálat keverékek zsugorodása, termikus hőtágulási együtthatója és a ezek kapcsolata a bányászott anyag ezen tulajdonságaival

3.2.2.2 Thermal expansion

Thermal stability of cementitious mortar and their dimensional compatibility with existing substrate may impact the repair success. Types of aggregates have main influence on this property, [39]. Dolomitic mortars represent the relatively lowest coefficients of thermal expansion (4.87E-06, 5.18E-06, and 5.44E-06) if compared with sand mortar value (6.56E-06), (*Table 4*). Mortar sample MD.C (with combined aggregates Dol.1&Dol.2) show good thermal stability and compatibility with the substrate without any additives. EPP mortars show gradual decrease of thermal expansion coefficients from 5.45E-06 to 5.18E-06 value. This may be referred to the good thermal insulation properties of EPP. That gives EPP mortars high chance to be used as a repairing material in spite of its values are relatively lower than the studied concrete substrate. Unlike CS, mortars show increase in the thermal expansion values. The chemical composition with high alumina and iron oxides of CS may contribute to their high thermal expansion. Therefore, dolomitic mortars with high CS dosages and sand mortar may be considered less thermally stable; however they

have values close to that of the studied substrate. Such mixes should be avoided especially in repair dolomitic substrate because they may lead to poor bonding as recommended by [40].

3.2.3 Strength

3.2.3.1 Compressive strength

There is a variation in strength between all repair mortar samples *(Fig. 7*). This may relate to the difference in mineralogical composition and shape of the applied aggregate [25]. The strength ranges are 4.9-6.7, 9.4-18.7 and 24-30 MPa in the early curing ages 1, 3 and 7 days, respectively. Whereas the substrate strength value still considered the highest. The higher substrate strength value in early ages than studied repair mortars may be related to coarse aggregate size and high aggregate/cement ratio. Furthermore, mortars strengths begin to exceed the substrate strength where strengths increase to the range 34-54 and 35-56 MPa during the later curing ages 28 and 90days, respectively. The high rate of strength development at late ages can be explained by the good aggregate compaction that increases mix cohesion by increase in hydration time. Also most of these values can be compatible with substrate strength purposes and classified according to EN 1504-3 [41] into R4 and R3, (*Table.5*). It can be noticed that the highest strength values between dolomitic mortars (without mineral additives) are shown by MD.C mortar sample through all curing intervals 1, 3, 7, 28 and 90 days. The aggregates used in the mix of these samples be sounded, have good grading and show relative high mortar dimensional stability with good physico-mechanical properties. Unlike, MDol.3 sample mortar is incompatible with the substrate and displays lower strength value than the other dolomitic samples. This may be related to poor grading, abundance of large particles and poor quality of aggregate. Dolomitic mortars strength did not exceed sand mortar strength. This may be related to the high specific surface area of the fine sand aggregate which lead to high bond strength between the aggregate and cement paste and increase the compressive strength [42]. Therefore, dolomitic aggregates with high quality seem to be more suitable for repairing mortar mix.

The cement consumption and the compressive strength can be adjusted by add appropriate amount of mineral admixtures. EPP mortars show slight increase of compressive strength in the early ages (1, 3, 7days) with cement replacement up to 10%, and still lower than the control. At 28 days, they show the same behavior, while in later age (90 days), strength increase than the control mix up to 10% replacement. The strength decreased with 15% replacement although all EPP mortars are compatible with the substrate (*Table 5*). The cement replacement by 10% EPP leads to the highest compressive strength values for all samples after 90 days (*Fig.7*). It is shown that in case of EPP dense mortar form due to pozzolanic effect, as [43] indicated that perlite powder has a significant pozzolanic effect and is a good active mineral admixture for mortar. Unlike, mortars mixed with CS powder have relatively moderate strengths and are classified as (R3). These mortars show slight increase of strength up to 10% cement replacement at the early ages and strength decrease with the high replacement (15%). CS mortars show relatively higher strengths values than EPP mortars only during the first day. That means CS plays a major role as filler giving early dense mortar performance. The compressive strength of mortars with different SC dosages at 28 days show the highest value (43 MPa) with 5% replacement. Then the strength decreases gradually to (34 MPa) with 15%replacement. Therefore, coal slag is noticed to be reducing the compressive strength with increasing replacement percents and considered as undesirable for repair mixes. However, CS mortars are still compatible with the substrate, (*Table 5*). In general, the various behavior of repairing mortar compressive strength is not evident alone for good repairing material without bonding strength.

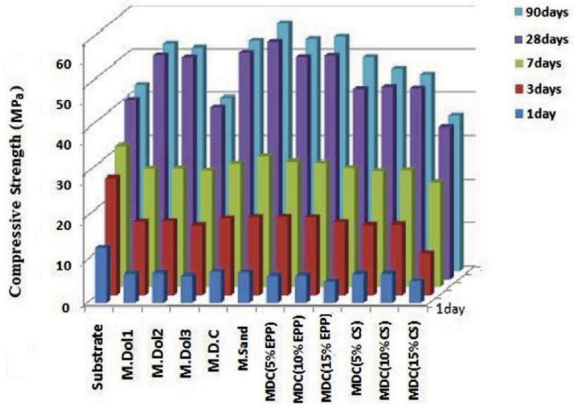

Fig. 7 Compressive strengths of all the studied repair cementitious mortars at different curing ages
7. Ábra A vizsgált cementalapú javítóhabarcsok nyomószilárdsága különböző szilárdulási korokban

Mortar Sample	Strength Classification according to EN 1504-3	Strength Relation	Bond strength Slant shear test 28d (MPa)	Bond failure
M.Dol.1	(R4)	R > C	26	Interface
M.Dol.2	(R4)	R > C	25	Interface
M.Dol.3	(R3)	R < C	20	Interface
M.D.C	(R4)	R > C	28	Interface
M. Sand	(R4)	R > C	33	Interface- with remains parts of C
M.D.C.5%EPP	(R4)	R > C	35	Interface- with remains parts of C
M.D.C.10%EPP	(R4)	R > C	26	Interface
M.D.C.15%EPP	(R3)	R > C	24	Interface
M.D.C.5%CS	(R3)	R > C	26	Interface
M.D.C.10%CS	(R3)	R > C	24	Interface
M.D.C.15%CS	(R3)	R < C	22	Interface

Table 5 Compressive strength classification, bond strength and bond failure of the studied mixes and their relations with the substrate
5. táblázat Nyomószilárdsági osztály, kötési szilárdság és kapcsolati tönkrement típusa a vizsgálat keverékeken és ezek kapcsolata a bányászott anyag tulajdonságaival

3.2.3.2 Bond strength (slant shear test)

It can be noticed that there is a correlation between bond strength and compressive strength, (*Fig 8*). The bond strengths of studied cementitious mortars range from 20 to 33 MPa, (*Table 5*). Most of the failure mode in the slant shear test was through the interface. This indicates that the bond strength between the cementitious repair mortar and substrate is weaker than the strength of the continuous substrate and the repair mortar themselves. Momayez et al., [44] predict low adhesion for cementitious repair materials and estimate slant shear values about 80% of the continuous sample. Therefore, additive should be applied to increase the cementitious bond.

On the other hand, natural sand mortar shows the highest bond strength value in all studied mortars. This may be related to the size and grading of its particles, which in turn cause good compacting and interlocking at the rough substrate surface. Also, the investigated dolomitic mortars show variations in bond strength. Since adherence occurs by penetration of the mortar's fine elements into the substrate's pores and forming a system of mechanical anchorage [30]. Mortars with good quality and more properly fine fractions as MDol.1 and MDol.2 show relatively higher bond than the coarser MDol.3. This means that the quality of the bond largely depends on the repair mortar characteristics.

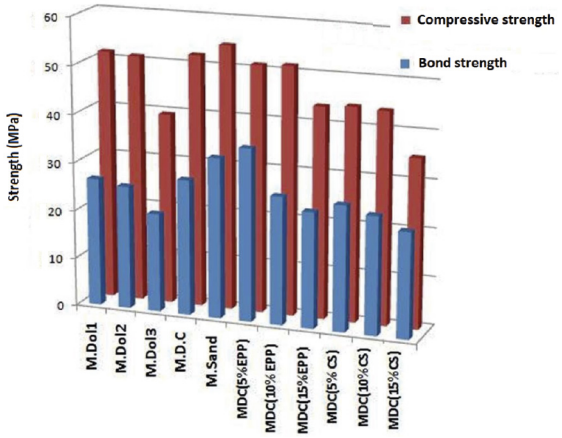

Fig. 8. The bond strength correlation between all studied cementitious mortars with different additives
8. ábra A kötési szilárdság korrelációja az összes vizsgálat cementalapú, különböző adalékanyagot tartalmazó habarcson

The selection of the repair mortars is based mainly on their bonding strength which may influence by mineral admixtures. Mortars mixed by EPP show bond strength decreasing from 35 (5%EPP) to 23 MPa (15% EPP). It is recommended that EPP could be used in small quantities as a cement replacement to prevent shrinkage and so debonding, due to its high water absorption capacity [34]. In spite of EPP mortars show relative decreasing in bond strength with replacement, however 5%EPP represents the highest bond strength value of all the studied cementitious mortars (*Fig.8*). The replacement level of all presented interface failure associated with partial damage and attached to traces of substrate (*Fig.9.a*). Good bonding of such mix may be related to the EPP pozzolanic activity, as filling voids of Interface Transition Zone (ITZ) which lead to cohesion of cement to other particles, resulting in enhancement of bonding to substrate.

Mortars mixed with CS show relatively high reduction in slant shear strength when compared with others. Replacement with 15% CS shows the lowest value (22 MPa) between all studied samples. The failure occurred only at the interface where complete separation of substrate and repair occurred, (*Fig 9.b*). The lack of pozzolanic activity in CS may be the main reason of reduction in its bond strength. Also, relatively high shrinkage observed by CS mortars may reduce bonding efficiency by initial tensile strain induced in the repair [45].

Fig. 9. a) 5% EPP mortar sample shows interface failure with partial damage and attached traces of substrate (right), b) interface failure with complete separation
9. ábra a) 5%-os EPP habarcs minta felületi tönkrementele az alapanyag részleges tönkremenetele mellett b) felületi tönkrementel teljes elválással

4. Conclusion

Well graded and dense dolomitic aggregates will positively affect interlocking and bonding by fissuring and decreasing void spaces. Avoid aggregate with high water absorption due to abundant fines, and iron oxides will be more safe in concrete repair.

Properties variation of cementitious repair mortar is due to variation in the used aggregates composition and characteristics. The studied dolomitic mortars show more dimensional stability than the comparable natural sandy

mortar. This fact enhances the compatibility between dolomitic repair mortar and the normal concrete substrate.

The different behavior of repairing mortar compressive strength is not evident alone for good repairing material without bonding strength. There is a correlation between bond strength and compressive strength, most of the failure mode in the slant shear test was through the interface. Therefore, additive should be applied to increase the cementitious bond. EPP added to dolomitic mortars is preferable than CS powder for good adherence. In general, the more compressive strength of dolomitic mortar contributes to increase the adhesion strength.

References

[1] Behfarnia, K. – Jon-nesari, H. – Mosharaf, A.(2005): The bond between repair materials and concrete substrate in marine environment, *Asian.J.Civil Eng* (Building and Housing). Vol.6, No.4, pp.267-272, https://behfarnia.iut.ac.ir/sites/behfarnia.iut.ac.ir/files/u32/bond_strength_6-4.pdf

[2] Bissonnette, B. – Vaysburd, A. – Von Fay, K. (2012): Best Practices for Preparing Concrete Surfaces Prior to Repairs and Overlays, Report Number MERL 12-17 U.S. Department of the Interior, Bureau of Reclamation, Technical Service Center, Denver, Colorado, USA, 92p

[3] Costa, C. (2015): Hydraulic Binders, in: M.C. Gonc ¸alves, F. Margarido (eds.), Materials for Construction and Civil Engineering Science, Processing, and Design, *Springer Inter. Publ. Switzerland* pp.1-52, https://doi.org/10.1007/978-3-319-08236-3

[4] Baldwin, N. – King, E. (2003): Field studies of the effectiveness of concrete repairs, Phase 1 research Report 175: Desk study and literature review, Mott MacDonald Ltd for the Health and Safety Executive, 42p

[5] ICRI, 320.2R., (2015): Guide for Selecting and Specifying Materials for Repair of Concrete Surfaces, Technical Guideline No. 320.2R, International Concrete Repair Institute, Rosemont, Illinois, UK, 92p

[6] Vaysburd, A. – Emmons, P. – McDonald, J. – Poston, R. – Kesne. K. (1999): Performance Criteria for Concrete Repair Materials, Phase II Summary Report, Technical Report REMR-CS-62, U.S. Army Engineers Waterways Experiment Station, Vicksburg, MS, 72p

[7] Emberson, N. – Mays, G. (1990): Significance of Property Mismatch in Patch Repair of structured concrete-Part1: properties of Repair Systems, *Magazine of Concrete Research*, Vol.42, pp.147-160

[8] VonFay, K. – Bissonnette, B. – Vaysburd, A. (2009): Development of Test Methods to Evaluate Cracking Tendency of Repair Materials, Field Study, Phase II, Research Report 2009-1,CREEP, U.S. Department of Interior, Bureau of Reclamation, Denver, Colorado.

[9] Amenta, M. – Karatasios, I. – Maravelaki-Kalaitzaki, P. – Kilikoglou, V. (2017): The Role of Aggregate Characteristics on the Performance Optimization of High Hydraulicity Restoration Mortars, *Construction and Building Materials*, Vol.153, pp.527-534, https://doi.org/10.1016/j.conbuildmat.2017.07.134

[10] ASTM C33 (2008): Standard Specification for Concrete Aggregates, ASTM International, West Conshohocken, PA, www.astm.org

[11] ECP-203. (2017): Egyptian Code for the design and implementation of concrete structures, Manual of testes, copy2017, HBNRC, Giza, Egypt, 132p

[12] ASTM C642. (2013): Standard test method for Density, Absorption and Voids in Hardened Concrete, ASTM International, West Conshohocken, PA, www.astm.org

[13] NT BUILD-367. (1991): Nordtest method, Concrete Repair Materials: Coefficient of Thermal Expansion, 2p

[14] ASTM C157/C157M. (2008): Standard Test Method for Length Change of Hardened Hydraulic-Cement Mortar and Concrete, ASTM Annual Book, 8p, www.astm.org

[15] ASTM C882 (1999): Standard Test Method for Bond Strength of Epoxy-Resin Systems Used With Concrete by Slant Shear

[16] Pettijohn, F. (1975): Sedimentary rocks, 3rd ed. Harper and row, New York, 526p

[17] Karagüler, M. – Yatagan (2018): Effect of Aggregate Size on the Restrained Shrinkage of the Concrete and Mortar, *Civil Engineering* (MOJ), Vol.4, pp.16-22, https://medcraveonline.com/MOJCE/MOJCE-04-00092.pdf

[18] Langer, W. (1993): Natural aggregates of the conterminous United States, *U.S. Geological Survey Bulletin*, Second Printing, pp.1-3.

[19] ASTM D448 (2017): Standard Classification for Sizes of Aggregate for Road and Bridge Construction, ASTM International, West Conshohocken, PA, www.astm.org

[20] ICRI, 320.3R (2012): Guideline for Inorganic Repair Material Data Sheet Protocol, Technical Guideline No. 320.3R, International Concrete Repair Institute, Rosemont, Illinois, UK, 7p

[21] Arumugam, B. (2014): Effect of Specific Gravity on Aggregate Varies the Weight of Concrete Cube, *International Journal of Civil Engineering* (SSRG-IJCE), Vol.1, 9p, http://www.internationaljournalssrg.org/IJCE/2014/.../IJCE-V1I3P101.pdf

[22] Satoh, A. – Satoh, M. – Yamada, K. (2015): Improvement of adhesion performance of mortar-repair interface with inducing crack path into repair, *Frattura ed Integrità Strutturale*, Italy, Vol.34, pp.397-405

[23] Fujiwara, T. (2008): Effect of Aggregate on Drying Shrinkage of Concrete, *Journal of Advanced Concrete Technology*, Vol.4, pp.31-44, https://doi.org/10.3151/jact.6.31

[24] Korkanc, M. – Tugrul, A. (2004): Evaluation of selected basalts from Nigde, Turkey as source of concrete aggregate, *Engineering Geology,* Vol.75, pp.291-307, https://doi.org/10.1016/j.enggeo.2004.06.015

[25] Abd-Allah, A. – Baghdady, A. – Dawood, Y. (2018): Adequacy of Carbonate Aggregates as an Alternative for Chert Aggregates in Concrete Manufacture, Construction and Building Materials, Vol.181, pp.94–105, https://doi.org/10.1016/j.conbuildmat.2018.06.019

[26] ASTM C142/C142M (2017): Standard Test Method for Clay Lumps and Friable Particles in Aggregates, ASTM International, West Conshohocken, PA, www.astm.org

[27] BS-8007 (1987): British Standard Code of Practice for Design of Concrete Structure

[28] ASTM C 127. (2001): Standard Test Method for Density, Relative Density (Specific Gravity), and Absorption of Coarse Aggregate, ASTM International, West Conshohocken, PA, www.astm.org

[29] BS 812-120 (1990): Testing Aggregate Method for Testing and Classifying Drying Shrinkage of Aggregates in Concrete

[30] Colen, I. – Brito, J. (2015): Renders, in: Gonc M.C. ¸alves, Margarido. F., (eds.), Materials for Construction and Civil Engineering Science, Processing, and Design p938, *Springer International Publishing Switzerland* pp53-122, https://doi.org/10.1007/978-3-319-08236-3_2

[31] ACI 224.1R. (2007): Causes, Evaluation, and Repair of Cracks in Concrete Structures, ACI committee report, American Concrete Institute, 22p

[32] Abu Seif. E. (2013): Performance of Cement Mortar Made with Fine Aggregates of Dune Sand, Kharga Oasis, Western Desert, Egypt: An Experimental Study, *Jordan Journal of Civil Engineering*, Vol.7, pp.270-284.

[33] Asamoah, M. – Afrifa, R. (2010): A study of concrete properties using phyllite as coarse aggregates, (Technical Report), *Materials and Design,* Vol.31, pp.4561-4566, https://doi.org/10.1016/j.matdes.2010.03.041

[34] Bektas, F. – Turanli, L. – Monteiro, P. (2005): Use of Perlite Powder to Suppress the Alkali-Silica Reaction, Cement and Concrete Research, Vol.35, pp.2014-2017, https://doi.org/10.1016/j.cemconres.2004.10.029

[35] Decter, M. – Keeley, C. (1997): Durable Concrete Repair-Importance of Compatibility and Low Shrinkage, *Construction and Building Materials*, II, NOS5-6, pp.267-213, https://doi.org/10.1016/s0950-0618(97)00047-0

[36] Morgan, D. (1996): Compatibility of Concrete Repair Materials and Systems, *Construction and Building Materials*, Vol.10, pp.51-61, https://doi.org/10.1016/0950-0618(95)00060-7

[37] Grassl, P. – Wong, H. – Buenfeld, N. (2009): Influence of Aggregate Size and Fraction on Shrinkage Induced Micro-racking of Mortar and Concrete, *Cement and Concrete Research*, Vol.40, pp.85-93, https://doi.org/10.1016/j.cemconres.2009.09.012

[38] Fardis, M. (ed.) (2012): Innovative Materials and Techniques in Concrete Construction, ACES Workshop, Library of Congress, 386p, https://doi.org/10.1007/978-94-007-1997-2

[39] King, D. (2012): The Effect of Silica Fume on the Properties of Concrete as Defined in Concrete Society Report 74, Cementitious Materials, 37th Conference on Our World in Concrete and Structures, Singapore
[40] Bissonnette, B. – Courard, L. – Fowler, D. – Granju, J. (2011): Bonded Cement-Based Material Overlays for the Repair, the Lining or the Strengthening of Slabs or Pavements, State-of-the-Art Report of the RILEM Technical Committee 193-RLS, V3, 199p, https://doi.org/10.1007/978-94-007-1239-3
[41] EN 1504-3(2006), European Standard, Products and systems for the protection and repair of concrete structures-Definitions, requirements, quality control and evaluation of conformity -Part 3: Structural and non-structural repair, European Committee for Standardization
[42] Al-Oraimi, S. – Taha, R. – Hassan, H. (2006): The effect of the mineralogy of coarse aggregate on the mechanical properties of high-strength concrete, *Construction and Building Materials*, Vol.20, pp.499-503, https://doi.org/10.1016/j.conbuildmat.2004.12.005
[43] Yu, L. – Ou, H. – Lee, L. (2003): Investigation on pozzolanic effect of perlite powder in concrete, *Cement and Concrete Research*, Vol.33, pp.73-76, https://doi.org/10.1016/s0008-8846(02)00924-9
[44] Momayez, A. – Ehsani, M. – Ramezanianpour, A. – Rajaie, H. (2005): Comparison of methods for evaluating bond strength between concrete substrate and repair materials, *Cement and Concrete Research*, Vol.35 pp.748–757, https://doi.org/10.1016/j.cemconres.2004.05.027
[45] Mangat, P. – Limbachiya, M. (1995): Repair material properties which influence long-term performance of concrete structures, *Construction and Building Materials*, Vol.9, pp.81-90, https://doi.org/10.1016/0950-0618(94)00003-k

Ref.:
El-Fakharany, M. E. – **Ezzat,** M. – **Gad,** A. – **Ghafour,** N. G. Abdel – **Baghdady,** A. R.: *Performance of dolomitic cementitious mortars as a repairing material for normal concrete in Egypt*
Építőanyag – Journal of Silicate Based and Composite Materials, Vol. 71, No. 2 (2019), 33–42. p.
https://doi.org/10.14382/epitoanyag-jsbcm.2019.7

Rheological properties of NBR/CR blends as a function of silicon dioxide grain size gradation

Ali I. AL-MOSAWI ▪ University of Miskolc, Hungary ▪ qkoali76@uni-miskolc.hu
Mohammed H. AL-MAAMORI ▪ College of Engineering Materials, University of Babylon, Iraq ▪ mat.mohammed.hamzah@uobabylon.edu.iq
Kálmán MAROSSY ▪ University of Miskolc, Hungary ▪ polkal01@uni-miskolc.hu

Érkezett: 2018. 12. 25. ▪ Received: 25. 12. 2018. ▪ https://doi.org/10.14382/epitoanyag-jsbcm.2019.8

Abstract

This study focuses on the extent to which the rheological properties of acrylonitrile butadiene rubber (NBR)/chloroprene rubber (CR) blends are affected by the variation of silicon dioxide grain size. Silicon dioxide (SiO_2) as a nanopowder filler has been added with 50 wt.% and different grain size particles (0-150 nm), and studied the effect of these additives on viscosity, scorch time, cure time and max torque for NBR/CR blends. The results obtained from the rheological tests showed that viscosity and max torque increased with increasing of silicon dioxide grain size, while the result was inverse with scorch and cure time, where the larger grain size of silicon dioxide will lead to reduce both the scorch- and the cure time.

Keywords: NBR/CR, SiO_2 grain size, Rheological properties, Rubber blends
Kulcsszavak: NBR/CR, SiO_2 szemcseméret, Reológiai tulajdonságok, Gumi keverékek

Ali I. AL-MOSAWI
PhD student in Polymers engineering, Institute of ceramic and polymer engineering, Faculty of materials science and engineering, University of Miskolc, Hungary. M.Sc. and B.Sc. in materials engineering, Faculty of engineering, University of Babylon, IRAQ. Research interests: Polymers, Composite materials, Rubber technology, Flame retardants, Materials testing, Materials processing.

Mohammed H. AL-MAAMORI
Professor of Rubber technology at Faculty of materials engineering, University of Babylon, IRAQ. Recent research interests: Rubber technology, Materials testing, Materials processing.

Kálmán MAROSSY
Professor of Polymer engineering at institute of ceramic and polymer engineering, University of Miskolc, Hungary. Recent research interests: Polymer Blends, Multiphase polymer systems, Relaxation phenomenon, Polymer degradation, Composite materials, Rubber.

1. Introduction

It is widely thought that, "Rheology" as a science, only used for the applications of material science and engineering, but in fact it is widely applied in other scientific fields such as mathematics, physics, geology, chemistry, biology.., etc. [1-2]. In materials processing, the rheological properties have a considerable and important influence and through the stages of using material (rubber as example) for many industries, because of their impact on the development of the fabrication and stability to operate of the product and performance in the final form. Many scientific literatures were published about the effectiveness of fillers or working conditions and their relation to rheological properties of rubber [3-8]. Al-Maamori in his Ph.D thesis investigated the mechanical and rheological properties of rubber parts fabricated from NBR with silicon dioxide and rise husk powder additions [2]. Al-Maamori, Al-Mosawi and Abdulsada studied the effect of the novolac nanoparticle additives (0-40 wt.%) on viscosity, max torque, scorch time, and cure time of NBR/CR blends [9-10]. Al-Maamori and Al-Mosawi in a patent have been studied the mechanical and rheological properties of rubber parts with different amounts of cement and rise husk waste [11], Thomas et. al. investigated the effect of adding TiO_2, $Ca_3(PO_4)_2$ and layered silicate on the mechanical and rheological properties of the nitrile rubber, where, they indicated that particle geometry of additives have a clear effect on glass transition temperature values for the rubber blends [12].

2. Methodology

a. Materials: Acrylonitrile Butadiene Rubber (30% AN) and Chloroprene Rubber as a blend, silicon dioxide nanoparticles (10-150nm).

b. Mixing process and samples preparation: The two batches composition used in this article shown in *Table. 1*, and these two batches were prepared by roll milling process with Comerio Ercole Busto Arsizio roll mill machine. The samples were prepared as a disc shape with 6 mm in thickness and 40mm in diameter and 6mm in thickness by using hydraulic mould at 1.4 MPa pressure and temperature 150°C.

c. Calculating of rheological properties: Oscillating disc Rheometer (Rheometer ODR 2000E) was used calculating of rheological properties according to (ASTM D1646-68) standard and with operational conditions 0.35 MPa bar pressure and 185°C in 6 min [13].

d. Preparation of silicon dioxide and tests: The silica nanoparticles were prepared by precipitation method. Atomic force microscope (AFM) imaging was performed for checking the surface roughness and grains distribution (see *Fig. 1* and *Fig. 2*).

Compounding Ingredients	Parts per hundred rubber (pphr)
NBR/ CR	50/50
Silicon dioxide	0 and 50
Zinc oxide	3
Stearic acid	1
DOP	1
TMTD	1.5
6PPD	1.5
Sulfur	1.5

Table 1. Composition of batch
1. táblázat A keverék összetétele

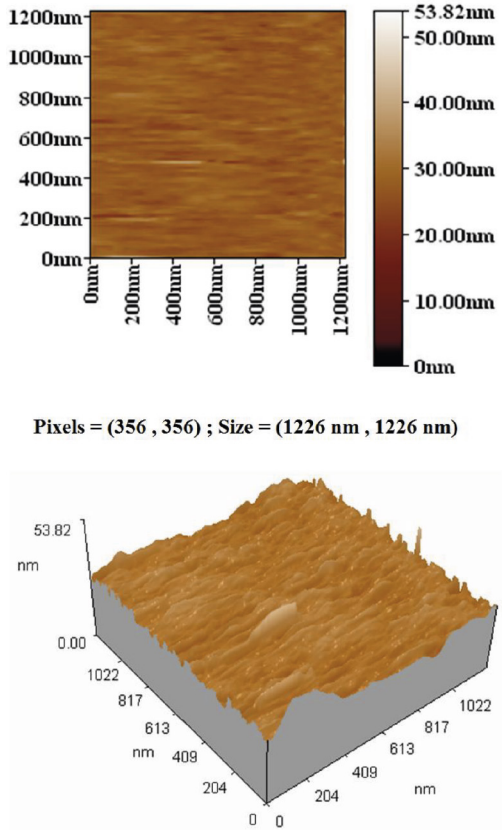

Fig. 1. AFM imaging analysis for silicon dioxide grains
1. ábra A szilícium-dioxid szemcsék AFM analízise

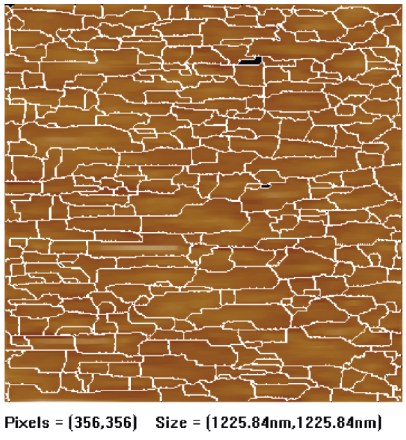

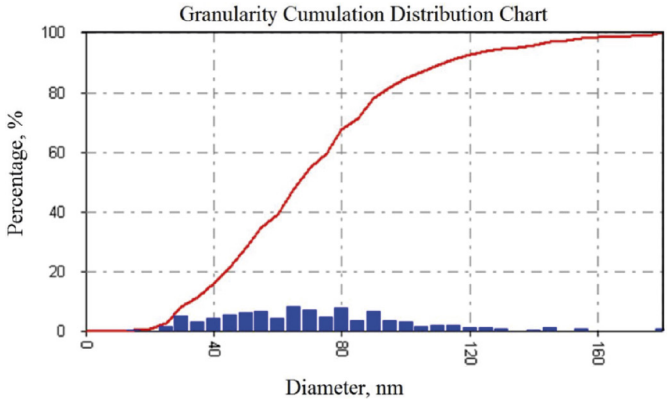

Fig. 2. Granularity cumulative distribution for silicon dioxide grains
2. ábra A szilícium-dioxid szemcsék kumulatív eloszlása

3. Resluts and discussion

Fig. 3 and *Fig. 4* represent the behavior of viscosity and max torque as a function of silicon dioxide grain size respectively. From these two figures we noted that viscosity and torque are increasing as silicon dioxide grain size increases, because the small grain size particles will diffuse more easily than large grain size particles through the chains of rubber, therefore the viscosity and torque will increase. On the other hand, the large grain size particles inhibit diffusion process and rubber chains movement. This means that the silicon dioxide is an active filler, no wonder the viscosity is about double with the same quantity as filler as rubber itself and triple with 100 pphr. The torque is more or less proportional to viscosity; therefore the torque increase can be taken as relative viscosity. The relative viscosity increase is higher than calculated from the Einstein's law ($\eta_{sp} = 2.5\Phi$, where Φ is the volume fraction of dispersed particles) therefore silicon dioxide has reinforcing effect.

The comparison between the results for fixed weight percent of silicon dioxide of various sizes shows that the higher grain size of silicon dioxide results in decreasing scorch and cure times as shown in *Fig. 5*. This is due to the grain size which resembles a measure for the specific surface area in contact with the rubber, where as this area decreased (i.e. more fine size contact area) results in decreasing in the physical bonds with the rubber chains and causes reduction in both scorch and cure times.

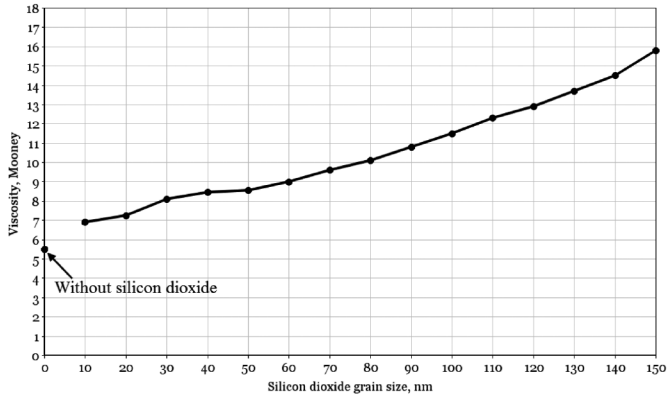

Fig. 3. Viscosity vs. silicon dioxide grain size
3. ábra Viszkozitás a szilícium-dioxid szemcseméret függvényében

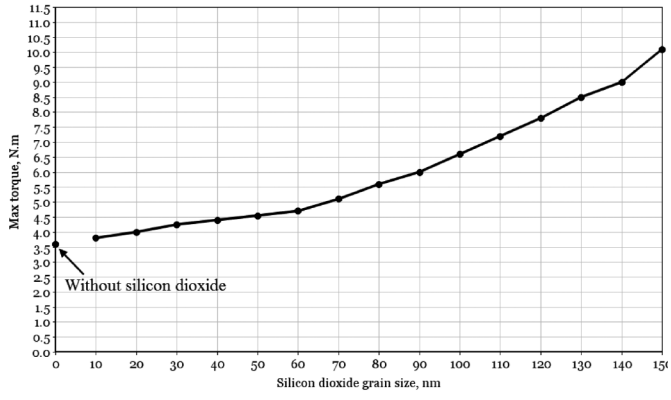

Fig. 4. Max torque vs. silicon dioxide grain size
4. ábra Maximális nyomaték a szilícium-dioxid szemcseméret függvényében

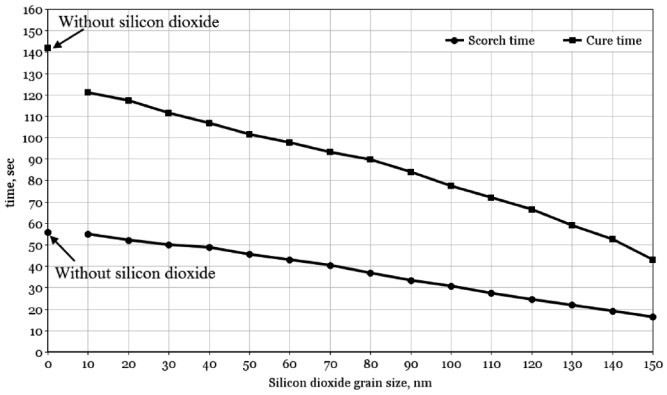

Fig. 5. Scorch and cure time vs. silicon dioxide grain size
5. ábra Scorch és keményedési idő a szilícium-dioxid szemcseméret függvényében

4. Conclusions

1. The practical results showed that silicon dioxide has an accelerating effect on the crosslinking reaction of rubber blends.
2. The crosslinking will increase due to the interaction between silicon dioxide and sulfur, where the scorch process is about 3.6 times faster and the difference is more than 40% if it is not present. Similarly, the cure time is also shorter about three times.
3. Increasing grain size of silicon dioxide particles resulted in higher viscosity and maximum torque.

References

[1] Gömze, L. A. (2015): Compilation of Scientific Papers I, GREX Engineering Service Ltd. publisher, Hungary. ISBN: 978-963-12-3088-8.

[2] Motiee, F. – Ganjali, S. T. – Malekzadeh, M. (2013): Investigation of correlation between rheological properties of rubber compounds based on natural rubber/styrene-butadiene rubber with their thermal behaviors, *International Journal of Industrial Chemistry*, Vol.4, issue.1, pp.1-8. https://doi.org/10.1186/2228-5547-4-16

[3] Al-Maamori, M. H.: Mechanical properties of polymeric composite materials, PhD thesis, UOT, IRAQ, 2006.

[4] Sreevalsa, S. – Sreekumar, S. – Sambhudevan, S. – Shankar, B. (2018): Cure characteristics and rheological properties of organically modified lanthanum oxide-natural rubber composites, *IOP Conf. Series: Materials Science and Engineering*, Vol. 360, 012037. https://doi.org/10.1088/1757-899X/360/1/012037

[5] Technical report (2016): Rheology and Viscosity, Malvern Panalytical Ltd.

[6] Shashok, Zh. S. – Prokopchuk, N. R. – Vishnevskii, K. V. – Krauklis, A. V. – Borisevich, K. O. – Borisevich, I. O. (2018): Rheological properties of rubber compounds with finely divided carbon additives, *Journal of Engineering Physics and Thermophysics*, Vol.91, issue.1, pp. 146-151. https://doi.org/10.1007/s10891-018-1728-9

[7] Linhares, F. N. – Gabriel, C. F. S. – de Sousa, A. M. F. – Nunes, R. C. R. (2018): Mechanical and rheological properties of nitrile rubber/fluoromica composites. *Applied Clay Science*, Vol.162, pp. 165-174. https://doi.org/10.1016/j.clay.2018.06.004

[8] Kim, J. – Oh, T. – Lee D. (2003): Morphology and rheological properties of nanocomposites based on nitrile rubber and organophilic layered silicates, *Polymer International*, Vol. 52, issue.7, pp.1203-1208. https://doi.org/10.1002/pi.1249

[9] Al-Maamori, M. H. – Al-Mosawi, A. I. – Abdulsada, S. A. (2016): Rheological behavior of Rubber Blends, I*nternational Journal of Engineering Technology*, Management and Applied Sciences, Vol. 4, issue. 11, pp:91-94.

[10] Al-Maamori, M. H. – Al-Mosawi, A. I. (2017): The impact of novolac wt.% nano additives on rheological properties of NBR/CR blends, *International Journal of Fracture and Damage Mechanics*, Vol. 3, issue. 1, pp. 19-23.

[11] Al-Maamori, M. H. – Al-Mosawi, A. I. (2014): Manufacturing of composite rubber material for the manufacturing of rubber rubbles and other reinforced by a brass Bushes used in mechanical and electrical couplings, Central Organization for Standardization and Quality Control (COSQC), International Classification (C08C19/42) , No.3913, Iraqi Classification (4) .

[12] Thomas, P. C. – Jose, E. T. – George, G. – Thomas, S. – Joseph K. (2014): Dynamic mechanical and rheological properties of nitrile rubber nanocomposites based on TiO_2, $Ca_3(PO_4)_2$ and layered silicate, *Journal of Composite Materials*, Vol. 48, issue.19, pp.2325-2339. https://doi.org/10.1177/0021998313498101

[13] ASTM D1646-17 (2017): Standard Test Methods for Rubber-Viscosity, Stress Relaxation, and Pre-Vulcanization Characteristics (Mooney Viscometer), ASTM International, West Conshohocken, PA. https://doi.org/10.1520/D1646-17

Ref.:
Al-Mosawi, Ali I. – **Al-Maamori**, Mohammed H. – **Marossy**, Kálmán: *Rheological properties of NBR/CR blends as a function of silicon dioxide grain size gradation*
Építőanyag – Journal of Silicate Based and Composite Materials, Vol. 71, No. 2 (2019), 43–45. p.
https://doi.org/10.14382/epitoanyag-jsbcm.2019.8

Technological parameters of ceramics creation on the basis of slavsonite

G. V. LISASCHUK ▪ National Technical University, Kharkiv Polytechnic Institute, Ukraine ▪ lisachuk @ kpi.kharkov
R. V. KRYVOBOK ▪ National Technical University, Kharkiv Polytechnic Institute, Ukraine ▪ krivobok491@gmail.com
A. V. ZAKHAROV ▪ National Technical University, Kharkiv Polytechnic Institute, Ukraine ▪ zakharovartem106@gmail.com
E. V. CHEFRANOV ▪ National Technical University, Kharkiv Polytechnic Institute, Ukraine ▪ eugene@chefranov.name
O. M. LAPUZINA ▪ National Technical University, Kharkiv Polytechnic Institute, Ukraine ▪ elapuzina@gmail.com
V. V. VOLOSHCHUK ▪ National Technical University, Kharkiv Polytechnic Institute, Ukraine ▪ valenty93vol@gmail.com
N. N. SAMOILENKO ▪ National Technical University, Kharkiv Polytechnic Institute, Ukraine ▪ samoilenko@kpi.kharkov.ua

Érkezett: 2018. 11. 27. ▪ Received: 27. 11. 2019. ▪ https://doi.org/10.14382/epitoanyag-jsbcm.2019.9

Abstract

The rationalization of technological parameters of products' manufacturing based on previously developed compositions of Slavsonite ceramics using a full-factor experiment of 2^3 type was studied. Equations of regression that describe adequately the dependencies of selected reviews (water absorption, dielectric permittivity, compressive strength) from grinding time and firing temperature were obtained. Based on the conducted research, a technological scheme for the manufacture of simple-shaped ceramic products that are capable of performing the functions of protective radio-transparent structural elements has been developed.

Keywords: slavsonite, radiotransparent ceramics, full-factor experiment, dielectric permittivity, dielectric loss tangent, water absorption, compressive strength, pressing pressure, grinding time, firing temperature

Kulcsszavak: szlavszonit, sugárzás áteresztő kerámiák,teljes faktorális kísérlet, dielektromos permittivitás, dielektromos veszteségi tangens, vízfelvétel, nyomószilárdság, préselési nyomás, csiszolási idő, égetési hőmérséklet

George Lisaschuk
Doctor of Sciences, full Professor. Specialist in material sciences of resource saving and energy-saving technologies, new structural ceramic materials and coatings. Head of Research department of NTU "KhPI".

Ruslan Krivobok
Ph.D, Senior researcher. Specialist in material sciences of new special-purpose ceramic materials and coatings. Deputy Head of Scientific and Research Part NTU "KhPI"

Artem Zakharov
Ph.D, NTU "KhPI". Fields of interests: development and physico-chemical properties of radiotransparent ceramic, functional materials.

Yevgen Chefranov
Ph.D. student, NTU "KhPI", Department of technology of ceramics, refractories, glass and enamels. Specializes in the study of radiotransparent ceramic materials.

Olena Lapuzina
Candidate of pedagogical sciences. Fields of interests: innovative teaching methods, distance learning; interdisciplinary coordination; theory and practice of teaching business ethics.

Voloshchuk Valentyna
Ph.D. student, NTU "KhPI", Department of technology of ceramics, refractories, glass and enamels. Specializes in the study of radiotransparent ceramic materials.

Nataliia Samoilenko
PhD, Professor, National Technical University "Kharkiv Polytechnic Institute", Professor of the department of chemical engineering and industrial ecology; Kharkov, Ukraine.

1. Introduction

The prospect of products' manufacturing based on Slavsonite (strontium aluminosilicate – $SrAl_2Si_2O_8$) is in the ability to combine a complex of dielectric and physical-mechanical characteristics of this material, such as radiotransparency, high strength, temperature resistance, and to have a low cost of raw materials. Slavsonite, besides the low dielectric permittivity value $\varepsilon \sim 6.2…6.8$, has the lowest dielectric loss $\tan\delta \sim 0.0001$ ... 0.0002 from among the crystalline phases, suitable for creating radioceramics [1].

Such materials are most often used when creating protection elements for aircraft antenna transmitters under high temperature and mechanical loads. For radiotransparent ceramic materials, low dielectric losses ($\tan\delta < 0.001$) and high stability of properties with temperature changes are typical. For example, the dielectric permittivity of sitalls does not change by more than ± 1%, and the tangent of dielectric loss increases by no more than ± 20% when the temperature changes from –60 ° to +1,200 °C [2].

The relevance of the study is creation of high-strength products of simple shape from the developed masses of radio transparent material based on the crystalline phase of Slavsonite.

2. Analysis of literature data and problem statement

The problem of creating densely sintered materials, firstly, lies in the difficulty of consolidating the dispersed powder after its synthesis. Scientists from many countries are involved in solving this problem, using various methods.

Researchers in the study [3] considered titanium oxide, zircon and glass as additives for sintering glass ceramics of cordierite composition. It is established that the minimum values of porosity (2-5%) are samples with the addition of glass, and its sufficient amount is 5 weight % (wt.%).

The author [4] obtained stoichiometric Slavsonite glass ceramics using cold isostatic pressing and sintering. In this case, the specific gravity of the material reached 94% and 97% of the theoretical.

The effect of various heat treatment modes on the sintering density of slavsonite glass ceramics is described in the study [5]. This work is relevant because the density of the material obtained becomes a critical factor in its application. For this study, the strontium aluminosilicate composition was used, which forms monoclinic Slavsonite as the primary crystalline phase already at a temperature of 1,200 °C.

In the study [6] the synthesis of Slavsonite by the sol-gel method and the preparation of high-density glass ceramics was carried out. The peaks of this crystalline phase begin to appear clearly on the radiograph of the synthesized material already at a temperature of 1,100 °C and at 1,250 °C the Slavsonite of the monoclinic syngony makes up 100% of the entire crystalline phase.

At the previous stages of research, the influence of the method of magnetic-pulse pressing (MPP) was studied [7]. The apparent density determined the effect of this method on the degree of sintering of the samples and the completion of the Slavsonite formation, and the amount of $SrAl_2Si_2O_8$ in the phase of the samples' composition annealed at a temperature of 1,250°, 1,350° and 1,450 °C, depending on the intensity of the impact action (number of cycles). According to research results, compared with the properties of the samples created by the method of static semi-dry pressing, it was found that the use of MPP significantly improves the characteristics of sintering the samples: the effect of 6 cycles of percussion and firing at a temperature of 1,250 °C is equivalent to a temperature rise on 120 °C. This method of formation on the processes of formation of the slavsonite phase at a given burning temperature is almost negligible: the increase of the Slavsonite amount using MPP does not exceed 2%.

It is important to note that the synthesis of Slavsonite takes place in the presence of a liquid phase in the above works. Liquid phase sintering is the most common process in ceramics technology, especially with the participation of aluminosilicates. The melt formed during ceramic firing plays the main role; it dissolves the raw materials and is the source of the new crystalline phase. Therefore, it is possible to control the synthesis process by changing the characteristics of the melt (viscosity, surface tension, activity).

In the study [8] the effect of additives of B_2O_3 and P_2O_5, which are glass-forming oxides was studied, but in this case they also played the role of mineralizers, reducing the temperature of crystallization to the beginning of Slavsonite 1,020 °C.

In the study [4] the preparation of high-strength ceramic materials with low values of dielectric properties is described. Moreover, it is said that the additives B_2O_3, LiF, Cr_2O_3, and $ZrSiO_3$ contribute to the transition of Slavsonite from the hexagonal form to the stable monoclinic form. This is due to the cracking of the ceramic body, possible at the stage of cooling during the polymorphic transformation of the hexagonal form, which takes place with an increase in volume on 3%.

Analyzing the methods of obtaining materials on the basis of Slavsonite are considered, it has been found that in most cases they are obtained by glass-ceramic technology, which requires additional energy costs for the transition of the hexagonal form of Slavsonite to the monoclinic form. In previous studies in studies [1, 9] the compositions of Slavsonite ceramics were developed, corresponding to the specified indicators of properties. Thus, in further studies it is advisable to carry out the selection of the optimal method of slavsonite powder consolidating to create products of simple form.

3. The purpose and objectives of the study

The aim of the study was the development of technological parameters for obtaining simple-shaped products from the developed masses of densely sintered, radio-transparent material with high mechanical properties with two-stage ceramic technology based on the crystalline phase of Slavsonite.

To achieve the goal, the following tasks were set:

- to choose the optimal binder and its amount from among the solutions of dextrin and methylcellulose;
- to investigate the influence of the grinding mode of the synthesized material, the pressing pressure and the firing temperature on the studied properties;
- to develop a technological scheme for the manufacture of simple-shaped products from the developed ceramic radio transparent materials on the basis of the conducted complex of studies.

4. Materials and research methods

Selection of the binder material was carried out by a separate experiment, while other parameters were made in a fully factorial experiment. The pre-synthesized ceramic material based on the crystalline phase of Slavsonite was ground in a planetary mill at 400 revolutions per minute with a grinding time of 15 minutes. For the study, dextrin and methylcellulose were selected as a binder in an amount from 1 to 3 wt. % with pace of 0.5% for dextrin and in an amount from 2 to 4 wt. % with pace of 0.5% for methylcellulose. The amount of binder was injected with more than 100 wt. % of the mixture pre-dissolved and aged for 24 hours in water in an amount equal to 8% of the humidity of the press powder. Samples were formed in the form of cylinders with a diameter and height of 25 mm, at a pressing pressure of 30 MPa with the previous pseudo-granulation at a pressure of 50 MPa. Samples were kept for 24 hours at room temperature, after which part of the series was dried to a moisture content of not more than 0.5% and burned at a temperature of 1,300 °C, and another part of the series was used to determine the strength of the raw material. Determination of strength was performed by the method of compression and the effect of the binder and its amount on the degree of water absorption was determined on the scorched samples. The results of both studies are shown in Table 1.

Properties	Binder additive and its content, wt.%									
	Dextrin					Methylcellulose				
	1	1.5	2	2.5	3	2	2.5	3	3.5	4
Compressive strength of raw material, MPa	0.31	0.54	0.76	0.97	1.09	0.92	1.75	2.05	2.18	2.33
Water absorption,%	0.14	0.29	0.33	0.58	0.75	0.19	0.27	0.31	0.57	0.9

Table 1 Results of the study of the effect of the binder
1. táblázat A kötőanyag hatása az eredményekre

The data obtained indicate that the optimal binder is methylcellulose in an amount of 3 wt.%, since an increase in its amount with an increase in strength will lead to an increase in the value of water absorption by more than 0.5%.

Experiment Planning

For carrying out an experiment of establishing the best technological parameters, a full-factor experiment of type 2^3 was used, in which factors were grinding time, pressing pressure and heat treatment temperature.

To clarify the experiment, it was decided that a point with the following zero values of the factors should be chosen as the center of the plan: grinding time is 15 minutes; pressing pressure is 30 MPa; firing temperature is 1,325 °C. The interval of the grinding time varying is 5 minutes, the pressing pressure is 10 MPa, and the firing temperature is 25 °C. *Figure 1* illustrates the arrangement of experiments of type 2^3 in three-dimensional space.

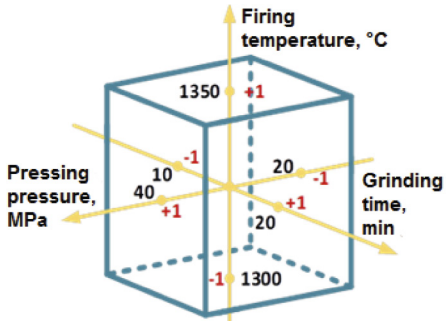

Fig. 1 The arrangement of experiments of type 2^3 in three-dimensional space
1. ábra 23 háromfaktoros teljes faktorális kísérleti tervelrendezés három dimenziós térben ábrázolva

In accordance with the developed natural plan of the experiment (*Table 2*), samples by the classical technology were obtained. The grinding of the synthesized mass was carried out in a planetary mill to a residue on sieve №0063 not more than 1.5%, it was thoroughly mixed with a binder solution, and the humidity of the press powder was 8%.

Composition cipher	Cipher sample in the series	Factors in natural form		
		Grinding time x, min	Pressing pressure y, MPa	Firing temperature z, °C
Composition «0»	0-8	20	40	1,350
	0-7	10	40	1,350
	0-6	20	20	1,350
	0-5	10	20	1,350
	0-4	20	40	1,300
	0-3	10	40	1,300
	0-2	20	20	1,300
	0-1	10	20	1,300
	0-9	15	30	1,325
Composition «2»	2-8	20	40	1,350
	2-7	10	40	1,350
	2-6	20	20	1,350
	2-5	10	20	1,350
	2-4	20	40	1,300
	2-3	10	40	1,300
	2-2	20	20	1,300
	2-1	10	20	1,300
	2-9	15	30	1,325

Table 2 Plan of the experiment in its natural form
2. táblázat A kísérleti terv eredeti formájában

The formation of semi-finished products took place in two stages, the first was granulation, formation of briquettes at a pressure of 50 MPa, followed by "wiping" through a sieve № 05; the second stage included pressing of the specified samples at a pressure of 20, 30 and 40 MPa. The next steps were drying in a drying oven and firing at a temperature of 1,300°, 1,325° and 1350° C with an exposure of one hour at the maximum temperature. The plan-matrix with natural values of factors according to the selected interval of variation is shown in Table 2.

5. The research results of indicators of obtained ceramic samples

During the experiment, the main technological properties of radiotransparent ceramics, such as water absorption, dielectric permittivity and flexural strength were determined (Table 3).The obtained results were processed with the Excel software application. For each experiment series, adequate third order equations that characterize the dependencies were obtained:

"grinding time – pressing pressure – firing temperature – water absorption",

"grinding time – pressing pressure – firing temperature – dielectric permittivity",

"grinding time – pressing pressure – firing temperature – flexural strength".

Dependencies with coded factors for different series are:

for a series of composition "0":

$$W, \% = 0.579 - 0.155 \cdot x - 0.263 \cdot y - 0.119 \cdot z + 0.063 \cdot y \cdot z - 0.019 \cdot x \cdot y \cdot z \quad (1)$$

$$\varepsilon = 6.565 + 0.081 \cdot x + 0.059 \cdot y + 0.158 \cdot z + 0.032 \cdot x \cdot y + 0.023 \cdot y \cdot z \quad (2)$$

$$\sigma_{fl}, \text{ MPa} = 48.69 + 6.233 \cdot x + 3.612 \cdot y + 9.841 \cdot z + 2.019 \cdot x \cdot y + 0.983 \cdot x \cdot z + 0.809 \cdot y \cdot z + 0.12 \cdot x \cdot y \cdot z \quad (3)$$

for a series of composition "2":

$$W, \% = 0.079 - 0.022 \cdot x - 0.066 \cdot y - 0.007 \cdot z + 0.01 \cdot x \cdot y + 0.01 \cdot x \cdot z \quad (4)$$

$$\varepsilon = 6.327 + 0.053 \cdot x + 0.045 \cdot y + 0.027 \cdot z + 0.029 \cdot x \cdot z + 0.021 \cdot y \cdot z + 0.029 \cdot x \cdot y \cdot z \quad (5)$$

$$\sigma_{fl}, \text{ MPa} = 50.875 + 5.371 \cdot x + 1.524 \cdot y + 0.798 \cdot z + 1.977 \cdot x \cdot y + 0.703 \cdot x \cdot z - 0.348 \cdot y \cdot z + 1.499 \cdot x \cdot y \cdot z \quad (6)$$

For equations 1 – 6:

$$x = \frac{\tau \text{ (Grinding time, min.)} - 15}{5}$$

$$y = \frac{\text{P (Pressing pressure, MPa)} - 30}{10}$$

$$z = \frac{t \text{ (Firing temperature, °C)} - 1{,}325}{25}$$

The analysis of the obtained regression equations for the two compositions allows us to estimate the influence of the technological parameters of obtaining the sintered material with high strength characteristics. Thus, the influence of factors on water absorption for both compositions is similar: an increase in the grinding time increases the water absorption

values, and the pressing pressure and the firing temperature decrease the water absorption values. Negative coefficients with factors for indicators of the dielectric permittivity of both compositions are observed. This indicates that with increasing the values of the studied parameters, the dielectric permittivity will also increase, which is most likely, caused from the glass phase increasing. Moreover, it should be noted the different importance of the parameters when affecting the dielectric constant: for the composition "0" the more important parameter is the sintering temperature, whereas for the composition "2" the more important parameter is the grinding time. For clarity, the diagram (Fig. 2) shows the significance of the influence of parameters on the studied properties. The effect of factors on the bending strength indices for both compositions is completely different. Only the effect of grinding time increasing is common, which is expressed as a strength decreasing. The increasing of pressing pressure and the firing temperature have a positive effect on the strength for the composition "0", whereas increasing of these factors reduce the strength characteristics for the composition "2".

From the diagram in Figure 2, it can be seen that the significance of factors is more different for individual properties as compared with significance for research compositions. Water absorption for both compositions is most influenced by pressing pressure. Whereas, the dielectric permittivity and strength characteristics of the composition "2" are influenced more by the grinding time, at the same time the dielectric permittivity and strength characteristics of the composition "0" are influenced more by the firing temperature. This fact can be explained by a large amount of glass phase in the synthesized material, which contributes to a more dispersed powder during the same grinding time.

Composition cipher	Cipher sample in the series	Sample Properties		
		Water absorption W, %	Dielectric permittivity, ε	Bending Power Limit, σ МПа
Composition «0»	0-8	0.08	6.89	72.3
	0-7	0.44	6.72	53.6
	0-6	0.53	6.69	59.2
	0-5	0.79	6.59	49.0
	0-4	0.23	6.58	48.8
	0-3	0.51	6.30	34.5
	0-2	0.86	6.42	39.4
	0-1	1.19	6.32	32.7
	0-9	0.57	6.34	47.1
Composition «2»	2-8	0	6.52	62.4
	2-7	0	6.32	48.3
	2-6	0.12	6.31	53.1
	2-5	0.17	6.27	47.9
	2-4	0	6.35	57.1
	2-3	0.05	6.30	46.8
	2-2	0.11	6.34	52.4
	2-1	0.19	6.21	44.0
	2-9	0.06	6.22	49.5

Table 3 Properties of the experimental compositions
3. táblázat A kísérleti összetételek tulajdonságai

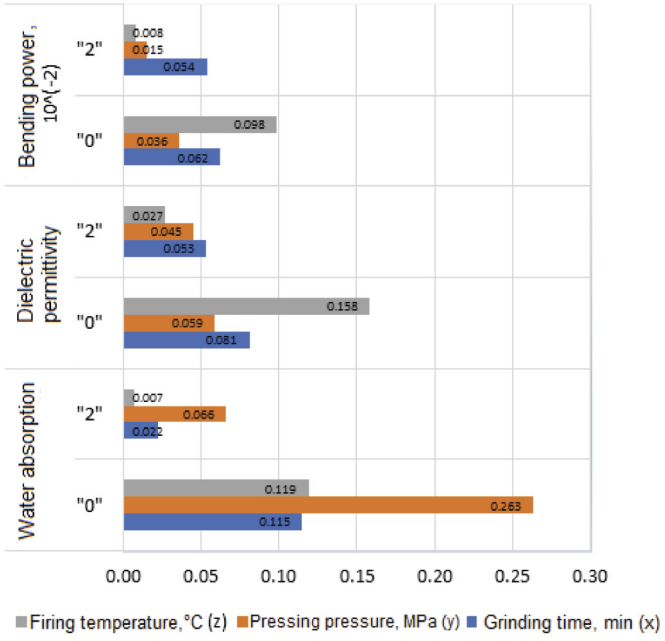

Fig. 2 Comparative chart of the coefficients for individual factors in the "technological parameters – properties" equation
2. ábra Összehasonlító diagram a technológiai paraméterek – tulajdonságok egyenletében található egyes tényezők együtthatóiról

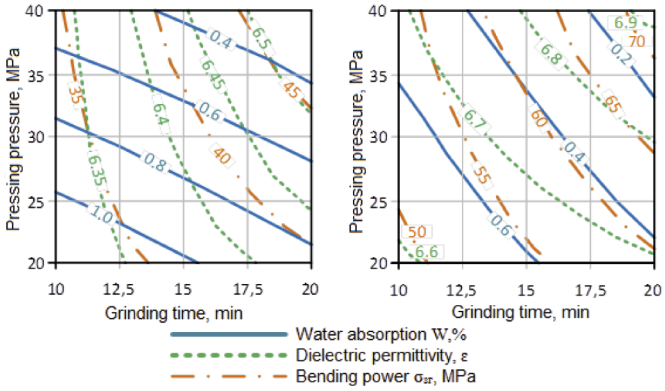

Fig. 3 Dependence of water absorption, dielectric constant and power limits for bending samples of the composition "0", scorched at temperatures 1,300 and 1,350 °C from technological parameters
3. ábra 1300 és 1350 °C-on égetett "0"-s összetételű hajlító minták függősége a vízfelvételtől, dielektromos állandótól és teljesítménylimitektől

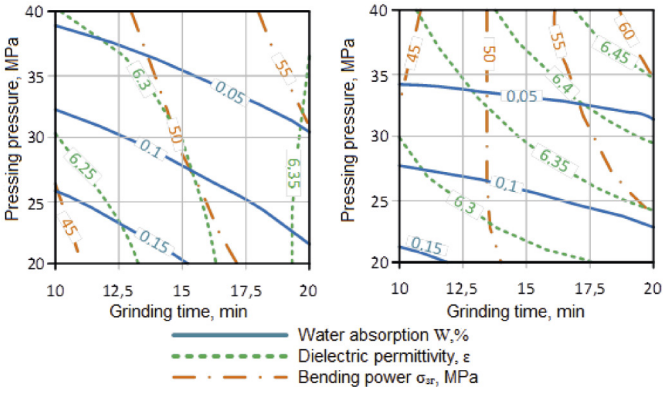

Fig. 4 Dependence of water absorption, dielectric permittivity and tensile strength in bending of samples of the composition "2" scorched at temperatures 1,300° and 1,350 °C from technological parameters
4. ábra 1300 és 1350 °C-on égetett "2"-s összetételű hajlító minták függősége a vízfelvételtől, dielektromos állandótól és teljesítménylimitektől

The use of the obtained models allows predicting the indicators of water absorption, dielectric permittivity and strength of materials with sufficient accuracy that will be manufactured using the selected compositions and according to the specified technological parameters.

For graphical interpretation of the obtained data, the diagrams with lines of equal values for water absorption, dielectric permittivity and bending strength were constructed for extreme values of the firing temperature factor. Excel software was used for this purpose (Fig. 3 and 4).

The results of the experiment showed that within the selected interval of variation of technological parameters, an increasing of the duration of synthesis products grinding, pressure of semi-dry pressing and firing temperature of products the water absorption is decreasing, the flexural strength is increasing, when storing dielectric permittivity values within 6.25 ... 6.9. This effect is caused by the amount of melt that compacts the material increasing. The influence of individual parameters on the properties of samples of ceramics of the composition "2" is more pronounced: strength indicators are more influenced by grinding time, and water absorption is more influenced by pressing pressure; it is especially clearly observed with the firing temperature increasing to 1,350 °C.

Based on the conducted research, a technological scheme for the simple-shaped products manufacturing from developed ceramic radiotransparent materials has been developed (Fig. 5).

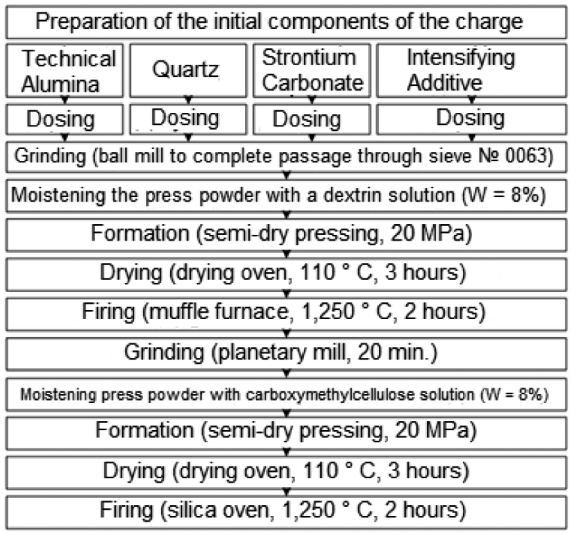

Fig. 5 The developed technological scheme for the radiotransparent ceramics creation
5. ábra A sugárzás áteresztő kerámiák készítésére kidolgozott technológiai eljárást bemutató folyamat ábra

6. The discussion of the results

According to the results of comprehensive studies, the following technological parameters of production are recommended: slavsonite firing at the stage of synthesis at a temperature of 1,250 °C with an hour-long exposure; fusion products grinding for 20 minutes in a planetary mill to get particle sizes of not more than 0.15 mm; moisturizing with 4% solution of methylcellulose to become 8% the powder moisture; forming of semi-finished by semi-dry pressing at a pressure of 40 MPa; products' firing at a temperature of 1,350 °C with an hour-long exposure.

The properties of the developed compositions of radiotransparent ceramics that meet the requirements for radiotransparent materials and the characteristics of GOST 20419-83 [10] for a similar material from celsian are shown in Table 4. For the mass on the basis of the composition "0" with the addition of 1 wt. % Li_2O : SnO_2 the marking HRC-0 was made, and for the mass based on the composition "2" with the addition of 1 wt. % Li_2O the markings HRC-2 was made (HRC – high-temperature radiotransparent ceramics).

Properties	HRC-0	HRC-2	GOST 20419-83 (subgroup 420 celsian)	Require-ments for RTC
Apparent density, kg / m³	2,960	2,880	Not less than 2,700	Not less than 2,500
Water absorption, %	0.08	0.13	0.5	Less than 0.1
Dielectric permittivity at 1 kHz	6.42	6.07	–	Less than 10
Tangent of dielectric loss angle at 1 kHz	0.017	0.012	Less than 10^{-2}	10^{-4} – 10^{-2}
Specific volume resistance, Ohm · cm	$5.9 \cdot 10^{14}$	$3.2 \cdot 10^{14}$	10^{14}	–
Bending power, MPa	72.3	62.4	80	60
Operating temperature, °C	1,500	1,300	–	1,200

Table 4 Properties of the optimal compositions of radiotransparent ceramics
4. táblázat Az optimális sugárzás áteresztő kerámia összetétel tulajdonságai

7. Conclusions

Compositions of raw materials and technological principles of the ceramic radiotransparent materials manufacturing from them have been developed. According to the results of comprehensive studies, the following technological parameters of production are recommended: Slavsonite firing at the stage of it synthesis at a temperature of 1,250 °C with an hour-long exposure; fusion products grinding in a planetary mill for 20 minutes to get particle sizes of not more than 0.15 mm; moisturizing with 4% solution of methylcellulose to become 8% the powder moisture; forming of semi-finished by semi-dry pressing at a pressure of 40 MPa; products' firing at a temperature of 1,350 °C with delay with an hour-long exposure.

The developed materials are characterized by the following properties:

- **the HRC-2 composition:** dielectric permittivity is ε = 3.67 ... 4.12 and the dielectric loss tangent is tanδ = 0.0073 ... 0.0091 (at 26 – 37.5 GHz) water absorption is 0.13%; apparent density is 2,880 kg/m³; flexural strength is 62.4 MPa; volume resistance is $1.1 \cdot 10^{13}$ Ohm · cm); maximum temperature of operation is 1,200 °C;
- **the HRC-0 composition:** dielectric permittivity is ε = 4.93 ... 5.26; the dielectric loss tangent is tanδ = 0.0097 ... 0.0122 (at 26 – 37.5 GHz) water absorption is 0.08%;

apparent density is 2,960 kg/m^3; flexural strength is 72.3 MPa; volume resistance is $5.9 \cdot 10^{14}$ Ohm · cm; maximum operating temperature is 1,500 °C.

The resulting materials comply with the requirements of GOST 20419-83 for products made of Celsian ceramics (class 420) and meet the requirements for radiotransparent materials.

References

[1] Lisachuk, G. – Kryvobok, R. – Zakharov, A., et al. (2017): Influence of complex activators of sintering on creating radiotransparent ceramics in SrO – Al_2O_3 – SiO_2. *Eastern-European Journal of Eenterprise Technologies*, Vol. 1, № 6 (85), pp 10–15. https://doi.org/10.15587/1729-4061.2017.91110

[2] Romashin, A.G. – Gajdachuk, V.E. – Karpov, Ya.S. – Rusin, M.Yu. (2003) Radioprozrachnye obtekateli letatel'nyh apparatov. Proektirovanie, konstrukcionnye materialy, tekhnologiya proizvodstva, ispytaniya. ucheb. posobie, Nac. aehrokosm. un-t «Khar'k. aviac. in-t», Khar'kov. – 239 p.

[3] Goleus, V. I. – Karasik, O. V. – Homenko, O. S. (2017): Rozrobka sklokeramiki kordieritovogo skladu, *Recent Studies of Applied Sciences*, № 2, pp. 1–4.f3

[4] Bansal, N. P. – Drummond, C. H. (1993): Kinetics of hexacelsian to celsian phase transformation in $SrAl_2Si_2O_8$. *Journal of the American Ceramic Society*, Vol. 76, № 5, pp. 1321–1324. https://doi.org/10.1111/j.1151-2916.1993.tb03758.x

[5] Sung, Y.M. – Kwak, W.C. (2002) Influence of various heating procedures on the sintered density of Sr-celsian glass-ceramic. *Journal of Materials Science Letters*, 21, №11, pp. 841–843. https://doi.org/10.1023/A:1015710309425

[6] Uvarova, N.E. – Orlova, L.A. – Popovich, N.V. (2008) Nizkotemperaturnyj sintez besshchelochnoj alyumosilikatnoj steklokeramiki. *Uspekhi v himii i himicheskoj tekhnologii*, Vol. 22, № 7(87), pp. 59–62.

[7] Shchukina, L.P. – Bolyuh, V.F. – Ligezin, S.L., ta in. (2018) Vpliv metodu konsolidaciï poroshkiv na fazoutvorennya tekhnichnoï keramiki, *Integrovani tekhnologiï ta energozberezhennya*. № 3, pp. 3–7.

[8] Shchegoleva, N.E. – Grashchenkov, D.V. – Sarkisov, P.D. i dr. (2012) Vliyanie dobavok V_2O_3 i R_2O_3 na kristallizacionnuyu sposobnost' stroncijalyumosilikatnogo stekla, *Tekhnika i tekhnologiya silikatov*. Vol. 19, № 2, pp. 7–14.

[9] Lisachuk, G.V. – Krivobok, R.V. – Zaharov, A.V. i dr. (2015) Intensifikaciya processa spekaniya Sr-keramiki putem vvedeniya mineralizatorov spekaniya, *Kosmicheskaya tekhnika. Raketnoe vooruzhenie*. № 3, pp. 74–78.

[10] Materialy keramicheskie elektrotehnicheskie. Klassifikatsiya i tehnicheskie trebovaniya: GOST 20419-83. – [Deystvuet s 1985-01-01]. – M. : Mezhgosudarstvennyiy sovet po standartizatsii, metrologii i sertifikatsii, 1985. – 9 s.

Ref.:

Lisaschuk, G. V. – **Kryvobok**, R. V. – **Zakharov**, A. V. – **Chefranov**, E. V. – **Lapuzina**, O. M. – **Voloshchuk**, V. V. – **Samoilenko**, N . N.: *Technological parameters of ceramics creation on the basis of slavsonite*

Építőanyag – Journal of Silicate Based and Composite Materials, Vol. 71, No. 2 (2019), 46–51. p.

https://doi.org/10.14382/epitoanyag-jsbcm.2019.9

Electrochemical characterization of micro- and nano-particles of ceftriaxone in human blood serum samples using cyclic voltammetry

Muhammed Mizher RADHI ▪ Radiological Techniques Department, Health and Medical Technology College-Baghdad, Iraq ▪ mmradhi@yahoo.com
Intesar Nadhum KHELKAL ▪ Biology Department, Science College, Mustansiriah University
Eman Natiq NAJI ▪ Biology Department, Science College, Mustansiriah University
Alaa Laebi ABDULLAH ▪ Biology Department, Science College, Mustansiriah University

Érkezett: 2019. 02. 02. ▪ Received: 02. 02. 2019. ▪ https://doi.org/10.14382/epitoanyag-jsbcm.2019.10

Abstract

The present study has selected one important antibiotic compound in a microcrystalline of ceftriaxone (CRX) and then it was converted into nano-particles (NPs) by lyophilization (freeze-drying method). The CRX NPs was characterized by electrochemical analysis using cyclic voltammetric method by glassy carbon electrode (GCE) in human blood serum medium. It was found that CRX has oxidation-reduction current peaks at 0.9 and -0.75 V respectively, while the cyclic voltammogram of CRX NPs was illustrated the reduction current peak at -0.75 V and the oxidation peak cannot be seen, so this phenomena explains that CRX NPs act as antioxidant antibiotic in serum medium. Also, the study included the electrochemical behavior of nano antibiotic CRX NPs in different pH and concentration. Scanning electron microscopy (SEM) and atomic force microscopy (AFM) was applied.

Keywords: ceftriaxone, cyclic voltammetry, antibiotic nano-particles, serum medium
Kulcsszavak: ceftriaxon, ciklikus voltammetria, antibiotikum nano-részecskék, vérsavó közeg

Muhammed Mizher RADHI
Professor, Department of Radiological Techniques, Health and Medical Technology College-Baghdad, Middle Technical University, Baghdad, Iraq. Received his PhD from University Putra of Malaysia (UPM) in 2010 in Electrochemistry, Nanotechnology. Research topics: conductivity of grafted polymer with nano-deposit and fabrication of sensors by nanomaterials to study drugs in blood medium by electrochemical analysis.

Intesar N. KHELKAL
Professor in the Department of Biology and Microbiology, Mustansiriah University, College of Science. Received her Bachelor's degree in science at Baghdad University, College of Science, Department of Biology (1991). Received her MSc and PhD degrees in Microbiology at Mustansiriah University (1998, 2004). Her study focused on pathogenic bacteria, Physiology and taxonomy. Currently she is a lecturer in Biology department, College of Science, Mustansiriah University, Iraq, Baghdad.

Eman Natiq NAJI
Professor in the Department of Biology and Microbiology, Mustansiriah University, College of Science. Received her Bachelor's degree in science at Baghdad University, College of Science, Department of Biology (1994). Received her MSc and PhD degrees in Microbiology at Mustansiriah University (1998, 2004). Her study focused on pathogenic bacteria and viruses, diagnostic microbiology and laboratory techniques. Currently she is a lecturer in Biology department, College of Science, Mustansiriah University, Iraq, Baghdad.

Alaa Laebi ABDULLAH
Received her Bachelor's degree in science at Baghdad University, College of Science, Department of Biology (2009). Received his MSc degree in Microbiology at Mustansiriah University (2015). Currently he is PhD student in Mustansiriah University, College of Science, Department of Microbiology.

1. Introduction

Currently scientists have been studied the redox process of nano antibiotics to find the mechanism of oxidative effect in whole blood or serum media of in vitro study [1-6].

Ceftriaxone, sold under the trade name Rocephin, is an antibiotic useful for the treatment of a number of bacterial infections. Ceftriaxone is commercially available as a white to yellowish-orange crystalline powder for reconstitution, the structure of ceftriaxone is shown in *Fig. 1* [7].

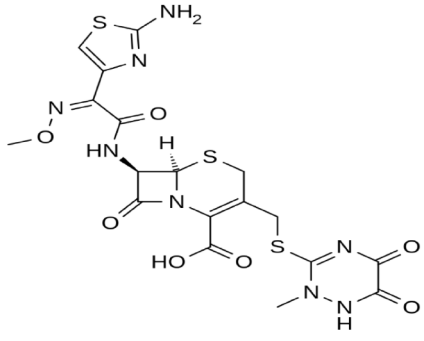

Fig. 1. Chemical structure of ceftriaxone micro-particles
1. ábra Ceftriaxone mikro-részecskék kémiai szerkezete

Electrochemical studies have been carried out on ceftriaxone by glassy carbon (GC-CNT) electrode modified with carbon-nanotube in a phosphate buffer solution, pH = 7.40. Cyclic voltammetric technique was indicated that the oxidation process is irreversible and diffusion-controlled. The number of electrons exchanged in ceftriaxone is oxidized via a one-electron step of oxidation process. Diffusion coefficient of ceftriaxone was found to be 2.74×10^{-6} cm^2 s^{-1}. Ceftriaxone has a detection limit of 4.03×10^{-6} M in the study [8].

Electrochemical sensor based on the use of Nafion/MWCNT modified screen-printed carbon electrodes (SPCEs) was used to study this antimycobacterial drug in human urine and human blood serum samples. Nafion/MWCNT-SPCEs provided excellent biocompatibility, good electrical conductivity, low electrochemical interferences and a high signal-to-noise ratio, providing excellent performance towards ETB quantification in microvolumes of human urine and human blood serum samples [9].

Cyclic voltammetric technique was used to determine ceftizoxime by a modified glassy carbon electrode with a film of nano-diamond/graphite nano-mixture decorated with Ag nano-particles (AgNPs/NDG/GCE). The prepared modified

electrode has good electrochemical properties such as simple preparation, high sensitivity, excellent repeatability and reproducibility and long-term stability [10].

Ceftizoxime (CFX) is used to reduce the infection caused by both gram-negative and gram-positive bacteria. The study included silver and gold nano-particles (Ag/AuNPs) on 5-(5-bromo-2-hydroxybenzylidenamino)-2 mercapto-benzimidazole and GCE was used to determine the electrochemical properties of CFX with good results of the detection limit which was calculated to be 2.0 × 10 − 12 M. Also, the experimental variables such as deposited amount of the modifier suspension, pH of the supporting electrolyte and accumulation potential and time were optimized [11, 12].

In this study, the electrochemical analysis was included cyclic voltammetric technique to determine the chemical properties of ceftriaxone at micro- and nano-particles in blood serum medium.

2. Experimental

2.1. Preparation of ceftriaxone nanoparticles

Lyophilization (freezing method) was used to prepare ceftriaxone nano-particles by dissolving 0.75 g of ceftriaxone micro particles in 150 ml of distilled water. The ceftriaxone suspension was cooled and the ice crystals of pure water formed at -18 °C. The second step involved blending the ice from the frozen product by passing thermal air from the lyophilization tool rack to the frozen solution in the flask, and leaking the flying ice and water vapor through the dried part of the product to the surface of the material. Water vapor is transported from the product surface through the chamber to the condenser, and the water vapor condenses on the condenser. At the end of the sublimation step a porous dam is formed. Its pores correspond to the areas occupied by ice crystals. The third step is drying that involves removing the absorbed water from the product. All steps must be continuous for about 48-72 hours [13].

2.2. Materials

Ceftriaxone compound in the form of yellowish powder was bought from HANGZHU Ruijiang Chemical (China) and blood samples were extracted from healthy humans which received from the center medicine of Baghdad City was used in the analysis after separation of the serum from the whole blood by electric centrifuge type 8-1 (3000 cycles/min) . Deionized water was used for the preparation of aqueous solutions. All the serum of blood samples were diluted with deionized water by a ratio of 1:9 mL (serum: deionized water), 10 mL of diluted serum was replaced in the cyclic voltammetric cell.

2.3. Apparatus

2.3.1. Cyclic voltammetric technique

Instrument series EZstat (Potentiostat / Glvanostat) from NuVant Systems Company (USA) was used. The electrochemical analytical cell was connected with the potentio-stat device and monitored through a program that was installed on the PC to conduct periodic voltammetry (CV). Silver electrode contains silver/silver chloride (Ag/AgCl in 3 M KCl) and platinum wire (diameter 1 mm) was used as reference and counter electrodes respectively. The glass working carbon electrode (GCE) was used in this study after cleaning by polishing with an alumina solution and treated with ultrasonic water path for ten minutes for measurement performance.

2.3.2. Lyophilization instrument

Lyophilization instrument from LABCONCO Company (USA) was used for the preparation of ceftriaxone nano-particles from micro-particles by deep freezing technique as shown in *Fig. 2*.

Fig. 2. Lyophilization instrument, LABCONCO Company (USA)
2. ábra Liofilizáló készülék LABCONCO Company (USA)

2.4. Scanning Electron Microscopy (SEM)

Fig. 3 shows the Scanning Electron Microscopy of the prepared ceftriaxone nano-particles which illustrates the morphology details of the nano-particles as spherical forms with diameter range of 20-38 nm.

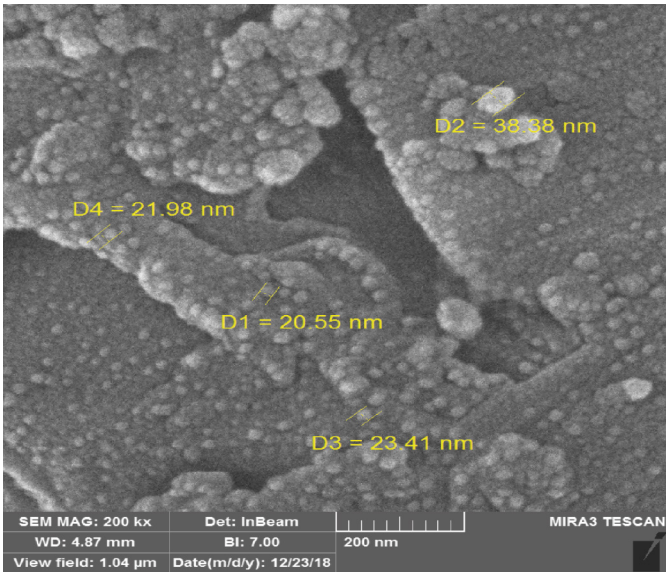

Fig. 3. SEM of the ceftriaxone nano-particles
3. ábra Ceftriaxon nano-részecskék pásztázó elektronmikroszkópos felvétele

2.5. Atomic Force Microscopy (AFM)

Atomic Force Microscopy technique was used to identify the diameter of the nano-particles. The diameter of the prepared ceftriaxone nano-particles was found as average diameter of 115 nm, shown in *Figs. 4* and *5* together with *Table 1*.

Diameter (nm)<	Volume (%)	Cumulation (%)	Diameter (nm)<	Volume (%)	Cumulation (%)	Diameter (nm)<	Volume (%)	Cumulation (%)
60.00	0.32	0.32	100.00	9.39	23.30	140.00	17.80	87.38
70.00	1.62	1.94	110.00	13.92	37.22	150.00	12.62	100.00
80.00	5.50	7.44	120.00	15.86	53.07			
90.00	6.47	13.92	130.00	16.50	69.58			

Table 1. Diameter (nm) of the prepared ceftriaxone nano-particles
1. táblázat Ceftriaxon nano-részecskék átmérője (nm)

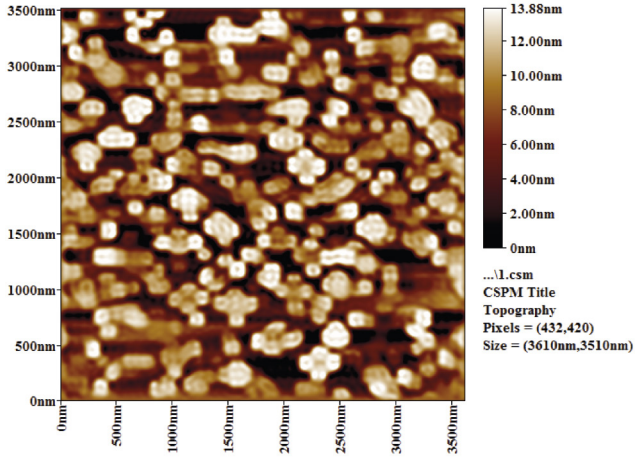

Fig. 4. AFM of the ceftriaxone nano-particles
4. ábra Ceftriaxon nano-részecskék AFM felvétele

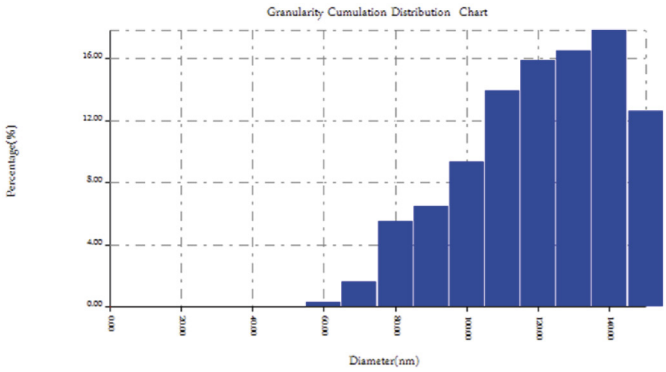

Fig. 5. Cumulative distribution diagram of ceftriaxone nano-particles diameter
5. ábra Ceftriaxon nano-részecskék átmérőjének kumulatív eloszlása

3. Results and discussion

3.1. Effect ceftriaxone micro- and nano-particles on blood serum components

The comparison study between the micro- and nano-particles of ceftriaxone was characterized in blood serum medium by cyclic voltammetric technique at GCE as working electrode and Ag/AgCl as reference electrode. *Fig. 6* illustrates the oxidation current peak of ceftriaxone micro-particles at 1.0 V potential which disappeared in nano-particles form of the compound. But, the reduction current peak of ceftriaxone in both micro- and nano-particles was still present without any change in the blood serum medium. So, the ceftriaxone nanoparticles act as antioxidant reagent in blood serum medium. It can be used as antibiotic for different bacterial diseases without any side effects in the human body [14].

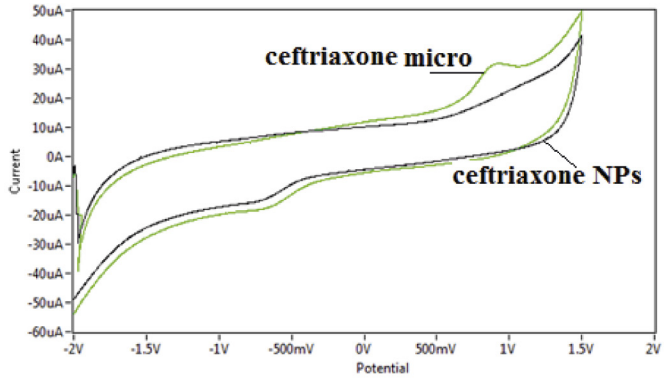

Fig. 6. Cyclic voltammogram of ceftriaxone micro- and nano-particles in blood serum medium at GCE as working electrode and Ag/AgCl as reference electrode
6. ábra Ceftriaxon mikro- és nano-részecskék ciklikus voltammogramja vérsavó közegben; mérő elektróda: GCE, referencia elektróda: Ag/AgCl

3.2. Effect of different serum pH on ceftriaxone micro- and nano-particles

The normal blood medium has a neutral pH=7 especially with the ceftriaxone micro particles and oxidation–reduction current peaks were found at +0.9 and -0.75 V respectively, but in the same pH (7) with ceftriaxone nano-particles reduction current peak was found at -0.75 V and disappearing the oxidation peak as shown in *Fig. 6*. So the ceftriaxone nanoparticles act as anti-oxidative antibiotic reagent.

3.2.1. Acidic medium

It was found from the results that acidic (pH=3) serum blood medium affected the electrochemical properties of the oxidation–reduction current peaks of the ceftriaxone micro-particles which acted as oxidative antibiotic reagent as shown in *Fig. 7*. Also, the same phenomena was found in the ceftriaxone nano-particles in acidic (pH=3) blood serum medium as shown in *Fig. 8*.

3.2.2. Alkaline medium

It was found in the results with alkaline (pH=12) blood serum medium that for both the micro- and nano-particles of ceftriaxone the oxidation current peak disappeared and the reduction peak enhanced as shown in *Figs. 7* and *8*, so we can consider the alkaline medium of the blood serum as a good medium for anti-oxidative antibiotic reagent of ceftriaxone.

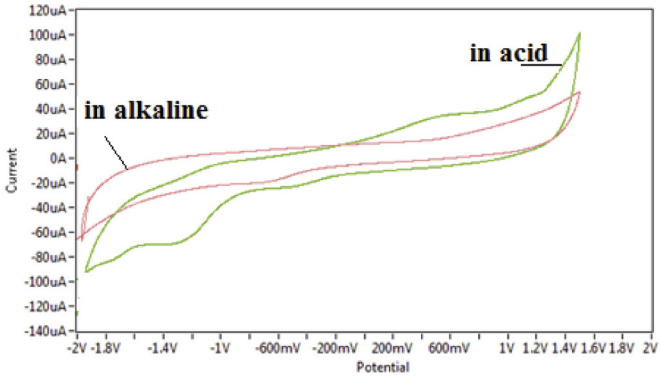

Fig. 7. Cyclic voltammograms for different pH (acidic and alkaline) blood serum medium with ceftriaxone micro-particles at GCE as working electrode and Ag/AgCl as reference electrode

7. ábra Ceftriaxon mikro-részecskék ciklikus voltammogramja eltérő kémhatású (savas és lúgos) vérsavó közegben; mérő elektróda: GCE, referencia elektróda: Ag/AgCl

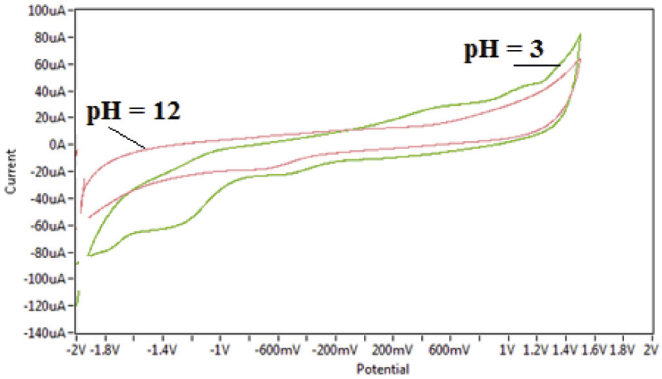

Fig. 8. Cyclic voltammograms for different pH (3 and 12) of blood serum medium with ceftriaxone nano-particles at GCE as working electrode and Ag/AgCl as reference electrode

8. ábra Ceftriaxon nano-részecskék ciklikus voltammogramja eltérő kémhatású (spH 3 és 12) vérsavó közegben; mérő elektróda: GCE, referencia elektróda: Ag/AgCl

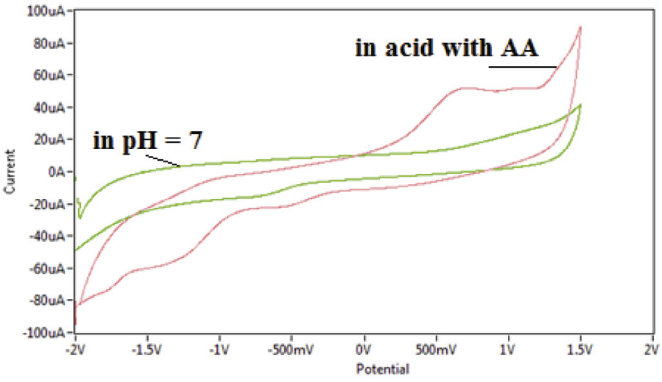

Fig. 9. Cyclic voltammogram of the ceftriaxone nano-particles in blood serum medium with and without AA with GCE as working electrode and Ag/AgCl as reference electrode

9. ábra Ceftriaxon nano-részecskék ciklikus voltammogramja aszkorbinsavval és anélkül vérsavó közegben; mérő elektróda: GCE, referencia elektróda: Ag/AgCl

3.3. Effect of ascorbic acid on ceftriaxone nano-particles in blood serum

One of the anti-oxidative reagents is ascorbic acid (AA) that can be used in electrochemical analysis, especially the voltammetric technique, to determine the oxidation-reduction current peaks of ceftriaxone nanoparticles in blood serum medium. *Fig. 9* shows the influence of AA on the enhancement of the cathodic current peak of the nano-particles of the antibiotic in blood serum medium which is enhanced and another reduction peak appeared to increase the anti-oxidative effect gaining the free radicals from the blood medium through the process. So, it can be said that using AA solution with nano antibiotic drug of ceftriaxone provides more safety [15].

4. Conclusions

Ceftriaxone compound was converted into nano-particles and studied by cyclic voltammetric technique to find the electrochemical behavior in blood serum medium at different pH and with ascorbic acid solution. It was found that ceftriaxone micro- and nano-particles can be considered as antioxidative antibiotic reagent in alkaline blood serum medium which showed two cathodic current peaks to appear and the oxidation current peak to disappear in the cyclic voltammogram. The study was indicated that ceftriaxone compound in both micro- and nano-particles are good antioxidant antibiotic reagents in alkaline blood medium especially with ascorbic acid.

References

[1] Muhammed Mizher Radhi, – Zuhair Numan Hamed, – Selda Sabah Ezzaldeen, – Emad Abbas Jaffar Al-Mulla (2017): Effect of Micro- and Nanoparticles of Ampicillin Trihydrate on Blood Medium: A Voltammetric Study. *Nano Biomedicine and Engineering*, 2017, Vol. 9, No. 3, pp. 185-190. https://doi.org/10.5101/nbe.v9i3.p185-190.

[2] Radhi, M. M. – Khalaf, M. S. – Ali, Z. O. – Omran, R. I. (2016): Voltammetric analysis of Zn (II) in present of each ascorbic acid (AA) and folic acid (FA) in human blood samples. *AASCIT Communications*, Vol. 3, No. 1, pp. 113-119.

[3] Yousif Kadhim Abdul-Amir, – Muhammed Mizher Radhi, – Emad Abbas Jaffar Al-Mulla (2017): Use of Nano-Sensors of the Interferences between Pb((II) with Each of Mg(II), Zn(II), Mn(II), Ca(II), Co(II) and PO4-3 in Blood Medium: An Electrochemical Study, *Nano Biomedicine and Engineering*, 2017, Vol. 9, No. 3, pp. 199-207. https://doi.org/10.5101/nbe.v9i3.p199-207

[4] Radhi, M. M. – Abdul-Amir, Y. K. – Khalaf, M. S. (2016): Electrochemical Effect of Acetylsalicylic Acid (Aspirin) in Present of Each Ascorbic Acid (AA) and Folic Acid (FA) in Normal Saline and Human Blood Samples, American Association for Science and Technology, *AASCIT Communications*, Vol. 3, No. 3, pp. 152-159.

[5] Radhi, M. M. – Al-Dulimy, W. G. – Khalaf, M. S. (2016): Electrochemical study of selenium (IV) mediated by carbon nanotubes modified glassy carbon electrode in blood medium, *Építőanyag-Journal of Silicate Based and Composite Materials*, Vol. 68, No. 3, pp. 90-93. https://doi.org/10.14382/epitoanyag-jsbcm.2016.16

[6] Radhi, M. M. – Abdullah, H. N. – Jabir, M. S. – Al-Mulla, E. A. J. (2017): Electrochemical effect of ascorbic acid on redox current peaks of CoCl2 in blood medium, *Nano Biomedicine and Engineering*, 2017, Vol. 9, No. 2, pp. 103-106. https://doi.org/10.5101/nbe.v9i2.p103-106

[7] Schichor, A. – Bernstein, B. – Weinerman, H. – Fitzgerald, J. – Yordan, E. – Schechter, N. (1994): Lidocaine as a diluent for ceftriaxone in the treatment of gonorrhea, *Archives of Pediatrics and Adolescent Medicine*, Vol. 148, No. 1, pp. 72–75. https://doi.org/10.1001/archpedi.1994.02170010074017

[8] Majdi, S. – Jabbari, A. – Heli, H. – Yadegari, H. – Moosavi-Movahedi, A. A. – Haghgoo, S. (2009): Electrochemical oxidation and determination of ceftriaxone on a glassy carbon and carbon-nanotube-modified glassy carbon electrodes, 2009, *Journal of Solid State Electrochemistry*, Vol. 13, No. 3, pp. 407-416. https://doi.org/10.1007/s10008-008-0567-6

[9] Couto, R. A. S. – Quinaz, M. B. (2016): Development of a Nafion/MWCNT-SPCE-Based Portable Sensor for the Voltammetric Analysis of

the Anti-Tuberculosis Drug Ethambutol. *Sensors*, 2016, Vol. 16, No. 7, p. 1015. https://doi.org/10.3390/s16071015

[10] Shahrokhian, S. – Ranjbar, S. – Ghalkhani, M. (2016): Modification of the Electrode Surface by Ag Nanoparticles Decorated Nano Diamond-graphite for Voltammetric Determination of Ceftizoxime. *Electroanalysis*, Vol. 28, No. 3, 2016, pp. 469-476, https://doi.org/10.1002/elan.201500377

[11] Beytur, M. – Kardaş, F. – Akyıldırım, O. – Özkan, A. – Bankoğlu, B. – Yüksek, H. – Yola, M. L. – Atar, N. (2018): A highly selective and sensitive voltammetric sensor with molecularly imprinted polymer based silver@ gold nanoparticles/ionic liquid modified glassy carbon electrode for determination of ceftizoxim, *Journal of Molecular Liquids*, Vol. 251, pp. 212-217. https://doi.org/10.1016/j.molliq.2017.12.060

[12] Sar, T. K. – Mandal, T. K. – Samanta, I. – Rahaman, A. – Chakraborty, A. K. (2010): Determination of ceftriaxone in plasma and ceftizoxime in milk of mastitic cows following single dose intravenous administration, *Indian Journal of Animal Sciences*, Vol. 80, No. 12, pp. 1182-1184, ref. 14.

[13] Abdelwahed, W. – Degobert, G. – Stainmesse, S. – Fessi, H. (2006): Freeze-drying of nanoparticles: formulation, process and storage considerations. *Advanced Drug Delivery Reviews*, 2006, Vol. 58, No. 15, pp. 1688-1713. https://doi.org/10.1016/j.addr.2006.09.017

[14] Sochor, J. – Dobes, J. – Krystofova, O. – Ruttkay-Nedecky, B. – Babula, P. – Pohanka, M. – Jurikova, T. – Zitka, O. – Adam, V. – Klejdus, B. – Kizek, R. (2013): Electrochemistry as a Tool for Studying Antioxidant Properties. *International Journal of Electrochemical Science*, 2013, Vol. 8, pp. 8464-8489 http://www.electrochemsci.org/papers/vol8/80608464.pdf

[15] Engin, C. – Yilmaz, S. – Saglikoglu, G. – Yagmur, S. – Sadikoglu, M. (2015): Electroanalytical Investigation of Paracetamol on Glassy Carbon Electrode by Voltammetry, *International Journal of Electrochemical Science*, 2015, Vol. 10, pp. 1916-1925. http://www.electrochemsci.org/papers/vol10/100201916.pdf

Ref.:
Radhi, Muhammed Mizher – **Khelkal**, Intesar Nadhum – **Naji**, Eman Natiq – **Abdullah**, Alaa Laebi: *Electrochemical characterization of micro- and nano-particles of ceftriaxone in human blood serum samples using cyclic voltammetry*
Építőanyag – Journal of Silicate Based and Composite Materials, Vol. 71, No. 2 (2019), 52–56. p.
https://doi.org/10.14382/epitoanyag-jsbcm.2019.10

About EGU

EGU, the European Geosciences Union, is Europe's premier geosciences union, dedicated to the pursuit of excellence in the Earth, planetary, and space sciences for the benefit of humanity, worldwide. It was established in September 2002 as a merger of the European Geophysical Society (EGS) and the European Union of Geosciences (EUG), and has headquarters in Munich, Germany.

It is a non-profit international union of scientists with about 15,000 members from all over the world. Membership is open to individuals who are professionally engaged in or associated with geosciences and planetary and space sciences and related studies, including students and retired seniors.

The EGU publishes a number of diverse scientific journals, which use an innovative open access format, and organises a number of topical meetings, and education and outreach activities. It also honours scientists with a number of awards and medals. The annual EGU General Assembly is the largest and most prominent European geosciences event, attracting over 14,000 scientists from all over the world in recent years. The meeting's sessions cover a wide range of topics, including volcanology, planetary exploration, the Earth's internal structure and atmosphere, climate, as well as energy and resources.

www.egu.eu

Optimum limestone powder amount in mortars with over silica fume

Paki TURGUT ▪ Inonu University, Civil Engineering Dept., Turkey ▪ paki.turgut@inonu.edu.tr
Abdullah OGRETMEN ▪ Atlasyol Dam Construction Co., Turkey ▪ abdullahogretmen63@gmail.com
Érkezett: 2019. 01. 12. ▪ Received: 12. 01. 2019. ▪ https://doi.org/10.14382/epitoanyag-jsbcm.2019.11

Abstract
The calcium hydroxide (CH) and the calcium silicate hydrate (CSH) are the main hydration products of Portland cement (PC) paste. The CH product causes the durability problems in the PC paste due to the leaching Ca^{2+} ions. Silica fume is an effective pozzolan to consume CH in the PC paste. It is only effective to convert all CH to CSH if used in excessive amounts in the PC paste. Some problems arise related to segregation, mechanical or physical properties when it is used in excessive amounts. In this study, the optimum limestone powder amount was determined to improve these problems in the mixtures.
Keywords: self-consolidating mortar, limestone powder, silica fume
Kulcsszavak: öntömörödő habarcs, mészkőliszt, szilikapor

Paki TURGUT
is a professor at Inonu University, Engineering Faculty, Civil Engineering Department. He has lectured about construction and building materials, seismic design of reinforced concrete and artificially intelligent systems. He published 23 SCI papers. His papers were cited about 650 times in different journals. He also worked as military officer in construction section of NATO. He has been working on the modelling of explosive damage effect on buildings.

Abdullah OGRETMEN
is a civil engineer. He worked as chief engineer on dam and pond constructions. He has been working at his construction company as planner.

1. Introduction

Self-compaction concrete (SCC) was firstly used in Japan 1990 and it has been effectively used in construction industry since this date [1]. SCC has the same main ingredients similar to the conventional concrete although the amount of powder in SCC is high compared to conventional concrete [2]. SCC is described as an easily flowable concrete having no segregation of its ingredients. In the fresh state, SCC is easily spreaded and fills moulds without compacting [3-4]. Many researches have been performed on hydration of mineral admixtures, mixture design and workability in SCC since it was invented [5]. The fresh SCC effectively covers the reinforcing bars as well as perfectly filling the moulds. The homogeneity of SCC is better than conventional concrete. Filling moulds, covering reinforcement bars and providing homogeneity of SCC is only possible by improving the rheological properties of the fresh SCC. The fresh SCC mixture should have enough plastic viscosity as well as low viscosity. The improved flowability and packing behaviour of fresh SCC can be obtained by adjusting amounts of the superplasticer and the powder amount [6]. The paste amount in SCC is also higher as compared with conventional concrete. Therefore, SCC is a landfill area for some powders having health and environmental hazards [3]. The maximum size of powder used in SCC is less than 0.125 mm. The used amount in it varies between 380 and 600 kg/m^3 [2]. The viscosity of SCC mixture increases when the interaction between powder particles increases because of the increase of powder amount. The powders make the solid section richer in SCC and the coarse aggregates are well covered by mortar [7]. The use of only Portland cement (PC) as powder in SCC is uneconomical approach. Another problem is that the use of high amount PC brings the durability problem in the concrete. That is why, the determined amounts of fly ash (FA), silica fume (SF), granulated blast furnace slag (GBFS), limestone powders (LP) etc. replaced with PC are used in the SCC as powder. Some quarry powders used in SCC has also been popular nowadays [8]. Some properties of fresh and hardened self-compacted mortars (SCMOs) were investigated. The effects of SF or LP on mortars or concretes were detailed given in literature review as below. Ye et. al. [4] showed that LP did not contribute in the chemical reaction in the cement paste system. This was confirmed by using thermal and BSE image analysis. They also pointed out that LP acted as an accelerator during early cement hydration. The high performance concretes having high durability properties were produced by using SF [9]. SF having effective pozzolanic properties produced discontinuous and impermeable pore structures in the cement paste system as compared with those without SF [10]. Cheng and Feldman [11] urged that SF accelerated the hydration of PC in the early hours because of released OH^- and alkali ions to the pore water in the paste. In the first hours, there was an increase in C_3S and C_3A hydrations. Feldman and Cheng [12] reported that the compressive strength of cement paste was decreased in the low water/binder ratios (water/binder: 0.25) when SF content increased. In high water/binder ratios (water/binder: 0.45), SF effectively increased the compressive strength at 1 and 180 days of age. The reason of the high compressive strength obtained in concrete with SF was the decreases in pore diameter, CH amount and the improved interface between paste and aggregate [12-14]. Rao [15] also investigated the effect of SF in the paste and mortar. The setting time, air content and workability were decreased when SF increased in these mixtures. The early drying shrinkage of mortars increased with the increase of SF amount while there was no any change in the late drying shrinkage. Similar results related to the drying shrinkage were found by other researchers [16-17]. Vikan and Justnes [18] performed some tests on the PC paste or mortar containing SF or LP. The viscosity of PC paste increased with the increase of SF amount, but decreased with the increase of superplasticizer amount. LP also decreased the viscosity of PC paste. It was argued that the LP distributed the PC particles more effectively than the SF. The LP had not any chemical reaction with the PC and it behaved as an inert material. In their work, the 9% LP addition effectively improved some properties of paste. Diamantonis et al. [19] made some rheological tests on the PC pastes with the natural pozzolan, SF, LP and FA or with their

combinations. The addition of fine materials to the PC paste had a great effect on its viscosity. PC replacement with 40% LP improved the viscosity. Thus, it was proved to be the best powder. On the other hand, the SF and natural pozzolan did not show the desired effect wanted in the decrease of viscosity. LP was the preeminent powder among the powders tested. The LP greatly improved the particle packing and the deformability of the cementitious paste and reduced the amount of mixing water in the SCC [20]. The PC replacement with 10% LP improved the compressive strength of pastes and reduced the amount of superplasticizer [21]. The LP had an improved effect on the packing, workability and stability of concrete mixtures and hardened properties of concrete by making the seeding points in the PC paste for the CH and CSH in the early hydration stage [22-26]. The LP improved the interface between PC paste and aggregate, and increased the density of PC paste [27-28]. The LP improved the shrinkage and creep deformations by influencing the interior moisture of concrete [29]. The LP having appropriate grain sizes generally improved the compressive strength of concrete [30]. It was found that the LP additive contribution to the early compressive strength was higher than both the FA and SF. The PC replacement with the 30% LP decreased the mechanical strengths in the mortars. It was argued that the PC replacement with the 5% or 10% LP was convenient in the mortars [31]. It was also suggested that the use of SF, FA and LP combinations in the mortars was more effective than the use of them separately [31]. The LP contributed to the improvement of cement grains distribution and enhanced the stability of the mixture when used in concrete or mortar [32-33]. It was noted that the LP was very effective on the concrete rheology and provided the better cohesion and plasticity in the concrete [32]. Neto and Campitelli [34] used a two-point test technique to characterize the rheology of PC paste with the LP. They observed a decrease in the yield stress of cement paste when LP amount increased. It was reported that the PC replacements with 5 to 28% LP effectively reduced the water bleeding and did not adverse effect on the air entraining [35]. The ultra-fine LP reduced the superplasticizer amount and enriched the workability of high performance concrete [36]. Kounakoff et al. [37] reported that the addition of LS or SF to the concrete increased slightly the slump-flow values in concrete. They urged that the flowability and the segregation resistance of concrete could be improved by replacing a certain volume of PC with an identical volume of LP or SF.

The durability of Self-Consolidated Mortars (SCMOs) was increased when the SF or F-class FA converted the CH to CSH in PC paste. Therefore, the high amount of SF was needed in SCMOs to consume the CH effectively. When the SF in SCMOs was high amount in mixtures, the segregation problem occurred in fresh mixture. It was reported in earlier studies that the segregation problem occurred in the SCC or SCMOs when PC replacement with the SF was higher than 15% by weight. Therefore, the aim of this study was to find the optimum LP amount when PC replacement with SF was 25%, and to investigate its effect on some properties of SCMOs.

2. Materials and methods

2.1 Properties of materials used

The type of PC used in this work was CEM I 42.5R. The SF and LP were used as powders. The LP was used in mixtures after sieved from 150 μm mesh. The chemical compositions of materials are given in *Table 1*. The densities of PC, LP and SF were 3.10, 2.54 and 2.25 g/cm^3 while their specific surface areas were 2047, 2186 (cm^2/g) and 20000(BET), respectively. The density, pH value and solid ratio of High range water reducer (HRWR) used were 1.06, 7.03 and 35.52%. The river sand had the maximum grain size of 2.36 mm and the water saturated surface dry density of 2.65 g/cm^3 was used. The percentages of sand by weight satisfying ASTM C33 [38] were 10, 20, 30 and 40% for 0.15-0.30, 0.30-0.60, 0.60-1.18 and 1.18-2.36 mm, respectively.

Weight %	CaO	SiO_2	Al_2O_3	Fe_2O_3	Na_2O	K_2O	MgO	SO_3	Cl^-	LOI
PC	63.59	18.90	5.15	3.36	0.31	0.77	1.57	2.65	0.02	3.59
LP	51.79	2.19	0.13	0.07	0.82	0.02	1.34	0.04	0.01	43.60
SF	1.30	83.14	0.19	0.24	0.64	2.62	4.24	1.04	0.18	4.77

Table 1. The chemical compositions of materials
1. táblázat A vizsgált anyagok kémiai összetétele

2.2 Sample preparation and tests

Five series of SCMs mixtures named as the Control, SF25, SF25LP5, SF25LP10 and SF25LP20 were prepared as given in *Table 2*. While the PC replacement with the SF was 25% by weight in the SF25 mixture, the Control mixture contained only PC as binder. The SF amount was constant in the mixtures containing the PC, SF and LP while the PC replacements with the LP were 5, 10 and 20% by weight. The PC replacements with the total of SF and LP were 30, 35 and 45% by weight in the mixtures LP. The mixture proportions were given in *Table 2*.

	W/B	W	PC	SF	LP	Sand	HRWR
Control	0.46	294	640	-	-	1293	1.28
SF25	0.46	294	480	160	-	1224	8.32
SF25LP5	0.46	294	448	160	32	1218	8.32
SF25LP10	0.46	294	416	160	64	1212	8.32
SF25LP20	0.46	294	352	160	128	1200	8.32

Table 2. Mixture proportioning of used materials (kg/m^3)
2. táblázat A felhasznált anyagok keverési aránya (kg/m^3)

The minimum PC amount was selected as 352 kg/m^3 to satisfy EN 206-1 [39] requirement which was 340 kg/m^3. The water/binder ratio (W/B) was selected as 0.46. During the preparation of fresh mixtures, the powder materials and sand were mixed for 1 min. as described in ASTM C109 [40]. Then, HRWRA and water was poured on these materials. The mixture was further mixed for 4 min. Following EFNARC standard [2], the suitability of fresh mortar mixtures was tested by the mini-slump and V-funnel apparatus. The specifications of mini-slump and V-funnel flow apparatus were given in

detail in EFNARC standard [2]. In the mini slump test, the frustum was placed on a flat surface and filled with mortar. Later, the frustum was lifted upwards. Thus, the diameter of the spread mortar was measured on perpendicular to one another. The average diameter was calculated from these two measurements. In the V-funnel flow test, the mortar was filled into the V-funnel flow apparatus. The gate at the bottom of the apparatus was opened and the discharge time (t) of the mortar was measured. The moulds were filled with fresh mixtures and they were demoulded after 24 hours. All samples were cured in water at 23 °C until testing. φ75×150 mm cylinder samples were used to determine compressive strengths after 7, 28 and 90 days. The dry unit weight, water absorption and sorptivity tests were also performed on the φ75×150 mm cylindrical samples at the age of 90 days.

The drying shrinkage tests on the mortar samples were performed in accordance with ASTM C596 [41]. This test method determined the change in length on the drying of mortar bar with dimensions of 25×25×285 mm. The moist cure of samples was made in the moulds for 48 h at 23 °C in water. Then samples were removed from moulds and cured in the lime-saturated water for 24 hours. The samples were taken from the water at the age of 72 hours and their surfaces were wiped with damp cloth. The lengths of samples were measured by the comparator. Then the samples were placed in the air storage for 25 days. The length readings for each sample were performed at 4, 11, 18, and 25 days of air storage. The length change of each sample at each age of air drying was determined by subtracting the initial length from the reading taken at each age of air drying.

The viscosity values were measured by Brookfield DV-E model viscometer having a smooth-walled concentric cylinder. At lower stress values, the slip in the wall occurred and this condition caused the low yield stress measurements. The slip was most pronounced at the low strain rates, which led to unusual low viscosity readings. The influence of slip decreased while the deformation rate increased. Therefore, the viscosity measurements were conducted at different rotational speeds. The mortar mixture was poured into the pot of the viscometer. The average viscosity values were measured by upwards and downwards of each rotational speed steps. The unit weight, water absorption and sorptivity tests were also performed on the φ75×150 mm cylinder samples by following ASTM C642 [42] and BS EN 772-11 [43].

3. Results and discussions

3.1 Slump, flow, segregation and rheological properties

All of the SCMs were produced to obtain a slump flow diameter of 25±1 cm by adjusting the dosage of HRWR admixture. As shown in *Fig. 1a*, the Control mixture made slight segregation between the sand and paste. In the SF mixture, there was an over segregation among the water, sand and paste. It was reported in earlier studies by different researchers that the segregation problem occurred in the SCMs or concretes when the PC replacement with the SF was higher than 15% by weight. Therefore, the segregation of SF25 mixture was an expected event. The water bleeding occurred at the outermost of flow ring as shown in *Fig. 1b* in the SF25 mixture. The slight segregation also occurred in the SF25LP5 mixture. When compared with the SF25 mixture, the segregation of SF25LP5 mixture was different than that of the SF25. The segregation occurred between the sand and paste in the SF25LP5 but there was also slight water bleeding on the outermost of flow ring as shown in *Fig. 1c*. As shown in *Figs. 1d* and *1e*, the SF25LP10 and SF25LP20 did not show any segregation and their surfaces were considerably smooth.

Li and Kwan [44] reported that the addition of LP into the concrete would increase the cohesiveness of mix to avoid segregation. Turgut et al. [45] showed in their newly developed segregation testing device that LP effectively prevented the segregation of SCC when compared with the SF and FA powders.

The apparent viscosity and RPM (Rotation per Minute) relationship of mixtures were shown in *Fig. 2a*. The viscosity of Control mixture was the lowest in all mixtures while those of the SF25 and SF25LP5 were higher. It could be said that the 5% LP did not decrease the viscosity of SF25LP5 mixture and did not effectively improve the rheological properties. The rheological properties of SF25LP10 and SF25LP20 mixtures were improved when the PC replacements with the LP were 10 and 20% in the SF25 mixture. The increase of LP amount decreased the viscosity value in the mixtures and this result was consistent with that of Vikan and Justnes [18]. Another important thing was that the HRWR amount stayed as constant although the water/binder powder ratio was the same in the SF25, SF25LP5, SF25LP10 and SF25LP20 mixtures. It was expected that the HRWR amount should have increased due to the increase of powder amounts in SF25LP5, SF25LP10 and SF25LP20 mixtures. This showed that the LP dispersed more effectively the PC and SF particles than the HRWR. Vikan and Justnes [18] also found that the LP dispersed the PC particles

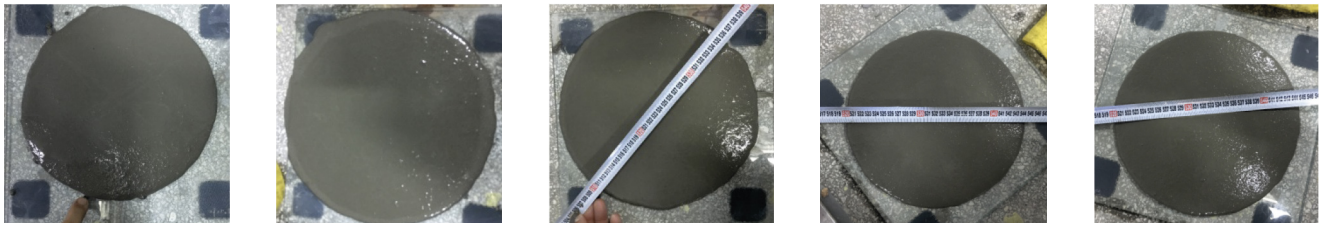

Control *SF25* *SF25LP5* *SF25LP10* *SF25LP20*

Fig. 1. Slump flow and segregation of SCMs
1. ábra Az SCM tartalmú minták terülése és szétosztályozódása

more effectively than that of the SF in their work. As shown in *Fig. 2b*, the V-funnel flow time of mixtures with LP was decreased as compared with the SF25 mixture.

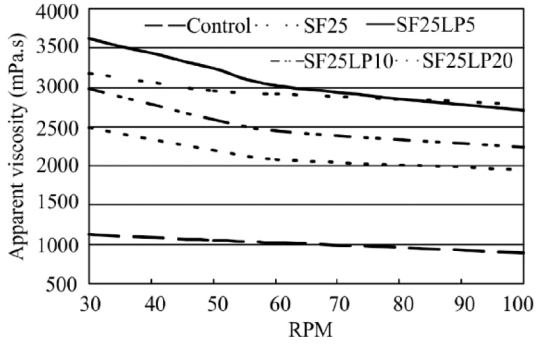

Apparent viscosity of mixtures

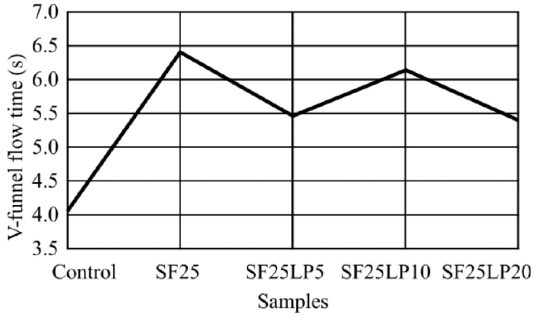

V-funnel flow time of mixtures

Fig. 2. Rheological properties of mixtures
2. ábra A keverékek reológiai tulajdonságai

3.2 Compressive strength

In *Fig. 3a* and *b*, the compressive strengths of samples are shown at 7, 28 and 90 days. At these time points, the compressive strength of Control sample was higher than those of the other samples containing the mineral admixtures. The decrease in the compressive strength at the 7 day was the proportional with the increase of LP amount. The compressive strengths of SF25 sample at the 28 and 90 days were lower than those of the Control sample at these time points. Moreover, the compressive strengths of SF25 sample were nearly identical at the 28 and 90 days although it was expected an increase in their values because of the pozzolanic effect of SF. It was pointed out earlier that the segregation occurred in the SF25. Why did the compressive strength decrease in the SF25 sample although the SF had an excellent pozzolanic property as mixed with the PC? Why did the compressive strengths increase again in the SF25LP5, SF25LP10 and SF25LP20 samples as compared with the SF25 sample? The analogy of decrease or increase in the compressive strength was shown in *Fig. 4*. As shown in *Fig. 4*, the PC and sand particles moved downward as the SF particles moved upwards because of segregation in the SF25 sample. The PC and sand amount were lower while the W/B ratio and the SF amount were higher in region 1 above the dotted line as compared to region 2 below this line. Thus, region 1 above the dotted line was firstly fractured because of the low strength value. It could be said that the SF did not efficiently show the pozzolanic effect because of higher SF and lower PC amounts in region 1. Another reason of strength decrease was the higher W/B ratio in this region. In the SF25 samples containing the LP, SF was uniformly distributed among the PC, LP and sand due to the effect of LP. As shown in *Fig. 4b*, the increase in the strength at the 90 day in these samples with LP might be due to the pozzolanic effect of SF. Chen and Kwan [46] argued that the LP particles might have acted as nuclei for precipitation of CSH, which increased the degree of PC hydration. They also reported that the LP reduced the bleeding in the concrete mixtures and thus, improved the bond strength of interfacial transition zone between the aggregate and mortar surface. Another thing was that the compressive strength increased in the SF25LP5, SF25LP10 and SF25LP20 samples as compared to the SF25 sample although the PC amounts were decreased in the samples with LP. As given in *Table 2*, the PC amounts were 480, 448, 416 and 352 kg/m^3 for the SF25, SF25LP5, SF25LP10 and SF25LP20 samples, respectively. The highest compressive strength increase at 90 days as compared to 28 days as percent was in SF25LP10 sample.

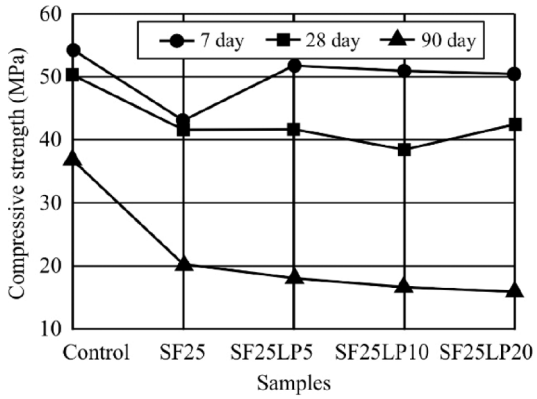

Strength of samples

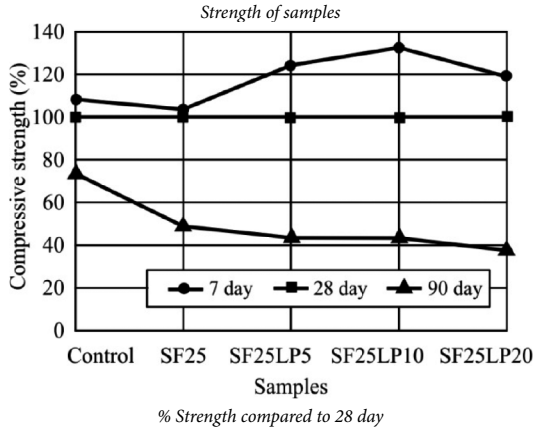

% Strength compared to 28 day

Fig. 3. Compressive strength variation of samples
3. ábra A vizsgált minták nyomószilárdságának változása időben

3.3 Fresh-hardened unit weight and water absorption-sorptivity

The fresh and hardened dry unit weight values of samples were shown in *Fig. 5a*. The fresh and hardened dry unit weight values of the Control sample were higher than those of the other samples with the SF and LP. This was the expected because the density of PC was higher than those of SF and LP. The unit weight values of SF sample was the lowest due to the increase of paste volume in the mixture. The interesting

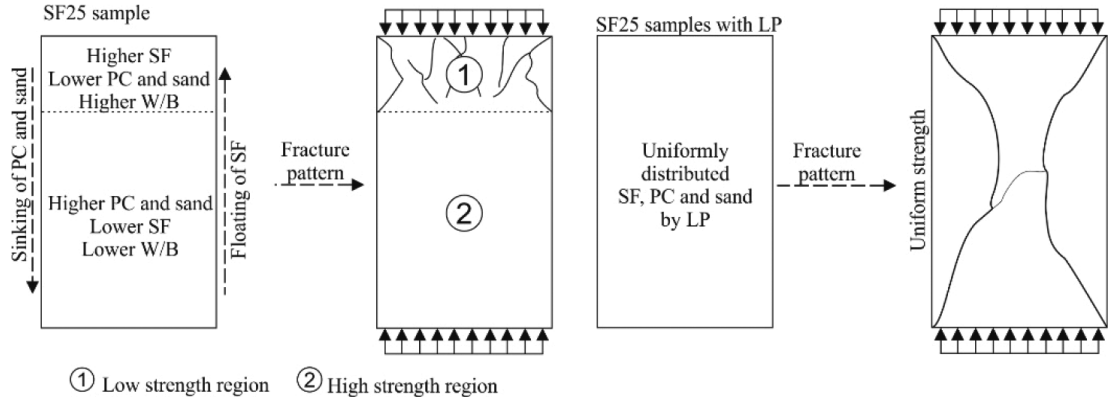

Fig. 4. Fracture pattern of SF25 and SF25 with LP samples
4. ábra Az SF25 valamint az LP tartalmú SF25 minták törésképe

situation occurred in the SF25LP5, SF25LP10 and SF25LP20 samples. It was expected that their unit weight values were lower than that of the SF25 sample due to the lower density of LP (2.54) as compared with the PC (3.1). The PC replacements with the total of SF and LP were 30, 35 and 45% in the SF25LP5, SF25LP10 and SF25LP20 samples. Moreover, the PC amounts were effectively decreased in these samples. The unit weight values of SF25LP5, SF25LP10 and SF25LP20 samples were higher than that of the SF25 sample. This could be originated from the various grain sizes of the SF and LP causing a good packing. The LP particles filled the pores between the large PC particles and the density of paste increased [27-28,47].

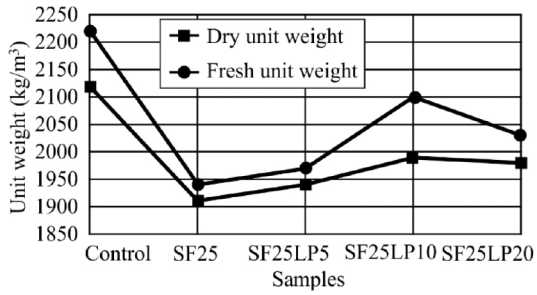

(a) Fresh and hardened dry unit weight

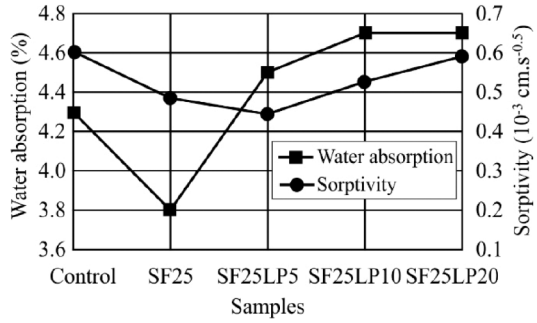

(b) Water absorption and sorptivity

Fig. 5. Fresh/hardened dry unit weights and water absorption/sorptivity of samples
5. ábra A minták friss / megszilárdult sűrűsége valamint vízfelvétele / kapilláris vízfelvétele

The water absorption and sorptivity of samples were shown in *Fig. 5b*. The lowest water absorption was obtained from the SF25 sample while the water absorptions were the highest in the SF25LP10 and SF25LP20 samples. The increase in the water absorption of samples with the LP could be originated from the porous structure of LP. As shown in *Fig. 5b*, the sorptivity had an optimum value in the SF25LP5 sample. Then, the sorptivity increased due to the increase of LP in the SF25LP10 and SF25LP20 samples. The sorptivity of Control and SF25LP20 sample were nearly identical. A hardened paste structure with fine pores due to the LP could be occurred in the SCC [48]. Thus, the capillary forces increased due to the increase in the total area of pore surface in the hardened paste. The sorptivity values of high performance concretes produced by Bharatkumar et al. [49] varied between $0.62\times10^{-3}\times cm.s^{-0.5}$ and $1.47\times10^{-3}\times cm.s^{-0.5}$. Tasdemir [50] also performed the sorptivity tests in the concretes with the LP, SF, FA and stone powder and reported that the sorptivity values varied between $0.46\times10^{-3}\times cm.s^{-0.5}$ and $0.77\times10^{-3}\times cm.s^{-0.5}$. In this work, the sorptivity values varied between $0.60\times10^{-3}\times cm.s^{-0.5}$ and $0.45\times10^{-3}\times cm.s^{-0.5}$ and were near the reference [49,50].

3.4 Drying shrinkage

The drying shrinkage (DS) values at 4, 11, 18 and 25th days are shown in *Fig 6*. The DS values of all samples increased with time. The DS value of SF25LP10 was the lowest at 4th day while that of the SF25 was the highest at 4th and 25th day. At 4th day, the DS value of Control sample was lower than that of the SF25. It was interesting that the DS values of the Control and SF25LP10 samples were nearly identical at 4th, 18th and 25th days. Setter and Roy [16] and Rao [17] found that the SF significantly increased the DS of concrete. They also reported that the SF did not increase the DS at later ages while increasing at early ages due to the starting of pozzolanic reaction effect of the SF. One of the reasons in the increase of the DS was the surface tension on the secondary CSH gels occurred with the reaction between the CH and SF. It was reported that the specific surface area of LP affected the DS of concrete [51-52]. The density of micro-structure of hardened paste increased when the specific surface area of LP was higher than that of the PC. Thus, the DS of mortar with the LP was decreased. As seen in *Fig. 5a*, the fresh and hardened unit weight values of SF25LP10 sample were higher than those of the other samples with the LP and SF. This showed that the DS of SF25LP10 sample was low due to its dense structure. Adam and Race [53] investigated several cements with the additions of grounded or blended LP. Their data indicated that the addition of 2 to 5% limestone in Type I or Type II cement could significantly

increase DS at 4th day. In this study, the DS values in the samples with the LP at 4th day were lower than those of the Control and SF25 although the LP amount increased in the samples. Dhir et al. [54] reported that the general trend for the DS was a reduction with the increase of LP amount in the PC concrete. Barrett et al. [55] investigated the DS of PC containing up to the 15% LP. They showed that the measured autogenous shrinkage in the PC and the PC containing LP systems were nearly equal.

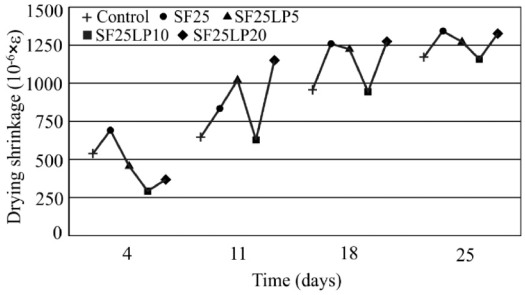

Fig. 6. Drying shrinkage
6. ábra A minták száradási zsugorodása

4. Conclusion

The paper dealt with optimum LP amount in SCM with 25% SF to improve some properties of SCM. The optimum amount of LP was found 10% in SCM containing 25% SF. 10% LP used in SCM increased the compressive strength by preventing segregation and decreased the drying shrinkage of SCM. Water absorption and sorptivity values of SCM increased in 10% LP compared to SCM with 25% SF but they were acceptable levels. The rheological properties of mixtures were also improved at 10% LP amount.

References

[1] Hayakawa, M. – Matsuoka, Y. – Shindoh, T. (1994): Development and application of super –workable concrete. *Proceedings of International RILEM workshop on the special concretes – workability and mixing*, 1994, 2: 183–90.

[2] EFNARC, Specifications and guidelines for self-compacting concrete, English ed. *European federation for specialist construction chemicals &concrete systems*, 2005.

[3] Khayat, K. – Hu, C. – Monty, H. (1999): Stability of self-consolidating concrete, advantages, and potential applications. *Proceedings of International RILEM symposium on self compacting concrete*, 1999, 1: 143–52.

[4] Ye, G. – Liu, X. – De Schutter G. – Poppe, A. M. – Taerwe, L. (2007): Influence of limestone powder used as filler in SCC on hydration and microstructure of cement pastes. *Cement and Concrete Composites*. Vol. 29, No. 2, pp. 94–2. https://doi.org/10.1016/j.cemconcomp.2006.09.003

[5] Oh, S. G. – Noguchi, T. – Tomosawa, F. (1999): Toward mix design for rheology of self-compacting concrete. *Proceedings of International RILEM symposium on self compacting concrete*, 1999, 1: 361-72.

[6] Skarendahl, Å. – Tangtermsirikul, S. – Kamal, K. – Petersson, Ö. (2000): Self-Compacting Concrete-State-of-the-Art Report of RILEM TC 174-SCC. *RILEM report*, 23.

[7] Sari, M. – Prat, E. – Labastire, J. F. (1999): High strength self-compacting concrete original solutions associating organic and inorganic admixtures. *Cement and Concrete Research*. Vol. 29, No. 6, pp. 813–8. https://doi.org/10.1016/s0008-8846(99)00037-x

[8] Galetakis, M., – Soultana, A. (2016): A review on the utilisation of quarry and ornamental stone industry fine by-products in the construction sector. *Construction and Building Materials*. Vol. 102, pp. 769–81. https://doi.org/10.1016/j.conbuildmat. 2015.10.204

[9] Neville, A.M. (2011): Properties of Concrete, 5th edition, Longman, Pearson Education.

[10] Bayasi, Z – Zhou, J. (1993): Properties of silica fume concrete and mortar. *ACI Materials Journal*. Vol. 90, No. 4, pp. 349–6. https://doi.org/10.14359/3892

[11] Cheng-Yi, H – Feldman, R. F. (1985): Hydration reactions in Portland cement-silica fume blends. *Cement and Concrete Research*. Vol. 15, No. 4, pp. 585–2. https://doi.org/10.1016/0008-8846(85)90056-0

[12] Feldman, R. F. – Cheng-Yi, H. (1985): Properties of Portland cement-silica fume pastes II. Mechanical properties. *Cement and Concrete Research*. Vol. 15, No. 6, pp. 943–2. https://doi.org/10.1016/0008-8846(85)90083-3

[13] Cohen, M. D. – Klitsikas, M. (1986): Mechanisms of hydration and strength developments in Portland cement composites containing silica fume particles. *Northeastern University*.

[14] Cohen, M. D. (1990): A look at silica fume and its actions in Portland cement concrete. *Indian Concrete Journal*. Vol. 64, No. 9, pp. 429–38.

[15] Rao, G. A. (2003): Investigations on the performance of silica fume-incorporated cement pastes and mortars. *Cement and Concrete Research*. Vol. 33, No. 11, pp. 1765–0. https://doi.org/10.1016/s0008-8846(03)00171-6

[16] Setter, N. – Roy, D. M. (1978): Mechanical features of chemical shrinkage of cement paste. *Cement and Concrete Research*. Vol. 8, No. 5, pp. 623–34. https://doi.org/10.1016/0008-8846(78)90045-5

[17] Rao, G. A. (1998): Influence of silica fume replacement of cement on expansion and drying shrinkage. *Cement and Concrete Research*. Vol. 28, No. 10, pp. 1505–09. https://doi.org/10.1016/s0008-8846(98)00127-6

[18] Vikan, H. – Justnes, H. (2007): Rheology of cementitious paste with silica fume or limestone. *Cement and Concrete Research*. Vol. 37, No. 11, pp. 1512–17. https://doi.org/10.1016/j.cemconres.2007.08.012

[19] Diamantonis, N. – Marinos, I. – Katsiotis, M. S. – Sakellariou, A. – Papathanasiou, A. – Kaloidas, V. – Katsioti, M. (2010): Investigations about the influence of fine additives on the viscosity of cement paste for self-compacting concrete. *Construction and Building Materials*. Vol. 24, No. 8, pp. 1518–22. https://doi.org/10.1016/j.conbuildmat.2010.02.005

[20] Bosiljkov, V. B. (2003): SCC mixes with poorly graded aggregate and high volume of limestone filler. *Cement and Concrete Research*. Vol. 33, No. 9, pp. 1279–86. https://doi.org/10.1016/s0008-8846(03)00013-9

[21] Felekoglu, B. (2007): Utilisation of high volumes of limestone quarry wastes in concrete industry (self-compacting concrete case). Resources, Conservation and Recycling. Vol. 51, No. 4, pp. 770–91. https://doi.org/10.1016/j.resconrec.2006.12.004

[22] Pera, J. – Husson, S. – Guilhot, B. (1999): Influence of finely ground limestone on cement hydration. *Cement and Concrete Composites*. Vol. 21, No. 2, pp: 99–05. https://doi.org/10.1016/s0958-9465(98)00020-1

[23] Bonavetti, V. – Donza, H. – Rahhal, V. – Irassar, E. (2000): Influence of initial curing on the properties of concrete containing limestone blended cement. *Cement and Concrete Research*. Vol. 30, No. 5, pp. 703–8. https://doi.org/10.1016/s0008-8846(00)00217-9

[24] Nehdi, M. (2000): Why some carbonate fillers cause rapid increases of viscosity in dispersed cement-based materials. *Cement and Concrete Research*. Vol. 30, No. 10, 1663–69. https://doi.org/10.1016/s0008-8846(00)00353-7

[25] Nehdi, M. – Mindess, S. – Aitcin, P. C. (1998): Rheology of high-performance concrete: effect of ultrafine particles. *Cement and Concrete Research*. Vol. 28, No. 5, pp. 687–97. https://doi.org/10.1016/s0008-8846(98)00022-2

[26] Ghezal, A. – Khayat, K. H. (2002): Optimizing self-consolidating concrete with limestone filler by using statistical factorial design methods. *ACI Materials Journal*. Vol. 99, No. 3, pp. 264–72. https://doi.org/10.14359/11972

[27] Tragardh, J. (1999): Microstructural features and related properties of self-compacting concrete. *Proceedings of International RILEM symposium on self compacting concrete*, 1999, 1: 175-86.

[28] Billberg, P. (1999): Fine mortar rheology in mix design of SCC. *Proceedings of International RILEM symposium on self compacting concrete*, 1999, 1: 47-58.
[29] Belarbi, N. – Pons, G. – Perrin, B. (1997): Delayed behaviour of concrete: influence of additions and aggregate characteristics in relation to moisture variations. *Cement and Concrete Research*. Vol. 27, No. 9, pp. 1429–38. https://doi.org/10.1016/s0008-8846(97)00125-7
[30] Petersson, O. (2001): Limestone powder as filler in self-compacting concrete-frost resistance and compressive strength. *Proceedings of International RILEM symposium on self compacting concrete*, 2001, 2: 277-84.
[31] Turkel, S. – Altuntas, Y. (2009): The effect of limestone powder, fly ash and silica fume on the properties of self-compacting repair mortars. *Sadhana*. Vol. 34, No. 2, 331–43. https://doi.org/10.1007/s12046-009-0011-3
[32] Bombled, J. P. (1986): Rhéologie du béton frais: Influence de lájout de fillers aux ciments. *Proceedings of 8th International Congress on the Chemistry of Cement*, 1986, 4: 190-96.
[33] Escadeillas, G. (1988): Les ciments aux fillers calcaires: Contribution a leur optimisation par l'étude des propriétés mécaniques et physiques des bétons fillérisés. *Doctoral dissertation, Thèse de Doctorat de l'Université Paul SABATIER, Toulouse*.
[34] Neto, C. S. – Campiteli, V. C. (1990): The influence of limestone additions on the rheological properties and water retention value of Portland cement slurries. In Carbonate additions to cement. *ASTM International*.
[35] Brookbanks, P. (1989): Properties of fresh concrete, performance of limestone filled cements. *Proceedings BRE/BCA seminar, Garston*. 1989: 4.
[36] Nehdi, M. – Mindess, S. – Aïtcin, P. C. (1997): Statistical modelling of the micro filler effect on the rheology of composite cement pastes. *Advances in Cement Research*. Vol. 9, No. 33, pp. 37-46. https://doi.org/10.1680/adcr.1997.9.33.37
[37] Kounakoff, B. A. – Hanzic, L., – Ho, J. C. M. (2017): Limestone and silica fume to improve concurrent flowability–segregation limits of concrete. *Magazine of Concrete Research*. Vol. 69, No. 23, pp. 1189–02. https://doi.org/10.1680/jmacr.16.00387
[38] ASTM C33 (2018): Standard specification for concrete aggregates. https://doi.org/10.1520/C0033_C0033M-18
[39] BS EN 206-1 (2013): Concrete: Specification, performance, production and conformity. https://doi.org/10.3403/30257890
[40] ASTM C109 (2016): Standard test method for compressive strength of hydraulic cement mortars (using 2-in. or [50-mm] cube specimens). https://doi.org/10.1520/C0109_C0109M-16A
[41] ASTM C596 (2018): Standard test method for drying shrinkage of mortar containing hydraulic cement. https://doi.org/10.1520/C0596-18
[42] ASTM C642 (2013): Standard test method for density, absorption, and voids in hardened concrete. https://doi.org/10.1520/C0642-13
[43] BS EN 772-11 (2011): Methods of test for masonry units. Determination of water absorption of aggregate concrete, autoclaved aerated concrete, manufactured stone and natural stone masonry units due to capillary action and the initial rate of water absorption of clay masonry units. https://doi.org/10.3403/30215381
[44] Li, L. G. – Kwan, A. K. (2015): Adding limestone fines as cementitious paste replacement to improve tensile strength, stiffness and durability of concrete. *Cement and Concrete Composites*. Vol. 60, 17–24. https://doi.org/10.1016/j.cemconcomp.2015.02.006
[45] Turgut, P. – Turk, K. – Bakirci, H. (2012): Segregation control of SCC with a modified L-box apparatus. *Magazine of Concrete Research*. Vol. 64, No. 8, pp. 707–16. https://doi.org/10.1680/macr.11.00144
[46] Chen J. J. – Kwan A. K. H. (2012): Adding limestone fines to reduce heat generation of curing concrete. *Magazine of Concrete Research*. Vol. 64, No. 12, pp. 1101–11. https://doi.org/10.1680/macr.11.00193
[47] Barnes, H. A. – Hutton, J. F. – Walters, K. (1989): An introduction to rheology. Elsevier. https://doi.org/10.1016/b978-0-444-87469-6.50005-6
[48] Valcuende, M. – Marco, E. – Parra, C. – Serna, P. (2012): Influence of limestone filler and viscosity-modifying admixture on the shrinkage of self-compacting concrete. *Cement and Concrete Research*. Vol. 42, No. 4, pp. 583–92. https://doi.org/10.1016/j.cemconres.2012.01.001
[49] Bharatkumar, B. H. – Narayanan, R. – Raghuprasad, B. K. – Ramachandramurthy, D. S. (2001): Mix proportioning of high performance concrete. *Cement and Concrete Composites*. Vol. 23, No. 1, pp. 71–80. https://doi.org/10.14359/9807
[50] Tasdemir, C. (2003): Combined effects of mineral admixtures and curing conditions on the sorptivity coefficient of concrete. *Cement and Concrete Research*. Vol. 33, No.10, pp.1637–42. https://doi.org/10.1016/s0008-8846(03)00112-1
[51] Van Khanh, B. – Montgomery, D. (1999): Drying shrinkage of self-compacting concrete containing milled limestone. *Proceedings of International RILEM symposium on self compacting concrete*, 1999, 1: 227-38.
[52] Klug, Y. – Holschemacher, K. (2003): Comparison of the hardened properties of self-compacting and normal vibrated concrete. *Proceedings of International RILEM symposium on self compacting concrete*, 2003, 3: 596-05.
[53] Adams, L. D. – Race, R. M. (1990): Effect of limestone additions upon drying shrinkage of Portland cement mortar. In Carbonate additions to cement. *ASTM International*.
[54] Dhir, R. K. – Limbachiya, M. C. – McCarthy, M. J. – Chaipanich, A. (2007): Evaluation of Portland limestone cements for use in concrete construction. *Materials and Structures*. Vol. 40, No. 5, pp. 459–73.
[55] Barrett, T. – Sun, H. – Villani, C. – Barcelo, L. – Weiss, J. (2014): Early-age shrinkage behaviour of Portland limestone cement. *Concrete International*. Vol. 36, No. 2, pp. 51–7.

Ref.:
Turgut, Paki – **Ogretmen**, Abdullah: *Optimum limestone powder amount in mortars with over silica fume*
Építőanyag – Journal of Silicate Based and Composite Materials, Vol. 71, No. 2 (2019), 58–64. p.
https://doi.org/10.14382/epitoanyag-jsbcm.2019.11

15TH INTERNATIONAL CONGRESS ON THE CHEMISTRY OF CEMENT

ICCC PRAGUE 2019

The ICCC 2019 will present cement and environmental development worldwide and renowned experts from all over the world are invited to present their work at the Congress. The scientific programme will cover the topics of the newest and the most important research and development describing cement and clinker chemistry (incl. kiln process technology), the nano and macro properties of the clinker and cement, hydration processes, the impact of additives and admixtures, leaching processes, the behaviour of trace elements, microscopy outputs, alternative binders, durability of concrete, standards and codes, as well as modern laboratory instrument equipment. The Congress will consist of many plenary lectures and parallel sessions on a variety of topics, offering to the scientists, researchers, producers and users from all over the world the opportunity to meet, to present and to exchange their research results and knowledge.

September 16–20, 2019

www.iccc2019.org

Lignit pernye alapú geopolimerek mechanikai tulajdonságainak szabályozása vibrációs tömörítéssel

SZABÓ Roland
A Miskolci Egyetem Mikoviny Sámuel Földtudományi Doktori Iskolájának doktorjelöltje 2018. februárjától. Előkészítéstechnikai mérnöki MSc diplomáját 2013-ban szerezte a Miskolci Egyetemen. Jelenlegi kutatási témája a speciális tulajdonságú geopolimerek fejlesztése, különös tekintettel a habszerkezetű geopolimer termékekre, elsősorban ipari hulladékokat felhasználva.

SZABÓ Roland ▪ Miskolci Egyetem, Nyersanyagelőkészítési és Környezeti Eljárástechnikai Intézet
Érkezett: 2019. 01. 17. ▪ Received: 17. 01. 2019. ▪ https://doi.org/10.14382/epitoanyag-jsbcm.2019.12

Kivonat
A geopolimerek tömörítése a betontechnológiában alkalmazott módszerekkel történhet, úgymint döngölés, csömöszölés, vibrációs tömörítés, kompaktálás. Jelen tanulmány a lignitpernye alapú geopolimerek vibrációs úton történő tömörítésével foglalkozik. A pernye főbb tulajdonságainak (szemcseméret-eloszlás, fajlagos felület, nedvességtartalom, ásványos és kémiai összetétel) meghatározása után a tömörítési paraméterek változtatásának (motor excentricitás (amplitúdó), frekvencia, tömörítési idő) a geopolimer próbatestek mechanikai tulajdonságaira gyakorolt hatását vizsgáltam. A próbatestek egytengelyű nyomószilárdságának és testsűrűségének meghatározása 7 napos vizsgálati korban történt. Az eredmények alapján megállapítható, hogy a tömörítési paraméterek változtatása a próbatestek testsűrűségében nem okozott jelentős eltérést, az értékek 1,4-1,45 g/cm^3 között változtak. A szilárdságvizsgálati eredményeknél azonban kimutatható volt a paraméterek módosításának hatása (az értékek 7,9-12,8 MPa között változtak). A vizsgálatok eredményei alapján tömörség és nyomószilárdság szempontjából optimális tömörítési paraméterek a következők voltak: excentricitás 10%, motorfrekvencia 50 Hz, tömörítési idő 1 perc.
Kulcsszavak: lignit pernye, geopolimer, vibrációs tömörítés, nyomószilárdság, testsűrűség

1. Bevezetés

A geopolimerek olyan új típusú, félig-kristályos, háromdimenziós szerkezettel rendelkező szervetlen polimerek, amelyek szilárd aluminoszilikátok vagy alkáli szilikát tartalmú anyagok lúgos (NaOH, KOH, Na-szilikát, K-szilikát) vagy savas (foszforsav) aktiváló oldatban való oldásával és reakciójával állíthatók elő. Alapanyagként természetes vagy mesterséges aluminoszilikát ásványi anyagok, illetve ipari aluminoszilikát melléktermékek/hulladékok (úgymint erőműi pernye, salak, agyag, vörösiszap, metakaolin, perlit, üveg vagy ezek keverékei) használhatók [1-6]. A geopolimerek tulajdonságait az alapanyag összetétele és reaktivitása, valamint az aktiváló oldat összetétele [6-10] mellett a kezelési hőmérséklet és idő [11-13], továbbá az alkalmazott tömörítési módszer is nagymértékben befolyásolja [13, 14].

A geopolimerek (illetve geopolimer betonok) tömörítése a betontechnológiában alkalmazott módszerekkel valósítható meg, melyek a következők lehetnek: vibrációs tömörítés, csömöszölés, döngölés valamint nagy nyomáson történő tömörítés (kompaktálás) [2, 8, 12-15]. A durva és/vagy finom aggregátumot nem tartalmazó geopolimerek esetén elsősorban vibrációs tömörítés az elterjedt.

Chindraprasirt és mtsai [12] lignit pernye alapú geopolimerek bedolgozhatóságát és szilárdságát vizsgálták különböző koncentrációjú NaOH (10, 15, 20 M) és Na-szilikát oldat eltérő arányú keverékét alkalmazva. A próbatestek tömörítését vibrációs asztalon végezték 10 s-ig. Az eredmények alapján megállapították, hogy a NaOH mennyiségének és koncentrációjának növelésével csökkent a geopolimer paszta bedolgozhatósága és ezáltal a próbatestek szilárdságértékei is.

Živica és mtsai [14] nagy nyomáson (300 MPa) kompaktált metakaolin alapú geopolimerek és kézi tömörítéssel előállított referenciatestek tulajdonságait hasonlították össze. Eredményeik alapján arra a megállapításra jutottak, hogy a nagy nyomáson tömörített próbatestekben megnőtt az azonos méretű pórusok mennyisége, és egy sokkal finomabb pórusszerkezet (átlagos pórusméret 59 nm) alakult ki bennük, mint a referencia mintákban (átlagos pórusméret 814 nm). Továbbá azt is megfigyelték, hogy a tömörítés homogénebb szemcseszerkezetet eredményezett, melyet a szemcsék felületének oldásával és ezáltal nagyobb fokú geopolimerizációs folyamattal magyaráztak.

Cheng és mtsai [15] szénmeddő alapú geopolimerek előállítási körülményeit és tulajdonságait vizsgálták. A kísérleteik során az aktiváló oldat/szilárd anyag arány mellett a NaOH koncentráció és NaOH/Na-szilikát arány hatását vizsgálták. A geopolimer paszta tömörítését vibrációs asztalon végezték 60 s-ig a kötőanyagban lévő levegő eltávolítása érdekében.

Jelen tanulmány a pernyealapú geopolimer tömörségének vibrációs úton történő szabályozásával foglalkozik. Az elvégzett vizsgálatok kiterjedtek a vibrációs asztal motorjának excentricitás és frekvenciamódosításával, illetve a tömörítési idő változtatásával a mintatestek nyomószilárdságában és testsűrűségében bekövetkező változások detektálására. Emellett vizsgáltam tömörítés hatására a geopolimer anyagszerkezetében bekövetkező változásokat is.

2. Anyagok, vizsgálati módszerek

Kísérletek során lignittüzelésből származó nyers erőműi pernyét használtam, amely főbb jellemzőit az *1. táblázat* tartalmazza. A pernye kémiai összetételének meghatározása röntgenfluoreszcens spektroszkópia elemzéssel (XRF) történt, amelynek eredményét a *2. táblázat* mutatja.

Származás	Mátrai Erőmű (Visonta, Magyarország)
Nedvességtartalom (%)	0,27
Halmazsűrűség (g/cm³)	0,72
Szemcsesűrűség (g/cm³)	1,93
x_{10} (μm)	10,8
x_{50} (μm)	52
x_{80} (μm)	119,3
Fajlagos felület (cm²/g)	1152

1. táblázat Lignit pernye jellemzői
Table 1. Properties of lignite fly ash

Komponens	Pernye alkotó mennyisége, m/m%
SiO_2	48,1
Al_2O_3	14,42
Fe_2O_3	10,97
Na_2O	0,37
K_2O	1,66
CaO	11,76
MgO	3,34
TiO_2	0,492
P_2O_5	0,264
MnO	0,171
SO_3	0,575
LOI*	2,2
egyéb	5,678

**Izzítási veszteség 950 °C-on (Loss on ignition at 950 °C)*

2. táblázat Lignitpernye kémiai összetétele (XRF vizsgálat alapján)
Table 2. Chemical composition of lignite fly ash (XRF measurement)

Az elemzés alapján megállapítható, hogy a pernyében lévő SiO_2/Al_2O_3 aránya 3,34, valamint a SiO_2, Al_2O_3 és Fe_2O_3 tartalom a pernye mintegy 73,49 m/m%-át adja. Emellett a mintaanyag relatíve magas CaO tartalommal (11,76 %) is rendelkezett.

A mintaanyag ásványos összetételének meghatározása röntgendiffrakciós szerkezetvizsgálati módszerrel (XRD) történt. A pernye fő ásványos összetevői a következők voltak: kvarc (20,34%), maghemit (4,22), hematit (3,91%), anhidrit (7,08%), albit (4,71%), albit K0.16 (5,58%), CaO (1,61%) és amorf rész (52,5%).

Asztal hasznos felülete	700 × 900 mm (0,63 m²)
Motor típusa	Italvibras MVSI 10/310-890-I
Motor teljesítménye (50 Hz)	0,35 kW
Motor fordulatszáma (50 Hz-en)	1000 1/perc (frekvenciaváltóval szabályozható)
Excenter súlyok	a bezárt szög állítható (0-180°)
Centrifugális erő (50 Hz)	3,14 kN

3. táblázat Vibrációs asztal műszaki jellemzői
Table 3. Technical characteristics of vibrating table

A geopolimerek előállításához használt aktiváló szer 8 M-os NaOH és vízüveg (Na_2SiO_3) oldatok keverékéből állt. A NaOH oldatot 99,99% tisztaságú szilárd NaOH granulátumok desztillált vízben való oldásával készítettem, míg a vízüveg 2,7% K_2O-ot, 13,7% Na_2O-ot, 25,3% SiO_2-ot és 58,3% H_2O-ot tartalmazott.

A geopolimer próbatestek tömörítésére szolgáló vibrációs asztal főbb műszaki jellemzői a *3. táblázat*ban találhatóak.

3. Kísérletek

A tömörítési vizsgálatok során először a geopolimer pasztát állítottam elő, amely a lignit pernye és az aktiváló oldat 2 percig történő keverésével történt. Az aktiváló szer/pernye aránya (L/S arány) 0,82 volt. A geopolimer paszta összetételének és hőkezelési körülményeinek (hőmérséklet, kezelési idő) megválasztása korábbi kísérletek eredményei [9] alapján történt. A kapott pasztát előre kiolajozott, 35 mm átmérőjű és 65 mm magasságú műanyag hengeres formákba töltöttem, majd vibrációs asztalon különböző paraméter beállítások mellett (motor excentricitás, frekvencia) egy percig tömörítettem. Tömörítés után a próbatestek hőkezelése történt, amelyet két lépcsőben hajtottam végre. Először a geopolimereket 24 órán keresztül levegőtől elzárva, kondicionáló kamrában 23 °C-on tároltam, majd elektromos kemencében 6 órán keresztül 30 °C-on hőkezeltem. Hőkezelést követően a próbatestek tárolása a nyomószilárdság-vizsgálat elvégzéséig kondicionáló kamrában történt 23 °C-on és 90%-os páratartalom beállítása mellett. A szilárdságvizsgálatra 7 napos korban került sor. Minden esetben 5 db próbatestet vizsgáltam, és a kapott eredmények átlagértékét diagramon ábrázoltam. A vibrációs asztal üzemi paraméterváltoztatása mellett a tömörítési idő hatását is vizsgáltam. A kísérlet során 0,5; 1; 2; 3; 5 és 10 perces tömörítést alkalmaztam. A próbatestek nyomószilárdsága mellett meghatároztam azok testsűrűségét, valamint Fourier-transzformációs infravörös spektroszkópia (FT-IR) elemzéssel a szerkezetükben - tömörítés hatására- bekövetkező változásokat.

4. Eredmények

4.1. Motor excentricitás (amplitúdó-kitérés) változtatásának hatása

A motor excentricitásának változtatásával a vibrációs asztallap x és y irányú kitérésének mértékét (amplitúdóját) tudjuk módosítani. Az *1. ábra* jól szemlélteti, hogy a vibromotoron található excentersúlyok pozíciójának módosításával hogyan változott az asztallap helyzete vibráció során. Az excentricitás mértékének növelésével az asztallap horizontális (x irányú) és vertikális (y irányú) kitérése 20%-os excentricitás értékig növekedett, majd ezt követően az y irányú kitérésben kismértékű csökkenés mutatkozott. Ezzel szemben az asztallap x irányú kitérése az excentricitás mértékének változtatásával növekedett. Ez a változás az

$$\ln(Y) = 0{,}054 * X - 1{,}017 \quad (1)$$

exponenciális függvénnyel jól jellemezhető, ahol a determinációs együttható értéke R^2=0,982.

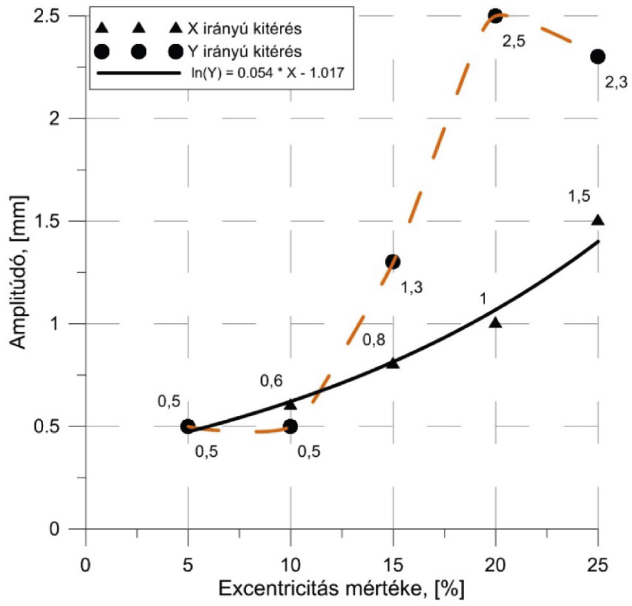

1. ábra Vibrációs asztal amplitúdójának változása az excentricitás függvényében
Fig. 1. Variation of amplitude of the vibrating table as function of the eccentricity

A *2. ábra* a próbatestek egytengelyű nyomószilárdság és testsűrűség értékeit ábrázolja a motor excentricitás változásának függvényében. Az ábra alapján elmondható, hogy a vibrációs asztallap amplitúdó változásának mértéke hatással volt a geopolimerek nyomószilárdságára, míg a testsűrűségükben nem történt jelentős változás, azok átlagosan 1,42-1,43 g/cm^3 közötti értéket vettek fel. Az excentricitás mértékének növelésével a geopolimerek nyomószilárdságában növekedés tapasztalható egy bizonyos értékig, majd csökkenés figyelhető meg. A legnagyobb szilárdságú geopolimer (12,8 MPa) 20% excentricitás beállításnál készült.

Fontos megjegyezni, hogy az irodalom alapján a pernye alapú geopolimerek szilárdsága a nyersanyag őrléssel megvalósított mechanikai aktiválásával fokozható [16-18].

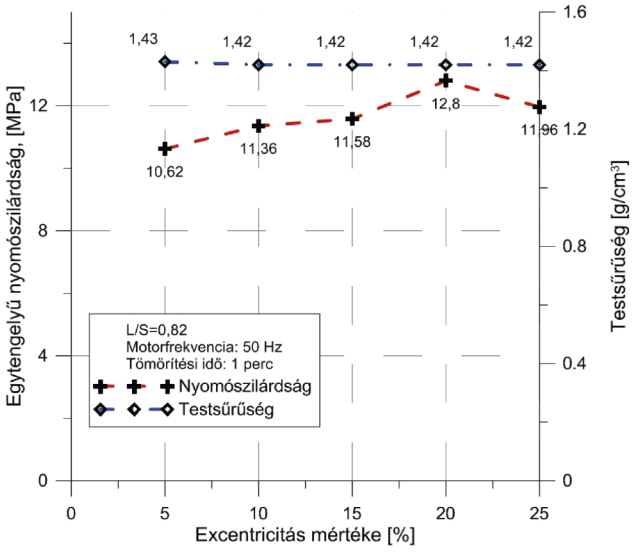

2. ábra Geopolimer nyomószilárdságának és testsűrűségének változása az excentricitás függvényében
Fig. 2. Compressive strength and specimen density of geopolymer as function of the eccentricity

A további vizsgálatot 10%-os beállítás mellett végeztem, mivel magasabb excentricitásnál (20 és 25%) az asztallap y irányú kitérésében bekövetkező ugrásszerű növekedés (*1. ábra*) a vibrációs asztal rögzítését hosszabb üzemeltetés esetén károsította volna. Továbbá a nyomószilárdság értékek relatív szórása (*4. táblázat*) is ennél a beállításnál volt a legkisebb (9,4%), míg a szilárdság értékek közötti legnagyobb eltérés 15%-os beállításnál mutatkozott (23,1%).

Motorexc. [%]	Nyomószil. relatív szórása [%]	Testsűrűség relatív szórása [%]
5	13,7	0,8
10	9,4	0,4
15	23,1	0,3
20	11,9	0,4
25	16,5	0,60

4. táblázat Geopolimer nyomószilárdságának és testsűrűségének relatív szórása az excentricitás változtatásával
Table 4. Coefficient of variation of compressive strength and density of geopolymer as function of the eccentricity

4.2 Motorfrekvencia változás hatása

Adott excentricitás (10%) és különböző motorfrekvencia beállítás mellett tömörített geopolimerek nyomószilárdságában és testsűrűségében bekövetkező változásokat a *3. ábra* szemlélteti. Az ábra alapján megfigyelhető, hogy a rezgésszám (frekvencia) növelésével a geopolimerek átlagos nyomószilárdsága is növekedett. Ugyanakkor az is megállapítható, hogy a vibrációs asztal túl alacsony (<40 Hz) és túl magas (60 Hz) rezgésszámon való üzemeltetése a geopolimerek mechanikai stabilitására már kedvezőtlenül hatott. Ezekben az esetben a geopolimerek 10,07-10,71 MPa közötti nyomószilárdsággal rendelkeztek. Ezzel szemben 45-55 Hz között készült próbatestek szilárdságértékei 11,31-11,53 MPa tartományban mozogtak.

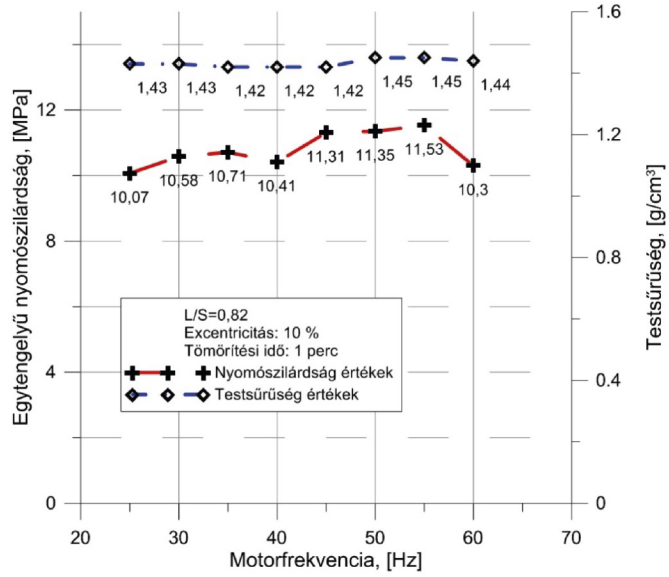

3. ábra Geopolimer nyomószilárdságának és testsűrűségének változása a frekvencia függvényében
Fig. 3. Compressive strength and specimen density of geopolymer as function of the motor frequency

A geopolimerek testsűrűségében nem történt jelentős változás, azok 1,42-1,45 g/cm³ között változtak. Legnagyobb testsűrűsége (1,45 g/cm³) 50 és 55 Hz-en készült próbatesteknek volt. (Ezekben az esetekben mértük a legnagyobb nyomószilárdságokat is.)

Az eredmények alapján megállítható, hogy a legmagasabb nyomószilárdsággal rendelkező geopolimerek a vibrációs asztal 45-55 Hz frekvencia tartományban való üzemeltetésével állíthatók elő. Továbbá a próbatestek nyomószilárdságának relatív szórása ezekben a tartományokban nem haladta meg a 13 %-ot (*5. táblázat*).

Motorfrekvencia [Hz]	Nyomószil. relatív szórása [%]	Testsűrűség relatív szórása [%]
25	5,8	0,7
30	9,6	0,7
35	14,9	0,5
40	12,8	0,4
45	10,9	0,3
50	12,8	0,6
55	10,6	0,5
60	12,4	0,7

5. táblázat Geopolimer nyomószilárdságának és testsűrűségének relatív szórásának alakulása a motor frekvencia változtatásával

Table 5. Coefficient of variation of compressive strength and density of geopolymer as function of the motor frequency

4.3 Tömörítési idő

Mivel 50 és 55 Hz-en közel azonos tulajdonságú geopolimerek készíthetőek, ezért a tömörítési idő változtatásának hatását 50 Hz (hálózati) frekvencia (és 10% excentricitás) beállításon vizsgáltam.

A vizsgálat eredményeit a *4. ábra* szemlélteti, míg a nyomószilárdság és testsűrűség értékek relatív szórását a *6. táblázat*ban foglaltam össze. Az ábra alapján megfigyelhető, hogy a geopolimerek nyomószilárdsága egy adott tömörítési ideig (1 perc) növekedett, majd ezt követően 5 perces tömörítésig csökkenő tendenciát mutatott. Ezután ismét szilárdságnövekedés tapasztalható. Ez a fluktuáció vélhetően a hosszabb ideig tartó tömörítés hatására a keverékben bekövetkező aktiváló oldat- szilárd anyag bizonyos mértékű szétválásával magyarázható, ami rendezetlen geopolimer szerkezet kialakulásához vezethetett. A legnagyobb szilárdságot 1 perc tömörítési időnél mértem (11,73 MPa), míg legkisebb szilárdsággal az 5 percig tömörített próbatestek rendelkeztek (7,92 MPa). A geopolimerek testsűrűsége a tömörítési idő növelésével, 2 perces tömörítésnél érte el a maximumot (1,45 g/cm³), ezt követően az értékük nem változott. A nem tömörített geopolimerek testsűrűsége átlagosan 1,42 g/cm³ volt.

A geopolimerek nyomószilárdság értékeinek relatív szórását megvizsgálva (*6. táblázat*), megállapítható, hogy az átlagtól való legnagyobb eltéréssel a tömörítetlen és az 5 percig tömörített geopolimerek rendelkeztek, mindkét esetben az eltérés 20% fölötti volt (21,1 illetve 29,6%). A többi esetben az eltérés 15% alatt maradt (6,7-14,2%).

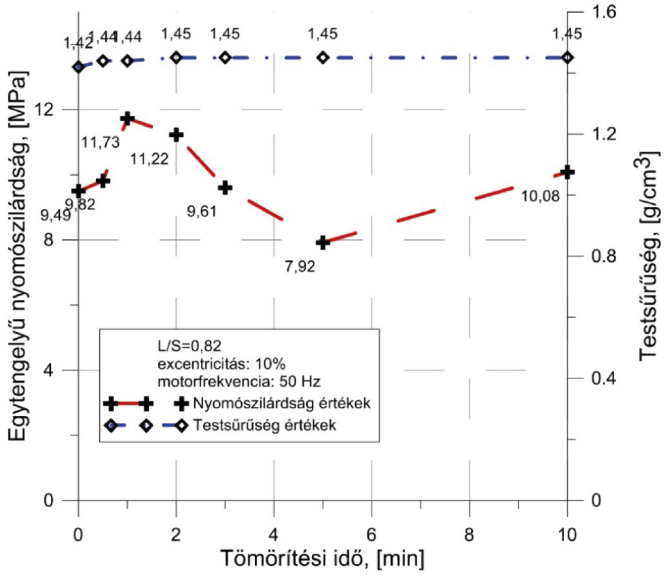

4. ábra Tömörítési idő hatása a geopolimer nyomószilárdságára és testsűrűségére

Figure 4. Effect of compression time on the compressive strength and specimen density of geopolymer

Tömörítési idő [min]	Nyomószil. relatív szórása [%]	Testsűrűség relatív szórása [%]
0	21,1	0,3
0,5	12,6	0,8
1	14,2	0,3
2	9,8	0,6
3	14,2	0,3
5	29,6	0,4
10	6,7	0,6

6. táblázat Geopolimer nyomószilárdságának és testsűrűségének relatív szórása változása a tömörítési idő függvényében

Table 6. Coefficient of variation of compressive strength and density as function of the compression time

4.4 FT-IR eredmények

4.4.1 Excentricitás

Az *5. ábra* különböző excentricitáson tömörített geopolimerek FT-IR spektrumát mutatja. Az ábrán látható, hogy az egyes spektrumok közel azonos lefutásúak. Eltérés leginkább az 1415 cm^{-1}-nél jelentkező sávokban (csúcsokban) mutatkozik, amely karbonát jelenlétére (O-C-O kötések nyújtó rezgéseire) utal [19]. E sávok intenzitása 10 és 20% excentricitáshoz tartozó geopolimereknél volt a legkisebb, amely magyarázatul szolgálhat a magasabb nyomószilárdság értékekre (10% exc.-nál 11,4 MPa, míg 20% exc.-nál 12,8 MPa). A geopolimerek 15% excentricitásnál is még átlagosan 11,5 MPa nyomószilárdsággal rendelkeztek, viszont az értékek ebben az esetben igen nagy relatív szórást mutattak (23%), ami az egyes próbatestekben fellépő karbonát képződés okozta szilárdságcsökkenés miatt következhetett be.

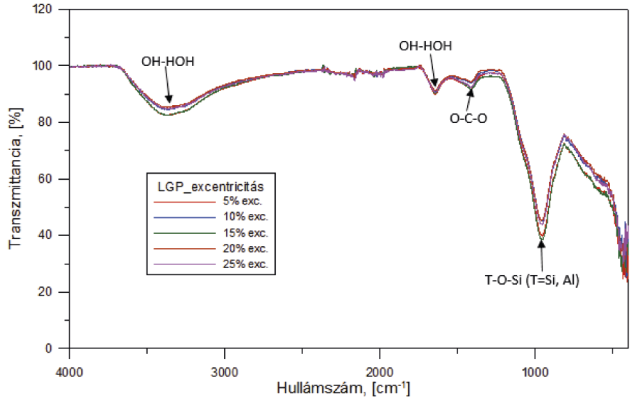

5. ábra Különböző excentricitáson tömörített geopolimerek FT-IR spektrumai
Fig. 5. FT-IR spectras of geopolymers (compression on various eccentricity)

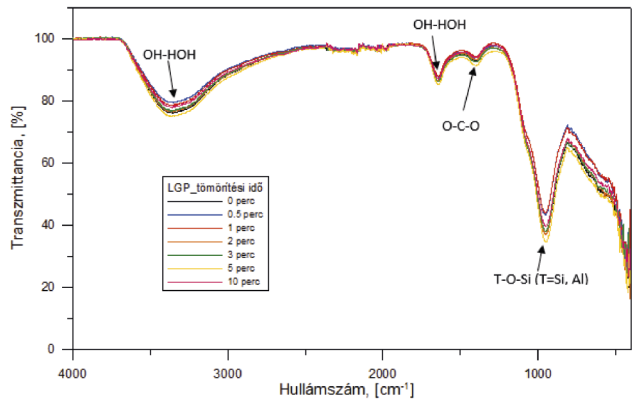

7. ábra Különböző ideig tömörített geopolimerek FT-IR spektrumai
Fig. 7. FT-IR spectras of geopolymers (compression on various compression time)

4.4.2 Frekvencia

Ha a különböző frekvencián tömörített geopolimerek FT-IR spektrumait megvizsgáljuk (*6. ábra*), megállapítható, hogy azokban nincs számottevő eltérés, a sávok szélessége és intenzitása is közel azonos volt. Mind a 3360 cm^{-1}-nél és 1645 cm^{-1}-nél jelentkező OH-HOH kötésekhez (víz), mind az 1416 cm^{-1}-nél jelentkező O-C-O kötésekhez (karbonát) valamint a 955 cm^{-1}-nél lévő T-O-Si (T=Si, Al) kötésekhez tartozó sávok (csúcsok) intenzitása és szélessége azonosnak tekinthető.

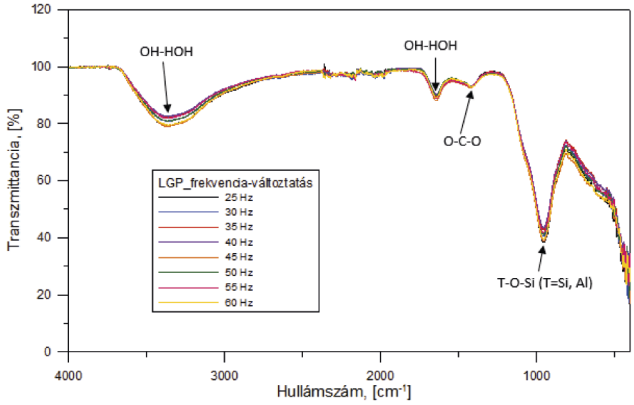

6. ábra Különböző frekvencián tömörített geopolimerek FT-IR spektrumai
Fig. 6. FT-IR spectras of geopolymers (compression on various frequency)

4.4.3 Tömörítési idő

A *7. ábra* a különböző ideig tömörített geopolimerek FT-IR spektrumát mutatja. Az ábrán látható, hogy az egyes geopolimerek spektrumaiban itt sincs számottevő eltérés. Ez alól kivételt képez az 5 percig tömörített geopolimer spektruma, amely kissé elkülönül a többitől. Eltérés leginkább az 1401 cm^{-1}-nél jelentkező csúcsnál mutatkozik, ami kissé nagyobb intenzitású, mint a többi próbatest esetén. Fontos megjegyezni, hogy a geopolimer 5 perces tömörítésnél rendelkezett a legkisebb nyomószilárdsággal (7,9 MPa), ami vélhetően a jelentősebb karbonátképződés miatt következett be. További eltérés a 950 cm^{-1} környékén jelentkező csúcsok intenzitásában mutatkozott, ami a T-O-Si (T=Si, Al) kötések aszimmetrikus nyújtó rezgéseire utal. Geopolimerizáció szempontjából ennek a csúcsnak a változása (csúcsmagasság és szélesség) jellemző a geopolimerizáció fokára [20].

5. Megállapítások

A kutatómunka során geopolimerek vibrációs úton történő szabályozásával foglalkoztam. Vizsgáltam különböző tömörítési paramétereknek (excentricitás, frekvencia, tömörítési idő) a geopolimerek mechanikai tulajdonságaira gyakorolt hatását.

A kísérletek eredményei alapján megállapítható, hogy ezen paraméterek változtatása jelentős hatással volt a geopolimerek nyomószilárdságára, míg a testsűrűségben nem volt lényeges változás. Az excentricitás növelése a vibrációs asztallap nagyobb mértékű x és y irányú kitérését (amplitúdó változását) eredményezte, amely változás a geopolimerek nyomószilárdságában is növekedést mutatott.

A motorfrekvencia változtatása során megállapítottam, hogy a rezgésszám növelése a geopolimerek mechanikai stabilitását javította, ugyanakkor túl magas (60 Hz) frekvenciaértéknél szilárdságromlás következett be. Optimális tartomány 45-55 Hz között volt.

A tömörítési idő is jelentős hatást gyakorolt a geopolimerek tulajdonságaira. A túl rövid (<1 perc) és túl hosszú (>2 perc) ideig tartó tömörítés relatíve alacsony szilárdságú (<10 MPa) geopolimert eredményezett, viszont az optimális tömörítési idő (1 perc) megválasztásával 11,7 MPa szilárdságú geopolimert állítottam elő.

Az FTIR mérések eredményei alapján megállapítható, hogy a tömörítési paraméterek változtatása a geopolimerek szerkezetében nem okozott jelentős átalakulást. Geopolimerizáció szempontjából fontos sávok (csúcsok) mind intenzitásukban mind szélességükben azonosak (vagy közel azonosak) voltak. Új sávok nem jelentek meg egyik esetben sem.

Az eredmények alapján tömörség és nyomószilárdság szempontjából optimális tömörítési paraméterek a következők voltak: excentricitás 10%, motorfrekvencia 50 Hz, tömörítési idő 1 perc. Ezen paraméter-beállítások mellett átlagosan 11,73 MPa nyomószilárdságú geopolimer állítható elő, amely érték a tömörítetlen geopolimerek szilárdságához képest (9,49 MPa) 23,6%-os szilárdságnövekedést jelent. A geopolimerek testsűrűsége a fentebb említett beállításokkal átlagosan 1,44 g/cm^3, ami kismértékű növekedést mutat a tömörítetlen geopolimerek sűrűségéhez képest (1,42 g/cm^3).

6. Köszönetnyilvánítás

A tanulmányban ismertetett kutatómunka az EFOP-3.6.1-16-2016-00011 jelű „Fiatalodó és Megújuló Egyetem – Innovatív Tudásváros – a Miskolci Egyetem intelligens szakosodást szolgáló intézményi fejlesztése" projekt részeként – a Széchenyi 2020 keretében – az Európai Unió támogatásával, az Európai Szociális Alap társfinanszírozásával valósult meg. A szerző köszönetét fejezi ki Móricz Ferenc tanársegédnek és Dr. Kristály Ferenc tudományos főmunkatársnak a pernyeminta kémiai és ásványos összetételének meghatározásáért, Dr. Debreczeni Ákos egyetemi docensnek az egytengelyű nyomószilárdság-vizsgálatok elvégzésében nyújtott segítségéért, továbbá Dr. Mucsi Gábor és Dr. Nagy Sándor egyetemi docensnek a témában való iránymutatásukért.

Irodalomjegyzék

[1] Davidovits, J. (2011): Geopolymer chemistry and application. *Institut Geopolimére*, ISBN: 9782951482050 pp. 283, 286.

[2] Mucsi G. – Lakatos J. – Molnár Z. – Szabó R. (2014): Development of geopolymer using industrial waste materials. ENVIRONMENTAL ENGINEERING, eISSN 2029-7092 / eISBN 978-609-457-640-9

[3] Komintsas, K. – Zaharaki, D. (2007): Geopolymerisation: A review and prospects for the mineral industry. Mineral Engineering 20, pp. 1261-1277. https://doi.org/10.1016/j.mineng.2007.07.011

[4] Bai, C. – Colombo, P. (2018): Processing, properties and applications of highly porous geopolymers: A review. Ceramics International 44:(14), pp 16103-16118, https://doi.org/10.1016/j.ceramint.2018.05.219

[5] Vaou, V. – Panias D. (2010): Thermal insulating foamy geopolymers from perlite. Minerals Engineering 23 (14) 1146–1151. https://doi.org/10.1016/j.mineng.2010.07.015

[6] Singh, S. – Aswath, M. U. – Ranganath, R. V. (2018): Effect of mechanical activation of red mud on the strength of geopolymer binder. Construction and Building Materials 177, pp. 91-101. https://doi.org/10.1016/j.conbuildmat.2018.05.096

[7] Davidovits, J. (1994): Geopolymers: inorganic polymeric new materials. J. Mater. Educ. 16, pp. 91-139.

[8] Kumar, S. – Kumar, R., (2011): Mechanical activation of fly ash: Effect on reaction, structure and properties of resulting geopolymer. Ceramics International 37, pp. 533–541. http://dx.doi.org/10.1016/j.ceramint.2010.09.038

[9] Molnár, Z. – Szabó, R. – Rácz, Á. – Lakatos, J. – Debreczeni, Á. – Mucsi, G. (2017): Optimization of activator solution and heat treatment of ground lignite type fly ash geopolymers. IOP CONFERENCE SERIES: MATERIALS SCIENCE AND ENGINEERING 175, pp. 1-8. https://doi:10.1088/1757-899X/175/1/012046

[10] Tchakouté, H. K. – Rüscher, C. H. – Kamseu, E. – Andreola, F. – Leonelli, C. (2017): Influence of the molar concentration of phosphoric acid solution on the properties of metakaolin-phosphate-based geopolymer cements. Applied Clay Science 147, pp. 184-194. https://doi.org/10.1016/j.clay.2017.07.036

[11] Palomo, A. – Grutzeck, M. W. – Blanco, M. T. (1999): Alkali activated fly ashes: A cement for the future. Cement and Concrete Research. 29 pp. 1323-1329. https://doi.org/10.1016/S0008-8846(98)00243-9

[12] Chindaprasirt, P. – Chareerat, T. – Sirivivatnanon, V. (2007): Workability and strength of coarse high calcium fly ash geopolymer. Cement and Concrete Composites, 29 (3); pp. 224-229. https://doi.org/10.1016/j.cemconcomp.2006.11.002

[13] Wallah, S. E. – Rangan, B. V. (2006): Low-calcium fly ash-based geopolymer concrete: Long-term properties, Research report GC2, Faculty of Engineering, Curtin University of Technology,

[14] Živica, V. – Balkovic, S. – Drabik, M. (2011): Properties of metakaolin geopolymer hardened paste prepared by high-pressure compaction. Construction and Building Materials 25 (5), pp. 2206–2213. https://doi.org/10.1016/j.conbuildmat.2010.11.004

[15] Cheng, Y. – Hongqiang, M. – Hongyu, C. – Jiaxin, W. – Jing, S. – Zonghui, L. – Mingkai Y. (2018): Preparation and characterization of coal gangue geopolymers. Construction and Building Materials 187, pp. 318-326. https://doi.org/10.1016/j.conbuildmat.2018.07.220

[16] Mucsi, G. (2016):_Mechanical activation of power station fly ash by grinding – A review. Építőanyag 68:(2) pp. 56-61. http://dx.doi.org/10.14382/epitoanyag-jsbcm.2016.10

[17] Mádai F. – Kristály F. – Mucsi G. (2015): Microstructure, mineralogy and physical properties of ground fly ash based geopolymers. Ceramics-Silikaty 59:(1) pp. 70-79.

[18] Kumar, R. – Kumar, S. – Mehrotra, S.P. (2007): Towards sustainable solutions for fly ash through mechanical activation. Resources, Conservation and Recycling 52, pp. 157–159. http://dx.doi.org/10.1016/j.resconrec.2007.06.007

[19] Panias, D. – Giannopoulou, I. P. – Perraki, T. (2007): Effect of synthesis parameters on the mechanical properties of fly ash-based geopolymers. Colloids and Surfaces A: Physicochemical Engineering Aspects 301 (1-3), pp.:246-254. https://doi.org/10.1016/j.colsurfa.2006.12.064

[20] Rattanasak, U. – Chindaprasirt, P. (2009): Influence of NaOH solution on the synthesis of fly ash geopolymer. Minerals Engineering 22 (12), pp. 1073–1078. https://doi.org/10.1016/j.mineng.2009.03.022

Control of mechanical properties of lignite fly ash based geopolymers by vibrating compression

The compression of geopolymer (and geopolymer concrete) can be performed by the usual methods used in the concrete technology, like compaction, tamping, and vibrating compression. This study focused on the vibrating compression of lignite fly ash based geopolymers. After the determination of the main properties of fly ash (like particle size distribution, specific surface area, moisture content, mineral and chemical composition) the effect of changing compression parameters (eccentricity, frequency and compression time) were investigated on the geopolymer properties. The uniaxial compressive strength and specimen density were measured at age of 7 days. Based on the results can be stated the changing of compression parameters resulted just a slight change on the specimen density (the values were between 1.4-1.45 g/cm3), but the compressive strength of geopolymer changed significantly (the values were between 7.9-12.8 MPa). Optimal compression parameters were the following: eccentricity of 10%, motor frequency of 50 Hz and the compression time of 1 minute.

Keywords: lignite fly ash, geopolymer, vibrating compression, compressive strength, specimen density

Ref.:

Szabó Roland: *Lignit pernye alapú geopolimerek mechanikai tulajdonságainak szabályozása vibrációs tömörítéssel*
Építőanyag – Journal of Silicate Based and Composite Materials, Vol. 71, No. 2 (2019), 66–71. p.
https://doi.org/10.14382/epitoanyag-jsbcm.2019.12

GUIDELINE FOR AUTHORS

The manuscript must contain the followings: title; author's name, workplace, e-mail address; abstract, keywords; main text; acknowledgement (optional)**; references; figures, photos with notes; tables with notes; short biography** (information on the scientific works of the authors).

The full manuscript should not be more than 6 pages including figures, photos and tables. Settings of the word document are: 3 cm margin up and down, 2,5 cm margin left and right. Paper size: A4. Letter size 10 pt, type: Times New Roman. Lines: simple, justified.

TITLE, AUTHOR

The title of the article should be short and objective.

Under the title the name of the author(s), workplace, e-mail address.

If the text originally was a presentation or poster at a conference, it should be marked.

ABSTRACT, KEYWORDS

The abstract is a short summary of the manuscript, about a half page size. The author should give keywords to the text, which are the most important elements of the article.

MAIN TEXT

Contains: materials and experimental procedure (or something similar), results and discussion (or something similar), conclusions.

REFERENCES

References are marked with numbers, e.g. [6], and a bibliography is made by the reference's order. References should be provided together with the DOI if available.

Examples:

Journals:

[6] Mohamed, K. R. – El-Rashidy, Z. M. – Salama, A. A.: In vitro properties of nano-hydroxyapatite/chitosan biocomposites. *Ceramics International.* 37(8), December 2011, pp. 3265–3271, http://doi.org/10.1016/j.ceramint.2011.05.121

Books:

[6] Mehta, P. K. – Monteiro, P. J. M.: Concrete. Microstructure, properties, and materials. *McGraw-Hill*, 2006, 659 p.

FIGURES, TABLES

All drawings, diagrams and photos are figures. The **text should contain references to all figures and tables**. This shows the place of the figure in the text. Please send all the figures in attached files, and not as a part of the text. **All figures and tables should have a title**.

Authors are asked to submit color figures by submission. Black and white figures are suggested to be avoided, however, acceptable.

The figures should be: tiff, jpg or eps files, 300 dpi at least, photos are 600 dpi at least.

BIOGRAPHY

Max. 500 character size professional biography of the author(s).

CHECKING

The editing board checks the articles and informs the authors about suggested modifications. Since the author is responsible for the content of the article, the author is not liable to accept them.

CONTACT

Please send the manuscript in electronic format to the following e-mail address: femgomze@uni-miskolc.hu and epitoanyag@szte.org.hu or by post: Scientific Society of the Silicate Industry, Budapest, Bécsi út 122–124., H-1034, HUNGARY

We kindly ask the authors to give their e-mail address and phone number on behalf of the quick conciliation.

Építőanyag – *Journal of Silicate Based and Composite Materials*, Quarterly peer-reviewed periodical of the Hungarian Scientific Society of the Silicate Industry, SZTE.
http://epitoanyag.org.hu

ESCM
EUROPEAN SOCIETY FOR COMPOSITE MATERIALS

THE SCIENTIFIC, ENGIEERING AND INDUSTRIAL COMMNITY INVOLVED WITH COMPOSITE MATERIALS

THE SOCIETY

OBJECTIVES OF THE SOCIETY

ESCM is a European, non-governmental, non-profit scientific and engineering organisation with the following objectives:

- To encourage the free interchange of information on all those aspects related to composite materials which of are interest to the scientific and engineering community.
- To provide a Europe-wide forum for the discussion of such topics, e.g. by organising the ECCM (European Conference on Composite Materials) and more specialised symposia related to composites.
- To guide and foster the understanding and utilisation of the science and technology of composite materials.
- To promote European co-operation in the study of topics in composite materials science and technology.
- To promote liaison with engineering and scientific bodies throughout Europe with similar aims and to serve as a facilitator for communication between such bodies.
- To foster an environment for timely and cost-effective research, development and implementation of advanced technology in composites.
- To encourage the education of young specialists in the disciplines supporting composite materials science and technology.
- To recognise individuals of outstanding achievement in the science, technology, engineering, and application of composite materials.

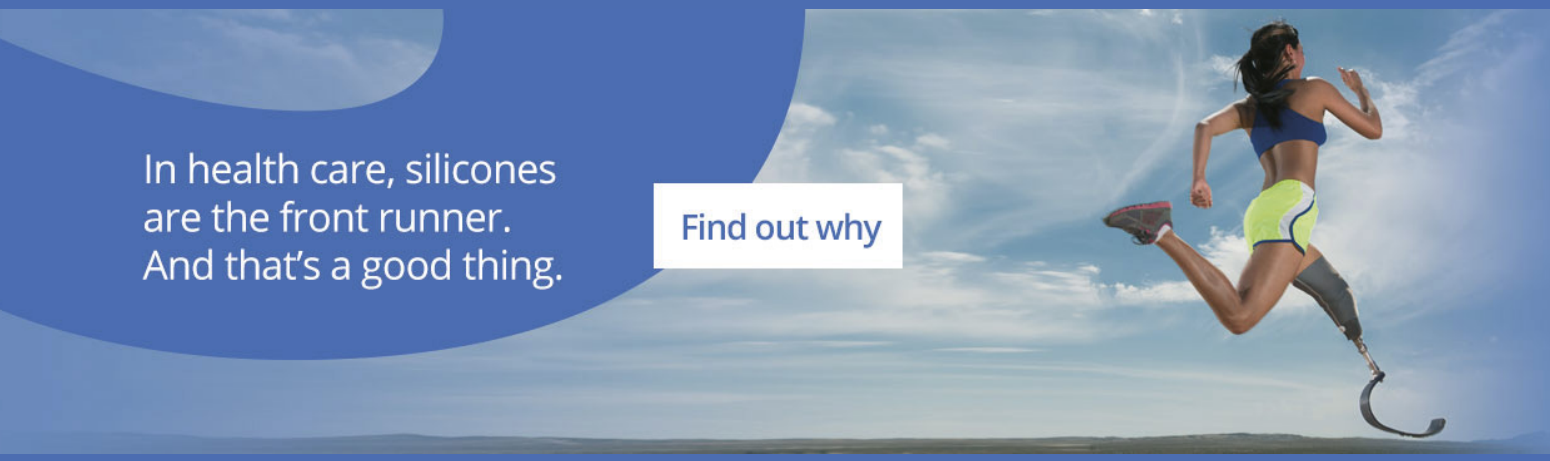

CES - SILICONES EUROPE

SILICONES & YOU

Silicones have literally thousands of applications that collectively bring safety, comfort and enjoyment to life. They improve the performance and reliability of millions of modern products.

THE SCIENCE

Silicones chemistry is one of the most versatile chemistries on the planet, rendering it full of possibilities and producing a wide range of formulations and uses from aesthetic to technical.

WHO IS CES?

We are a non-profit organisation representing all major producers of silicones in Europe. We provide information on silicones from a health, safety and environmental perspective.

WWW.SILICONES.EU